FEMALE CONTROL OF REPRODUCTIVE SUCCESS IN
ARABIDOPSIS THALIANA

by

Jing Yuan

A Dissertation

Submitted to the Faculty of Purdue University

In Partial Fulfillment of the Requirements for the degree of

Doctor of Philosophy
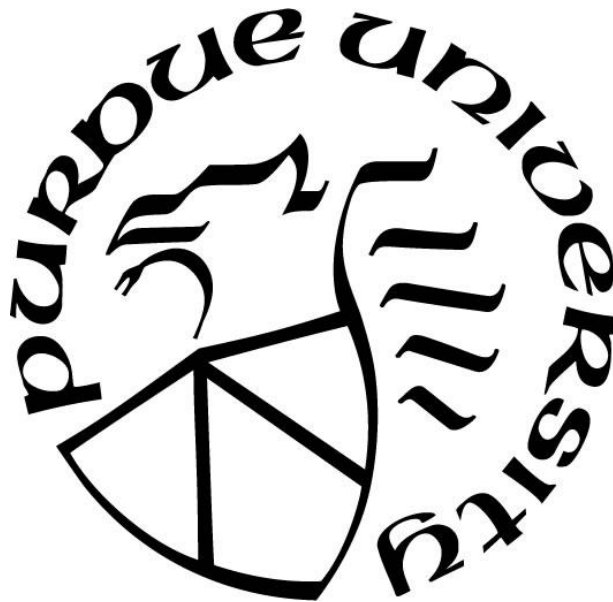
Department of Botany & Plant

Pathology West Lafayette, Indiana

August 2019

THE PURDUE UNIVERSITY GRADUATE SCHOOL
STATEMENT OF COMMITTEE APPROVAL

Dr. Sharon Kessler, Chair

    Department of Botany and Plant Pathology

Dr. Jody Banks

    Department of Botany and Plant Pathology

Dr. Yun Zhou

    Department of Botany and Plant Pathology

Dr. Chunhua Zhang

    Department of Botany and Plant Pathology

Dr. Brian Dilkes

    Department of Biochemistry

Approved by:

    Dr. Christopher Staiger

        Head of the Graduate Program

This dissertation is dedicated to my family for their supports.

Specially to my grandfather Wensui Yuan and my grandmother Jinmei Cui, who raise me, teach me and encourage me all the time!

ACKNOWLEDGMENTS

TABLE OF CONTENTS

LIST OF TABLES

LIST OF FIGURES

LIST OF MOVIES

EXTRA HEADINGS

AG   AGAMOUS

AHK   ARABIDOPSIS HISTIDINE KINASE

ANT   AINTEGUMENTA

BR   BRASSINOSTEROIDS

BUPS BUDDHA'S PAPER SEAL 1 AND 2 (BUPS1 AND BUPS2)

BZR   BRASSINAZOLE-RESISTANT 1

CC   CENTRAL CELL

CMM CARPEL MARGIN MERISTEM

CRC   CRABSCLAW

CRP   CYSTEINE-RICH POLYPEPTIDES

CUC   CUP-SHAPED COTYLEDON1 AND 2 (CUC1 AND CUC2)

DIC   DIFFERENTIAL INTERFERENCE CONTRAST

EC   EGG CELL

ES   EMBRYO SAC

EVN   EVAN

FA   FILIFORM APPARATUS

FDR   FALSE DISCOVERY RATE

FER   FERONIA

GAI   GA-INSENSITVE

GFP   GREEN FLUORESCENT PROTEIN

GWAS GENOME-WIDE ASSOCIATION STUDY

HAP   HAPLESS

HLL   HUELLENLOS

LM   LINEAR REGRESSION MODEL

LRE   LORELEI

LUG   LEUNIG

MAC   MINOR ALLELE COUNT

MLO   MILDEW RESISTANCE LOCUS O

MMC MEGASPORE MOTHER CELL

MS MURASHIGE AND SKOOG

NERD NEW ENHANCER OF ROOT DWARFISM1

NTA NORTIA

ONA OVULE NUMBER ASSOCIATED

PT POLLEN TUBE

QTL QUANTITATIVE TRAIT LOCUS

RAM ROOT APICAL MERISTEM

ROS REACTIVE OXYGEN SPECIES

SAM SHOOT APICAL MERISTEM

SEU SEUSS

SHP SHATTERPROOF1 AND 2 (SHP1 AND SHP2)

SRN SIRÈNE

SNP SINGLE NUCLEOTIDE POLYMORPHISM

SPT SPATULA

SYN SYNERGID CELL

TUN TURAN

ABSTRACT

Author: Yuan, Jing. PhD
Institution: Purdue University
Degree Received: August 2019
Title: Female Control of Reproductive Success in *Arabidopsis thaliana*.
Committee Chair: Sharon Kessler

In flowering plants, successful pollination is important for sexual reproduction. It involves a series of intercellular communication pathways between male and female tissues. This cell-cell communication includes the attraction and reception of the male gametophyte, or pollen tube (PT), by the synergid cells of the female gametophyte, also known as the embryo sac (ES). To achieve reproductive success, it is important to manipulate reproduction at both quality and quantity levels. In other words, flowering plants can only produce as many seeds as they produce ovules and these ovules must be able to be fertilized to make seeds. In *Arabidopsis thaliana*, *NORTIA (NTA)*, a member of the MILDEW RESISTANCE LOCUS O (MLO) family of proteins, plays a critical role in the communication process that regulates PT reception. Upon PT arrival at the filiform apparatus, *NTA* becomes polarly redistributed from the Golgi-associated compartment to the filiform apparatus of the synergid cell, indicating that PT-triggered regulation of the synergid secretory system is important for synergid function during pollination. In the first part of this dissertation, I will describe my research of the female controlled reproductive success at molecular and cell biology level with a focus on *NTA*. Moreover, the ovules contain the female gametophytes which are fertilized during pollination to initiate seed development. Thus, ovule development is an essential and crucial process during plant growth. More importantly, the number of ovules will limit the quantity of reproductive success. However, the major regulators are still poorly understood. The remaining chapters of my dissertation describe the identification of key components that affect the number of ovules during plant development by using natural variation in *Arabidopsis thaliana* and the correlations of ovule number with flowering time. Discovering new ovule number regulators could provide new tools for improving the agricultural productivity.

CHAPTER 1.   INTRODUCTION

1.1   Sexual reproduction in flowering plants

Unlike animals, land plants are non-motile, a feature which limits their dispersal and ability to outcross. Thus, how plants use various strategies to achieve successful sexual reproduction is an essential and important question to understand. Flowering plants, also known as Angiosperms, are the most abundant phylum in the plant kingdom. The Angiosperms are estimated to have 250,000-400,000 species, which can date back to about 150 million years ago (Fernandez-Mazuecos and Glover, 2017). Angiosperms undergo different phases of life cycles that alternate between a diploid (2n) sporophyte generation and a haploid (n) gametophyte generation (Hofmeister and Currey, 1862; Eames, 1961). The sporophyte period of the plants is the main phase among the overall life cycle (Mulcahy, 1979; Gifford et al., 1989; Ratcliffe et al., 1998). Typical Angiosperm flowers contain the same basic morphology with concentric whorls of sepals, petals, stamens, and carpels (Ross, 1985) (Figure 1.1 and 1.2). The sepals and petals protect the inner whorls of reproductive tissues and petals can also attract pollinators and provide space for them to land on the flower. The stamens consist of the anther and filament. Anthers generate haploid microspores that develop into the male gametophyte pollen grains. The innermost whorl is made up of the carpels, which provide a house for ovules. During ovule development, a sporophytic cell is specified as the megaspore mother cell which undergoes meiosis and develops into the female gametophyte, also known as the embryo sac (ES) (Mackiewicz, 1970; Iwanami, 1984; Yadegari and Drews, 2004) (Figure 1.1D-E and 1.2). The most common type of embryo sac contains seven cells and eight nuclei: two haploid synergid cells, one haploid egg cell, one diploid central cell, and three haploid antipodal cells (Maheshwari, 1950) (Figure 1.2).

In order to achieve reproductive success, pollen must be transported from the anther to the stigma. This can occur via pollinators such as wind, animals or self-pollination. After the pollen interacts with the stigma, pollen tubes grow by tip growth to transport the sperm to the ovules. It is crucial that a species be able to recognize and accept pollen from relatively closely related individuals and reject pollen that is too evolutionarily distant. Pollen-pistil interaction is an integral process in the reproductive biology of flowering plants. In recent years, pollen-pistil interactions have been studied at both the molecular and cellular level. The journey of pollination and fertilization in flowering plants can be divided into five phases (Dresselhaus and Franklin-Tong, 2013). In the first phase, the male gametophyte (pollen) lands on a compatible stigma, hydrates and germinates to grow the pollen tube. During phase 2, the pollen tubes grow through the style and transmitting tract, where a nutrient-rich extracellular matrix (ECM) supports the pollen tubes' tip growth. The style and transmitting tract tissue also enable the pollen tubes to be competent to perceive guidance signals from the female gametophyte (Higashiyama et al., 1998; Palanivelu and Preuss, 2006). Phase 3 begins when the pollen tubes leave the transmitting tract and are attracted by ovules. Synergid cells, part of the female gametophyte (embryo sac), secrete signals to attract pollen tube from the transmitting tract to complete successful double fertilization, which is the last phase of this journey (Kessler and Grossniklaus, 2011) (Escobar-Restrepo et al., 2007; Okuda et al., 2009; Kessler et al., 2010; Dresselhaus and Franklin-Tong, 2013; Lindner et al., 2015; Liu et al., 2016). In *Arabidopsis*, pollen tubes interact with different pistil cell types like stigma, style, transmitting tract, septum, funiculus, integument, and synergid cells before reaching their final destination (Palanivelu and Tsukamoto, 2012). After the pollen tube discharges the two sperms into the embryo sac, one sperm fuses with egg cell to form the zygote, while another one fuses with central cell to form the endosperm. This entire process is called double fertilization (Russell, 1992).

1.2   Synergid cells of the female gametophyte

The female gametophyte (embryo sac) initiates from the megasporocyte, which undergoes megasporogenesis and megagametogenesis (Maheshwari, 1950) (Figure 1.2). In angiosperms, multiple patterns of this female gametophyte development have been described The most common one is the Polygonum-type, which occurs in the Brassicaceae, Solanaceae, Gramineae, and other groups (Maheshwari, 1950; Yadegari and Drews, 2004), van Went 1984, Huang and Russell 1992). For instance, in the model plant *Arabidopsis thaliana*, the megaspore mother cell (MMC) goes through two rounds of meiosis and generates four megaspores. Three of them will die, and only the chalazal-most one will survive, which differentiates into the functional megaspore. Subsequently, the functional megaspore undergoes three rounds of mitosis, and cellularizes to become the seven-celled female gametophyte within the ovule (Willemse and Van Went, 1984; Huang and Russell, 1992). Among those cells, three antipodal cells always locate at chalazal end of ovule, one central cell with a large vacuole occupies most of the space within the embryo sac, and two synergid cells always sit side by side with egg cell at micropylar end of ovule (Maheshwari, 1950).

Although most of those specialized cells are very important for reproductive success, the synergid cells are the most essential cells for pollen tube attraction and reception. Normally, there are two synergid cells within an embryo sac and no differences have been found to differentiate the two from each other before pollination. A typical synergid cell contains a large vacuole, a nucleus, and the cytoplasmic complex with various organelles in their distinct distribution pattern (Jensen, 1965; Jones et al., 2018). The attraction signals for guidance of pollen tube to embryo sac were firstly identified in the synergid cells from *Torenia fournieri* (Higashiyama et al., 2001). When two

synergid cells were ablated by laser, pollen tube attraction was disrupted, however, when the other cells were ablated, there was no effect on pollen tube guidance (Higashiyama et al., 2001). This suggests that synergid cells are very important to guide and initiate fertilization, acting like the "gate-keepers" to open the door of double fertilization. Moreover, LUREs, cysteine-rich polypeptides (CRPs) that are secreted from synergid cells, have been found to be the attractants to guide pollen tubes (Okuda et al., 2009; Takeuchi and Higashiyama, 2012). A recent study showed that novel cysteine-rich XIUQIU peptides are non-species specific attractants from synergid cells which guide pollen tube attraction to ovules (Zhong et al., 2019). The synergids also act to prevent polytubey, or the attraction of multiple pollen tubes. Once the first pollen tube enters the synergid cell and release the sperm cells, the other pollen tubes are prohibited from entering or are not attracted (Beale et al., 2012; Kasahara et al., 2012). There is another special structure within the female gametophyte called the filiform apparatus (FA), which is a highly invaginated cell membrane of synergids (Gunning and Pate, 1969). Many important ligands and receptor-like kinases are located at the filiform apparatus region. More interestingly, pollen tubes will cease their growth for a short time period when they arrive at the filiform apparatus region of synergid cells (Palanivelu and Preuss, 2006). However, the reason why this short stop happens, and the precise communication between the pollen tube and the synergid cells are still not clear. Furthermore, more detailed structure and function of filiform apparatus still needs to be explored.

Another interesting topic of synergid cells is the initiation of synergid cell degeneration. Several studies report that synergid cell death is required for pollen tube entry to the receptive synergid cell and release of the two sperm cells (Faure et al., 2002; Punwani and Drews, 2008). However, other studies showed that the synergid degeneration accompanies successful pollen tube discharge

(Leydon et al., 2015). Moreover, the degeneration of the persistent synergid cell has been reported to initiate from fertilization (Volz et al., 2013). In our live imaging study, we found that both the receptive synergid cell and persistent synergid cell stayed alive after pollen tube entry into the synergid cell. Synergid cell death followed pollen tube rupture. However, the detailed timeline of synergid cell death initiation and termination and the relationship between the receptive synergid cell death and persistent synergid cell death still needs to be identified.

Taken all together, synergid cells are unique and important cells for the female and male gametophytes to perceive each other through various molecular signaling events. In other words, they are the both attractors and acceptors during pollen tube reception (Higashiyama, 2002). Although the synergid cells will degenerate after completing its function, they are very important and essential during successful pollen tube reception for double fertilization to occur during most of the angiosperm reproduction.

1.3　　Multiply signals are involved in female-male gametophyte communications

Several molecular players such as signaling peptides and small protein ligands have been identified to participate in pollen tube reception from both male and female side (Beale and Johnson, 2013; Johnson et al., 2019). As for the male gametophyte in Arabidopsis, MYB transcription factors (MYB97, MYB101, and MYB120) are induced during growth through the transmitting tract (Qin et al., 2009). Triple *myb* mutants have 70% of ovules with a pollen tube overgrowth phenotype in which pollen tubes are attracted to ovules but continue growing instead of bursting to release the sperm cells (Leydon et al., 2013; Liang et al., 2013; Leydon et al., 2017). Another discovery was reported in which the AUTOINHIBITED Ca^{2+} ATPASE 9 (ACA9), encoding a Ca^{2+} efflux pump, is also involved in pollen tube discharge during pollen tube reception (Schiott et al., 2004). These

results indicate that all three MYB transcription factors and ACA9 are important for successful pollen tube rupture. At the same time, it is also very important to maintain the integrity of pollen tube during tip growth through the reproductive tract, which has been found to be regulated by receptor-like kinases such as ANXUR1 and 2 (ANX1 and ANX2), and BUDDHA'S PAPER SEAL 1 and 2 (BUPS1 and BUPS2) (Ge et al., 2017; Zhu et al., 2018). These receptor-like kinases bind RALF ligands during growth to maintain tip integrity. Upon arrival at the synergids, these two pairs of receptor-like kinases are thought to bind other RALF ligands secreted from the ovule, such as RALF34, leading to disruption of tip integrity and pollen tube discharge (Ge et al., 2017; Johnson et al., 2019). However, the more detailed mechanisms of these networks still need to be explored. On the other hand, a group of synergid-expressed genes have been identified to regulate pollen tube reception. The first discovery of female controlled pollen tube reception was a gene called SIRÈNE (SRN) (Rotman et al., 2003). In *srn* embryo sacs, pollen tubes do not deliver their sperm cells, which causes failure of double fertilization (Rotman et al., 2003). Later analysis of FERONIA (FER), revealed that is allelic to SIRÈNE, and encodes a receptor-like kinase (Huck et al., 2003; Escobar-Restrepo et al., 2007). FER accumulates in synergids at a plasma membrane region called the filiform apparatus. In *fer* mutants, instead of pollen tube discharging, pollen tubes will continue to grow within synergid cells of the embryo sac, leading to only half of the ovules developing into seeds (Huck et al., 2003; Escobar-Restrepo et al., 2007). Similarly, several synergid-expressed genes like NORTIA (NTA), LORELEI (LRE), EVAN (EVN), TURAN (TUN), SCYLLA (SYL) and EARLY NODULIN-LIKE PROTEINS (ENs) have been found to regulate pollen tube reception, and their loss-of-function mutants lead to pollen tube overgrowth and failure of pollen tube rupture similar to the phenotype seen in *fer* mutants (Capron et al., 2008;

Kessler et al., 2010; Tsukamoto et al., 2010; Lindner et al., 2015; Hou et al., 2016). Detailed

mechanisms and collaborations of those proteins will be discussed in the following sections.

Other than those genes identified to regulate pollen tube reception in both the male and female

gametophytes, some other remarkable signaling changes like Ca^{2+} oscillations and reactive oxygen

species (ROS) accumulations also occur during pollen tube reception. For instance, $[Ca^{2+}]_{cyt}$ will

significantly increase in both the pollen tube tip and the micropylar end of two synergid cells when

the pollen tube is approaching. These oscillations may define the initiation of pollen tube reception,

followed by another $[Ca^{2+}]_{cyt}$ spike that occurs as the PT bursts and synergid degenerates (Iwano

et al., 2012; Denninger et al., 2014; Hamamura et al., 2014). Furthermore, changes of $[Ca^{2+}]_{cyt}$ also

regulate the delivery of sperm cells during pollen tube reception. The Ca^{2+} oscillations in the

synergids are mediated by the FER/LRE signaling pathway (Ngo et al., 2014). ROS has also been

reported to play a role in mediating pollen tube rupture (Duan et al., 2014). High levels of ROS at

the filiform apparatus region of synergid cells are correlated with pollen tube rupture and delivery

of sperm cells (Duan et al., 2014). Interestingly, ROS accumulation in synergid cells is also

regulated by the FER/LRE signaling pathways (Duan et al., 2014; Ngo et al., 2014). Together, the

components and signaling molecules work together in both the male and female gametophyte to

achieve successful pollen tube reception and double fertilization.

1.4   NORTIA MLO protein and the related networks mediating pollen tube reception

In *Arabidopsis thaliana*, only a handful synergid-expressed genes have been reported to regulate

pollen tube reception. *NORTIA (NTA)* is the one of those important genes that is involved in

regulating the pollen tube reception process (Kessler et al., 2010). NTA, or AtMLO7, is a member

of plant specific Mildew resistance locus O (MLO) family of proteins, which was originally

described in barley (*Hordeum vulgare L.*) (Buschges et al., 1997). There are fifteen members in the MLO family in Arabidopsis, and they are predicted to have a signal peptide, seven transmembrane domains, and a calmodulin-binding domain in its C terminal tail (Consonni et al., 2006; Acevedo-Garcia et al., 2014) (Figure 1.3). Different MLO members have been proposed to be involved in various pathways in the plant. The earliest identification of an MLO gene was described in barley leaf cell death and pathogen defense (Buschges et al., 1997). In homozygous barley *mlo* mutants, the plants show resistance to powdery mildew fungus, *Blumeria graminis* f.sp. *hordei* (Buschges et al., 1997). In Arabidopsis, the triple mutant *Atmlo2 Atmlo6 Atmlo12* is fully resistant to the powdery mildew species *Golovinomyces orontii* and *Golovinomyces cicboracearum* , where fungal penetration is terminated at the stage of host cell entry (Consonni et al., 2006; Acevedo-Garcia et al., 2014). Furthermore, MLOs also play a role in leaf spot disease resistance, which result in the decrease in grain yield (Schwarzbach E., 1976) (Acevedo-Garcia et al., 2014).

MLO genes have been proposed to be involved in regulating other pathways as well. For instance, AtMLO4 and AtMLO11 have functions in root thignomorphogenesis, and the single mutant of *Atmlo4* and *Atmlo11*, as well as the double mutants of *Atmlo4 Atmlo11* display a dwarf and curling root phenotype, compared to wild type seedlings with normal elongated roots (Chen et al., 2009). However, the mutant of ATMLO14, which is in the same clade with AtMLO4 and AtMLO11, does not have any phenotype during root development, suggesting the closest related genes do not necessarily have similar function (Acevedo-Garcia et al., 2014). Moreover, AtMLO5 and AtMLO9 are predicted to be expressed in pollen. These MLOs may have some function in maintaining pollen tube growth (Moriyama et al., 2006).

As for sexual reproduction, one of the MLO genes, *NTA*, or AtMLO7, was reported that has functions in regulating pollen tube reception (Kessler et al., 2010). *NTA* is a member of clade III, and is most closely related to AtMLO8 and AtMLO10 (Kessler et al., 2010; Jones et al., 2017). *NTA* is expressed in ovules, specifically in the synergid cells of the female gametophyte (Kessler et al., 2010). In a *nta-1* mutant, around 30% of ovules fails to fertilize. In those infertile ovules, instead of the pollen tube entering the female gametophyte and bursting, the pollen tubes continue growing within the receptive synergid cell, which is referred to as a pollen tube overgrowth phenotype. Mutants in AtMLO8 and AtMLO10 do not have the pollen tube overgrowth phenotype (Kessler et al., 2010). Most interestingly, before pollen tube arrival, NTA protein is contained in Golgi compartments throughout the whole synergid cells, and as the pollen tubes approaching, NTA redistributes to the filiform apparatus region (Jones et al., 2017). However, the timing and significance of this redistribution remains unclear. In chapter 2 of this dissertation, I will discuss my experiment, which addresses to identify the timing and significance of this redistribution using a semi-*in vivo* pollen tube guidance assay. Moreover, NTA did not re-localize to the filiform apparatus in *fer* mutant ovules, suggesting the redistribution of NTA is dependent on FER signaling pathways (Kessler et al., 2010). The mechanism of this pollen tube reception network is still not very clear. LORELEI (LRE), a putative glycosylphosphatidylinositol (GPI)-anchored membrane protein, also localizes at filiform apparatus of synergid cells (Capron et al., 2008; Tsukamoto et al., 2010). *lre* is also a female gametophyte mutant which has unfertilized ovules due to pollen tube overgrowth. A recent study revealed that the LRE collaborates with FER by assisting it transport from the endoplasmic reticulum (ER) to the filiform apparatus (Li et al., 2015). LRE also binds FER may act as co-receptor. LRE protein expressed from PT can complement *lre* phenotype (Tsukamoto et al., 2010; Liu et al., 2016). In all, the networking for regulating pollen

tube reception maybe consist of synergid expressed genes, and the major identified contributors are FER, LRE and NTA. Before PT arrival, LRE accompanies FER and moves from ER to filiform apparatus to perceive the signal of pollen tubes (Li et al., 2015). After a pollen tube gets close to the synergid cells, FER somehow delivers a signal to NTA, resulting in NTA re-localization to the filiform apparatus where it is predicted to have a function in PT reception. However, more detailed information such as the identity of the signals, how those proteins deliver and perceive the signals, their function at the filiform apparatus, and the reason for NTA re-localization to the filiform apparatus still remain to be discovered. Furthermore, if the other synergid-expressed genes such as EVN, TUN, SYL and ENs are also involved in this regulation system, or whether there are some novel distinct system for regulating the pollen tube reception still needs to be explored.

1.5   The number of ovules and the reproductive success

In order to achieve reproductive success, only manipulating the successful cell-to-cell communication is not enough. There are thousands of pollen grains within one flower. However, the number of ovules in the pistil limits the number of seeds that can be produced. Therefore, it is of agronomic interest to increase the number of ovules within a flower.

During plant reproduction, the ovules contain the female gametophytes, which are fertilized during pollination to initiate seed development. Thus, ovule development is crucial process during plant growth to ensure successful creation of progeny which can carry on the plant's genetic information. In *Arabidopsis*, ovule development can be summarized in a few main steps. First, a tissue called carpel margin meristem (CMM) will specialize into different functional regions known as the placenta, the septum, and transmitting tract. Once the placenta is created, the following step is the formation of the ovule primordia with appropriate divisions (Robinson-Beers et al., 1992).

Subsequently, the primordium will be organized in three different regions, which are the funiculus, the chalaza and the nucellus. And finally the mature haploid embryo sac is formed within the nucellus (Webb and Gunning, 1990; Cucinotta et al., 2014)(Figure 1.4).

In the last decades, only a few molecular components have been identified that affect ovule development. Among these are genes that are involved in carpel margin meristem formation, auxin gradients, ovule identity establishment, and ovule primordia initiation. For example, a transcription factor called AINTEGUMENTA (ANT) has a profound effect on ovule development and the *aintegumenta (ant)* mutant displays defects in integuments or even fail to form a female gametophyte (Klucher et al., 1996). The double mutant *lug-3 ant-9* did not form any ovules (Liu et al., 2000). ANT also interacts synergistically with SEUSS (SEU), while the double mutant *seu-3 ant-1* results in a complete loss of ovule initiation (Azhakanandam et al., 2008). CUP-SHAPED COTYLEDON1 (CUC1), CUC2 as well as SPATULA (SPT) are together required for ovule development. *spt cuc1* and *spt cuc2* present reduced ovule number (Nahar et al., 2012; Galbiati et al., 2013). Moreover, Brassinosteroid (BR) signal was also demonstrated to be involved in ovule initiation and development. BR-induced transcription factor BZR1 regulates HLL, ANT, and AP2, and the mutants display lower seed numbers and smaller seed size (Huang et al., 2013). qSS.C9 is a positive regulator of functional ovules per silique and encodes BnaC9.SMG7b which is a predicted small protein that plays a role in regulating the formation of a functional female gametophyte, thus determining the formation of mature ovules in *B. napus* (Li et al., 2015). More recently, a study also shows the regulators in other species. The miR157/SPL axis can affect ovule production and over-expression of the GhmiRNA157 precursor resulted in fewer ovules as well as

reduced seed production due to suppression of cell proliferation and cell elongation in cotton (*Gossypium hirsutum*) (Liu et al., 2017).

Although researchers have demonstrated that these genes play a role in ovule development, the major regulators that affect ovule number during plant development are still largely unknown. In the third chapter of this dissertation, I will describe my experiment which has identified a novel regulator of ovule number and fertility using a genome wide association study. I took advantage of *Arabidopsis* accessions that are naturally inbred lines and aim to identify the key components that are involved in ovule development. I also found the ovule number has a negative correlation of the flowering time, which could be helpful to manipulate the agricultural productivity. The discovery of new ovule number regulators could provide new tools for increasing crop yield.

1.6   Overview of this dissertation

The overall goal for this dissertation is to explore the female control of reproductive success. In chapter 2, I utilized multiple cell biology tools to explore the cell-to-cell communication during pollen tube reception. I took advantage of a semi *in-vivo* pollen tube guidance assay to examine NTA protein localization and its behavior during pollen tube arrival at the ovule. I found that the redistribution of NTA may function to facilitate PT rupture during fertilization. Then I described the female controlled of the reproductive success from the quantity level in chapter 3. I used both cell biology and bioinformatics methods to identify the regulators that affect the number of ovules within a flower. In chapter 4, I explored correlations between the number of ovules and flowering time, as well as some other reproductive traits. Since the female gametophyte plays an essential and important role during the reproductive growth phase, it is important to understand reproductive mechanisms for being able to manipulate them for agricultural benefits.

1.7   Figures
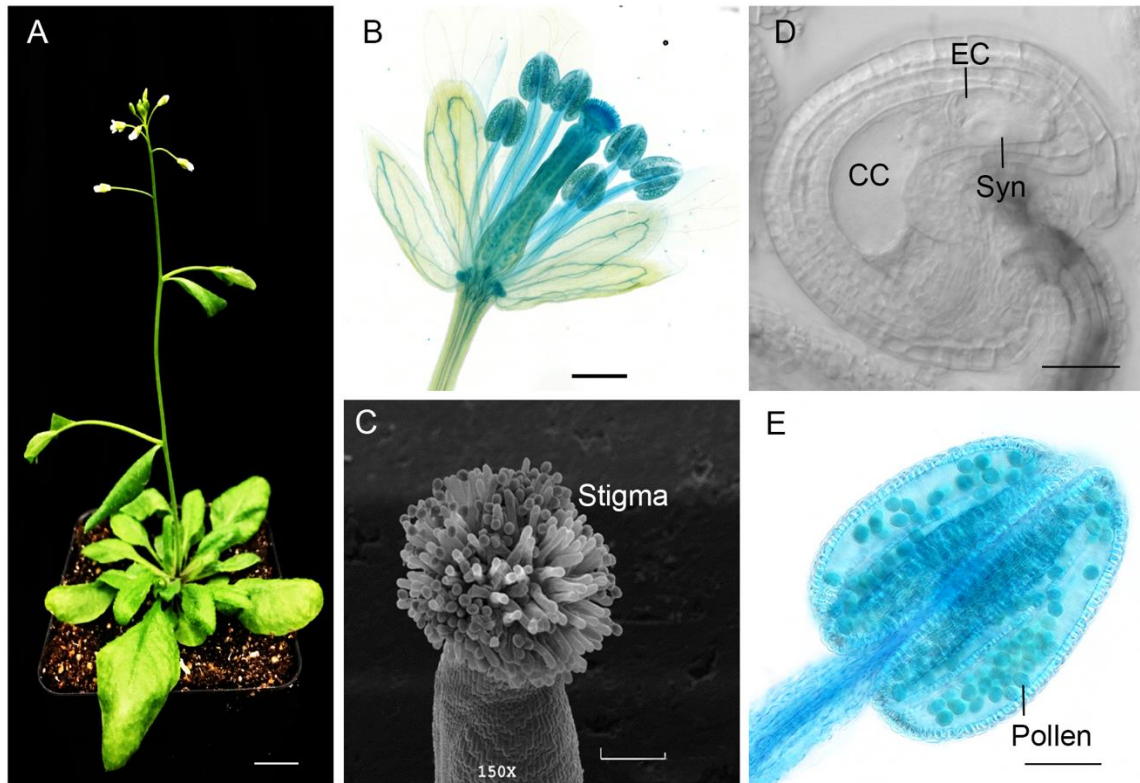
Figure 1.1 The reproductive tissues in flowering plants.

(A) A photo of typical Arabidopsis plant at four weeks after germination. (B) A GUS stained Arabidopsis flower. (C) A scanning electron microscope image of Arabidopsis stigma. (D) A DIC image of unpollinated ovule. CC: Central Cell, EC: Egg Cell, Syn: Synergid cell. (E) A GUS stained Arabidopsis anther with pollen grains. Bars = 3cm(A), 500μm (B), 200μm (C), 30μm (D), 100μm (E).
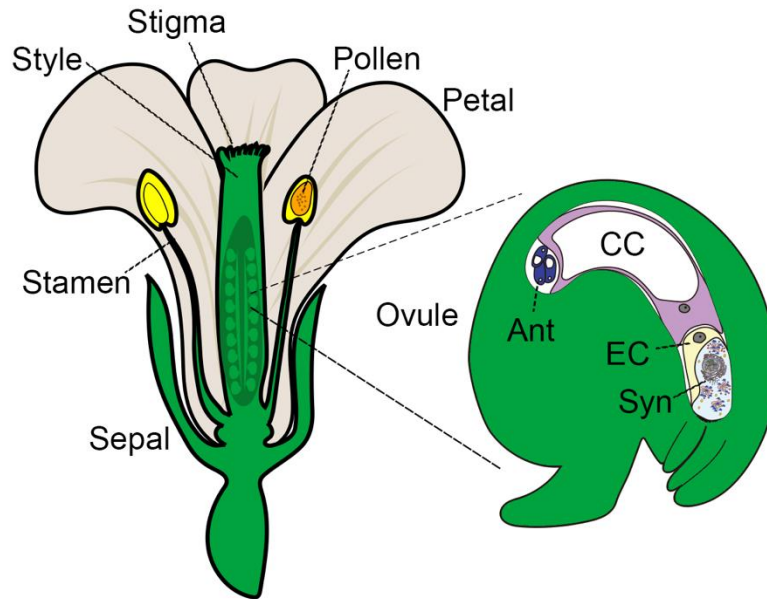
Figure 1.2 Diagram of flower and the female gametophyte in *Arabidopsis thaliana*.

A typical mature flower contains Petals, Sepals, male gametophyte (pollen) in stamen, as well as female gametophyte (embryo sac) in pistil. Ant: Antipodal cell, CC: Central Cell, EC: Egg Cell, Syn: Synergid cell.
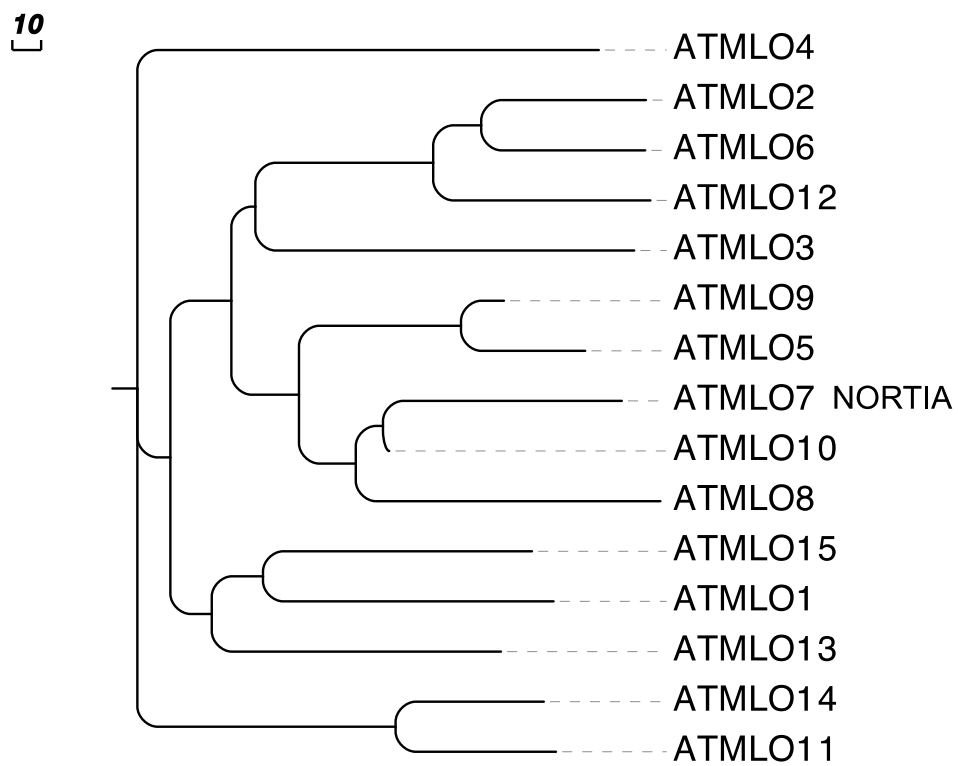
Figure 1.3 The phylogenetic tree of the MLO gene family.

The protein sequences were alignment by MUSCLE program; the Neighbor-Join tree was generated by MEGA7 software.
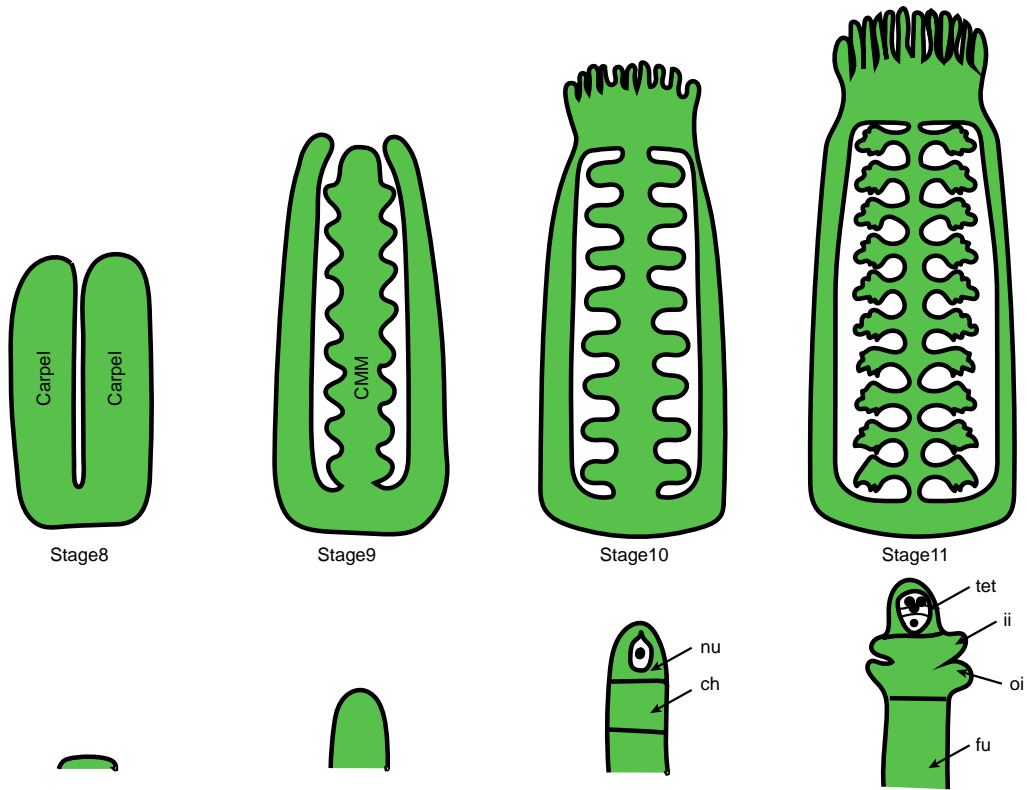
Figure 1.4 Ovule initiation and development in Arabidopsis thaliana.

From stage 9, the ovules start to initiate from carpel margin meristem (CMM). nu, nucellus; ch, chalaza; tet, tetrad; ii, inner integument; oi, outer integument; fu, funiculus.

CHAPTER 2. REDISTRIBUTION OF NORTIA IN RESPONSE TO POLLEN TUBE ARRIVAL FACILITATES FERTILIZATION IN *ARABIDOPSIS THALIANA*

Jing Yuan, Yan Ju, Daniel S. Jones, Weiwei Zhang, Noel Lucca, Christopher J. Staiger, and Sharon A. Kessler
doi: https://doi.org/10.1101/621599

Data Contributions

Daniel Jones made the MLO1 swaps constructs, and Yan Ju analyzed them for figure 2.7 and 2.11.

Daniel Jones and Patrick Day generated the CaMBD and NTA[Cterm] data for figure 2.8 and 2.9.

2.1 Abstract

During gamete delivery in Arabidopsis thaliana, intercellular communication between the attracted pollen tube and the receptive synergid cell leads to subcellular events in both cells culminating in the rupture of the tip-growing pollen tube and release of the sperm cells to achieve double fertilization. Live imaging of pollen tube reception revealed dynamic subcellular changes that occur in the female synergid cells. Pollen tube arrival triggers the trafficking of NORTIA (NTA) MLO protein from Golgi-associated compartments and the accumulation of endosomes at or near the synergid filiform apparatus, a region of highly invaginated membrane that acts as the site of communication between the pollen tube and synergid cells. Domain swaps and site-directed mutagenesis suggest that NTA's C-terminal cytoplasmic tail with its calmodulin-binding domain regulates NTA movement and function in pollen tube reception. Signal-mediated trafficking of NTA to the filiform apparatus upon pollen tube arrival may function to facilitate intercellular communication that leads to pollen tube rupture.

2.2   Introduction

Intercellular communication is central to the proper development and maintenance of all multicellular organisms. During this communication, signals from one cell are perceived by receptors in another cell and translated into various subcellular responses. These include signal transduction cascades leading to transcription of other genes, calcium signaling, and trafficking of proteins to different organelles or regions of the cell. A well-studied example of signal-induced protein trafficking in plant development is the redistribution of the PIN polar auxin transporters to different sides of the cell during important developmental events such as embryo patterning, leaf initiation and lateral root initiation (Petrasek et al., 2006; Naramoto, 2017; Salanenka et al., 2018). In plants, most intercellular communication occurs between cells that are genetically identical and connected by adjoining cell walls. One exception is pollination, in which pollen (the male gametophyte) is released from an anther, transported to a receptive stigma, and produces a tip-growing pollen tube that grows through the female tissues of the pistil and delivers the two sperm cells to the female gametophyte (also known as the embryo sac, Figure 2.1A). The pollen tube's journey through the pistil requires cell-to-cell interactions with the female that allows water and nutrient uptake and enables the detection of cues important for guidance toward the female gametes (Johnson et al., 2019).

In the model plant *Arabidopsis thaliana*, complex signaling events ranging from pollen landing on the stigma to fusion of gametes occur over several hours. Most of our knowledge about the signaling pathways involved along the pollen tube's journey through the female is limited to the final stages of pollination and involve a highly specialized pair of female gametophyte cells known as synergids. During female gametophyte development, meiosis followed by three rounds of

mitosis produce the egg cell and central cell along with 2 synergid cells flanking the egg cell and 3 antipodal cells on the chalazal end of the embryo sac (Drews and Yadegari, 2002), Figure 2.1A). The synergid cells are accessory cells that control the behavior of the pollen tube during the final stages of pollination. Before pollen tube arrival, they secrete cysteine-rich LURE peptides that act as short-range pollen tube attractants that are recognized by receptor-like kinases in the tip of the pollen tube to regulate the direction of pollen tube growth and guide the pollen tube to the micropyle of the ovule (Okuda et al., 2009; Takeuchi and Higashiyama, 2016; Wang et al., 2016). After pollen tube arrival, the synergids communicate with the pollen tube to induce changes that result in pollen tube rupture and delivery of the sperm cells (Kessler and Grossniklaus, 2011; Johnson et al., 2019). Thus, synergids are critical for ensuring that double fertilization can occur to produce seeds.

In Arabidopsis, live imaging has been used to examine the behavior of both the pollen tube and the synergids during the process of pollen tube reception. A pollen tube follows the gradient of LURE attractants, enters the micropyle of the ovule, and pauses its growth for 30 min to 1 h just outside the receptive synergid (Iwano et al., 2012; Denninger et al., 2014; Ngo et al., 2014). During this pause in pollen tube growth, communication occurs between the pollen tube and the synergids that leads to subcellular changes and ultimately to the death of both the pollen tube and the receptive synergid. Cytoplasmic calcium ($[Ca^{2+}]_{cyto}$) oscillations occur in both the tip of the pollen tube and in the 2 synergid cells during this communication phase. $[Ca^{2+}]_{cyto}$ levels continue to increase in both cell types until the pollen tube starts to grow again and bursts to release the sperm cells, a catastrophic event for both the pollen tube and the receptive synergid, which also degenerates (Iwano et al., 2012; Denninger et al., 2014; Ngo et al., 2014). Mutations in genes that

regulate communication between the synergids and pollen tube during pollen tube reception result in a pollen tube overgrowth phenotype in which the pollen tubes are attracted normally to the ovules, but do not get the signal to burst and release the sperm cells. Presumably, synergid-induced changes in the cell wall of the pollen tube tip do not occur in these mutants, therefore the pollen tube continues to grow and coil inside the embryo sac. Synergid-expressed genes that participate in pollen tube reception include the FERONIA (FER) receptor-like kinase, the GPI-anchored protein LORELEI (LRE), and the Mildew Resistance Locus-O (MLO) protein NORTIA (NTA, also known as AtMLO7) (Escobar-Restrepo et al., 2007; Capron et al., 2008; Kessler et al., 2010; Ngo et al., 2014; Li et al., 2015; Liu et al., 2016). Mutations in all of these genes lead to the pollen tube overgrowth phenotype due to disruption of the pollen tube-synergid communication pathway.

FER and LRE are necessary for the calcium oscillations that occur in synergids in response to pollen tube arrival (Ngo et al., 2014). In contrast, *nta-1* mutants have $[Ca^{2+}]_{cyto}$ oscillations at lower amplitudes, indicating that NTA may participate in modulating Ca^{2+} fluxes in the synergids during communication with the pollen tube and likely acts downstream of FER and LRE (Ngo et al., 2014). Like all members of the MLO gene family, NTA has seven membrane-spanning domains and a predicted calmodulin-binding domain (CaMBD) in its C-terminal intracellular tail (Devoto et al., 2003; Kusch et al., 2016). Calmodulin (CaM) is a small protein that binds Ca^{2+} and is involved in signal transduction for many cellular processes (Yang and Poovaiah, 2003). We previously showed that the C-terminal domain of NTA is necessary and sufficient for MLO function in pollen tube reception (Jones et al., 2017), but the significance of the CaMBD in pollen tube reception remains an open question.

The subcellular localization of these important pollen tube reception proteins is not always predictive of their function in communicating with the pollen tube. As expected for early response proteins, both FER and LRE are expressed in synergid cells where they localize in or near a specialized region called the filiform apparatus, a membrane rich area located at the micropyle end of the synergids (Huck et al., 2003; Rotman et al., 2003; Escobar-Restrepo et al., 2007; Capron et al., 2008; Li et al., 2015; Lindner et al., 2015; Liu et al., 2016). The filiform apparatus is thought to be important for the secretion of attractant peptides and is the first site of interaction between the pollen tube and synergid cell prior to pollen tube reception (Mansfield et al., 1991; Huang and Russell, 1992; Leshem et al., 2013). In contrast, before pollen tube arrival, NTA is sequestered in a Golgi-associated compartment within the synergid cell and excluded from the filiform apparatus region (Jones et al., 2017). At the end of pollen tube reception, NTA protein is only detected in the region of the filiform apparatus, indicating that this protein changes its subcellular localization during pollen tube reception (Kessler et al., 2010). This suggests that pollen tube-triggered regulation of the synergid secretory system may be a crucial subcellular response to pollen tube arrival and that NTA function may be related to its subcellular distribution; however, the precise timing and significance of NTA's redistribution are still unclear.

In this study, we take advantage of a live-imaging system to further characterize synergid cellular dynamics during pollen tube reception and to determine the timing and significance of the polar redistribution of NTA to the filiform apparatus. To investigate the link between Ca^{2+} and MLO function in pollen tube reception, we assayed the influence of the CaMBD on NTA's function and subcellular distribution through C-terminal truncations and a point mutation disrupting the CaMBD. We show that the polar redistribution of NTA is triggered by the approach of a pollen

tube, is important for pollen tube reception, and is regulated by the CaMBD. While most subcellular compartments remain distributed throughout the synergid cells during pollen tube reception, recycling endosomes respond to pollen tube arrival by accumulating towards the filiform apparatus. Moreover, we show that targeting NTA to the filiform apparatus before pollen tube attraction does not induce synergid cell death.

2.3   Materials and Methods

2.3.1   Plant materials and growth conditions

Arabidopsis thaliana lines expressing NTApro::NTA-GFP, MYB98pro::NTA-GFP, MYB98pro::MLO1-GFP Golgi-associated marker (Man49-mCherry), ER-associated marker (SP-mCherry-HDEL), TGN-associated marker (SYP61-mCherry), peroxisome-associated marker (Peroxisome-mCherry) and recycling endosome-associated marker (mCherry-RabA1g), were generated and described in previous publications (Kessler et al., 2010; Liu et al., 2016; Jones et al., 2017; Jones et al., 2018). Pollen tube marker lines, ACA9::DsRed (Boisson-Dernier et al., 2008) and Lat52::GFP (Palanivelu and Preuss, 2006) were generously provided by Dr. Aurelien Boisson-Dernier and Dr. Ravi Palanivelu. Seeds were sterilized and plated on ½-strength Murashige and Skoog (MS) plates. All plates were sealed and stratified at 4˚C for two days, and then transferred to the growth chamber (long day conditions, 16 h of light and 8 h of dark at 22˚C) for germination and growth. After 5-7 days, seedlings were transplanted to soil. Seeds from transformed lines were sterilized and plated on ½ MS plate with 20 mg/L hygromycin for selection of transgenic seedlings, which were then transplanted to soil and grown in long days.

2.3.2   Live Imaging of Pollination Using a Semi-*in vivo* Pollen Tube Guidance Assay

The semi-*in vivo* system of pollen tube reception was modified from (Palanivelu and Preuss, 2006).

Approximately 150 µL of pollen germination media (5 mM KCl, 1 mM $MgSO_4$, 0.01% (w/v) H_3BO_3, 5 mM $CaCl_2$, 20% sucrose, 1.5% agarose, and adjusted pH to 7.5 with KOH) was poured into a Glass Bottom Culture Petri Dish (MatTek Corporation, P35G-1.0-20-C) and spread out using a pipette. Pistils were emasculated and 2 d later were hand pollinated with ACA9::DsRed or Lat52::GFP pollen and returned to the growth chamber. Approximately 1 h after pollination, pistils were removed from plants and placed on double sided tape on a glass slide. Stigmas were cut using single-sided razor blade and placed on pollen germination media using forceps. 8-10 ovules were arranged around the cut style and the petri dish was returned to the growth chamber. After 4-6 h, pollen tubes grew through the stigma and style and emerged near the ovules. Imaging commenced when the pollen tubes approached ovules. Time-lapse images were acquired at 5 min intervals by spinning disk confocal microscopy using an Andor Revolution XD platform with a Yokogawa CSU-X1-A1 scanner unit mounted on an Olympus IX-83 microscope and a 20X/0.5 NA objective (Olympus). An Andor iXon Ultra 897BV EMCCD camera was used to capture GFP fluorescence (488-nm excitation) and red fluorescent protein (dsRed or mCherry) fluorescence (561-nm excitation).

For each experimental condition, at least 60 ovules were imaged over the time course from pollen tube approaching the ovule to completion of pollen tube reception (pollen tube rupture to release the sperm cells). Neighboring ovules that did not attract pollen tubes were imaged at the same time and served as controls for photoxicity.

2.3.3   Confocal laser scanning microscopy (CLSM)

CLSM to examine MLO variant subcellular localization was performed on ovules dissected 2 d after emasculation. FM4-64 staining was performed according to the protocol described in (Jones et al., 2017). CLSM was done using either a Nikon A1Rsi inverted confocal microscope according to (Yuan and Kessler, 2019) or a Leica SP8 upright confocal microscope according to (Jones et al., 2017).

2.3.4   Quantification of fluorescence signal intensity

Two-channel images were adjusted for brightness and contrast using Fiji (Schindelin et al., 2012). Then, they were input to NIS-Elements software (Ver. 5.02) to measure the fluorescence signal intensity. A line that spanned from the chalazal end to the filiform apparatus end of the synergid was used for the signal intensity measurements. For a more accurate representation of the total area of the synergid, signal intensities were recorded along the same length line at five parallel position within the synergid cell. Finally, all the measurement data were output as Excel files. Graphs and statistical analysis were performed with Prism software (www.graphpad.com).

2.3.5   Video processing

Images were filtered to remove the noise and cropped using Fiji (Version 2.0.0). QuickTime Player (Version 10.5) was used for movie editing and time-lapse analyses.

2.3.6   Cloning and Generation of Transgenic Lines

PCR amplification with PHUSION High-Fidelity Polymerase (NEB, M0535S) or Q5 High-Fidelity DNA Polymerase (NEB, M0419S) were used to generate the following constructs in this study. Genes were amplified with primers that had attB1 and attB2 sites for recombination via BP reaction into the Gateway-compatible entry vector pDONR207. Full-length NTA entry vectors

used in this study was generated as described previously (Jones et al., 2017) . NTA truncations were amplified using NTA full-length entry vector as a template with forward primer NTA-FattB1 and the following reverse primers: NTA450-RattB2 and NTA481-RattB2 (See all primer sequences in Table S1). The NTA^{W458A} point mutation was generated using the same *NTA* template and amplifying two fragments of *NTA* with desired point mutations introduced into the primers: NTA-FattB1 + NTAW458A-R and NTAW458A-F + NTA-RattB2. The two fragments were purified and pasted together with overlaps using a PCR-pasting protocol. The NTA-MLO1^{CTerm} construct was generated using the full-length entry vectors of NTA and MLO1 used in previous study (Jones et al., 2017) as templates and amplifying two fragments of *NTA* and *MLO1* using the two pairs of primers: NTA-FattB1 +NTA-R19 and MLO1-F + MLO1-RattB2. The two fragments were purified and pasted together with overlaps using a PCR-pasting protocol. The coding sequence from both truncations and the point mutation and the fusion sequence were fully sequenced in entry vectors. All entries were then recombined via LR reactions into the pMDC83 backbone with the MYB98$_{pro}$ (Muller et al., 2016) to drive expression of each NTA variant in synergid cells with a C-terminal GFP fusion.

For *nta-1* complementation assay and co-localization analyses, expression vectors were transformed into the *Agrobacterium tumefaciens* strain GV3101 and transformed into the *nta-1* mutant background or the Col-0 background (co-localization – Col-0 was stably expressing the Golgi or TGN synergid secretory markers) via the floral-dip method (Bent, 2006). Stable transgenic lines were selected using their respective selections described above. Homozygous T2 lines were used in *nta-1* complementation assay and co-localization imaging in the synergid was done in a T1 analysis.

2.3.7   *nta-1* Complementation Assays

3-4 independent insertion lines for each construct were taken to the T2 generation and screened for homozygosity using fluorescence microscopy to ensure transgene expression in synergids of every ovule. Unfertilized vs. fertilized ovule counts from self-pollinated flowers were assessed in at least three plants of each insertion line and compared to *nta-1*, Wassilewskija (Ws-2; wildtype), and the previously published full-length NTA (MYB98$_{pro}$::NTA-GFP in *nta-1* background, (Jones et al., 2017). Ovule counts were statistically analyzed using Prism (www.graphpad.com) with significance determined using a Student's *t*-test. Comparisons of the NTA variants were made to full-length NTA and the *nta-1* mutant.

2.4   Results

2.4.1   Time-lapse imaging of NORTIA redistribution using a semi-*in vivo* assay

Pollen tube reception is a complex process that requires the synergid cells to recognize the approaching pollen tube and to send signals back to the pollen tube that result in release of the sperm cells at the correct time and place. We previously showed that the NTA-GFP fusion protein localizes to a Golgi-associated compartment of the synergids before pollen tube attraction (Jones et al., 2017). When imaged after pollen tube reception, NTA-GFP is concentrated at the micropylar end of the synergid (in or near the filiform apparatus) (Kessler et al., 2010). NTA-GFP doesn't accumulate near the filiform apparatus in *fer* ovules with pollen tube overgrowth, suggesting that FER-mediated signaling that occurs during pollen tube reception triggers NTA-GFP redistribution that in turn contributes to the interaction of the synergid with the pollen tube (Kessler et al., 2010). An alternative hypothesis is that pollen tube rupture triggers NTA-GFP redistribution and is a symptom of pollen tube reception rather than an important contributor to the signaling pathway. To distinguish between these two possibilities, we used a semi-*in vivo* pollination system

combined with spinning disk confocal microscopy to determine the timing of NTA-GFP redistribution during the pollen tube reception process. In the semi-*in vivo* system, pollen tubes grow out of a cut style and are attracted to ovules arranged on pollen germination media (Palanivelu and Preuss, 2006). This system has previously been used to quantify and track pollen tube attraction to ovules and to image ($[Ca^{2+}]_{cyto}$ reporters during pollen tube reception (Hamamura et al., 2011; Hamamura et al., 2012; Denninger et al., 2014; Hamamura et al., 2014; Ngo et al., 2014). In order to follow subcellular changes in NTA-GFP protein localization before, during, and after pollen tube arrival, we used pollen from plants expressing the pollen-specific AUTOINHIBITED Ca^{2+-}ATPase9$_{pro}$::DsRed (ACA9$_{pro}$::DsRed) reporter and ovules expressing NTA$_{pro}$::NTA-GFP in the semi-*in vivo* system. Approximately 4 h after pollination, pollen tubes emerged from the style onto the media and were attracted to ovules (Figure 2.1B). Images in the red and green channels were collected every 5 min from when a pollen tube approached an ovule until after the pollen tube ruptured inside the ovule. In our system, most of the ovules displayed successful pollen tube attraction and reception, while others did not attract a pollen tube during the time course of the imaging experiments (Figure 2.1B and Figure 2.2). A second group were imaged under the same conditions and serve as a negative control for environmentally-induced changes in NTA-GFP localization. 83% of the ovules that attracted a pollen tube that successfully burst to deliver the sperm cells (n=93) displayed NTA-GFP redistributed to the micropylar end of the synergid cell (Figure 2.1C-E). Ovules without NTA-GFP redistribution displayed abnormal pollen tube behavior in which pollen tubes were attracted but stopped growing and never ruptured to release the sperm cells. Neighboring ovules that did not attract a pollen tube (n=103) but were imaged under the same semi-*in vivo* conditions did not have redistribution of NTA-GFP (Figure 2.1E), nor did ovules that were incubated on pollen germination media without a pollinated pistil

(n=133, Figure 2.1E). These data suggest that pollen tube arrival is necessary for NTA-GFP redistribution and that the imaging conditions do not trigger redistribution (Figure 2.1E).

Our semi-*in vivo* system also allowed us to determine the timing of NTA-GFP redistribution in relation to the position of the pollen tube as it approached the synergids. We defined the 0 min timepoint as the time where the pollen tube just reached the micropylar opening of the ovule (Figure 2.1C, ovules with yellow stars, Movies S1 and S2). In all cases, NTA-GFP movement also started from this time point. During the following 30–50 min, pollen tubes grew through the micropyle region of ovule and arrived at the filiform apparatus of the receptive synergid cell. During this time, three quarters to half of the NTA-GFP signal moved to the micropylar end of synergid cells, indicating that the approach of the pollen tube triggers NTA-GFP movement. As reported in (Ngo et al., 2014) and (Denninger et al., 2014), the arriving pollen tubes paused their growth outside the filiform apparatus for 30–50 min, presumably for cell-to-cell communication. During this period, NTA-GFP signal continued to move toward the filiform apparatus. The whole movement took around 70–80 min, and after the redistribution completed, pollen tubes resumed growth and ruptured to deliver the sperm cells and complete double fertilization (Figure 2.1C and Movies S1 and S2). Even though only one of the synergids receives the pollen tube, NTA-GFP was actively redistributed to the filiform apparatus in both synergid cells in response to pollen tube arrival, similar to the activation of $[Ca^{2+}]_{cyto}$ oscillations in both synergids during pollen tube reception reported in (Ngo et al., 2014).

2.4.2 The Golgi apparatus does not concentrate at the filiform apparatus during pollen tube reception

We previously determined that NTA is sequestered in a Golgi-associated compartment in synergid cells that have not attracted a pollen tube (Jones et al., 2017) . Our live-imaging data suggests that NTA-GFP is selectively moved out of the Golgi and trafficked to the region of the filiform apparatus in response to pollen tube arrival; however, it is possible that the observed NTA-GFP movement is a result of massive reorganization of subcellular compartments. To distinguish between these possibilities, we investigated the behavior of Golgi in synergid cells during pollen tube reception. We used the semi-*in vivo* imaging system described above with a synergid-expressed Golgi marker (Man49-mCherry) co-expressed with NTA-GFP (Jones et al., 2018). In all replicates, the Golgi marker was distributed throughout the synergids, excluded from the filiform apparatus, and co-localized with NTA-GFP as reported previously (Figure 2.3A). When a pollen tube approached the synergids, NTA-GFP redistributed to the filiform apparatus region of the synergids as observed previously (Figure 2.1), but the Golgi-mCherry marker remained consistently distributed throughout the synergid cells and did not concentrate near the filiform apparatus (Figure 2.3B). In order to examine the behavior of the Golgi during later stages of pollen tube reception, we used the synergid-expressed Golgi marker line (Man49-mCherry) and pollen that was expressing GFP (Lat52$_{pro}$::GFP). In all cases, the Golgi marker remained randomly distributed throughout the synergid cells, even after pollen tube rupture (Figure 2.3C-D, Movies S3 and S4). These results indicate that the movement of NTA-GFP during pollen tube reception is not linked to mass redistribution of the Golgi apparatus.

2.4.3   Distribution of cellular compartments in synergid cells during pollen tube reception

A signal from the arriving pollen tube seems to trigger the movement of NTA-GFP out of the Golgi-associated compartments. It is possible that pollen tube arrival triggers other changes to synergid subcellular organization. We previously reported the localization of synergid-expressed markers for the ER, peroxisome, endosome and the trans-Golgi Network (TGN) in unfertilized ovules *in vivo* using confocal laser scanning microscopy (Jones et al., 2018). Before pollen tube arrival, SP-mCherry-HDEL (an ER-associated marker), mCherry-SKL (a peroxisome-associated marker), and mCherry-RabA1g (a recycling endosome-associated marker) were all distributed evenly throughout synergid cells (Figure 2.4 and 2.5; (Jones et al., 2018). The TGN-associated marker SYP61 exhibited two types of distribution patterns before pollen tube arrival: in type 1 synergids, the marker accumulated near the filiform apparatus, whereas type 2 synergids displayed a punctate distribution pattern throughout the cells (Figure 2.4; (Jones et al., 2018). During pollen tube reception, no change was seen in the TGN marker distribution in either type of synergids (Figure 2.4C-D, Movies S5 and S6). Likewise, the ER and peroxisome markers maintained a diffuse distribution throughout the synergids and did not accumulate at the filiform apparatus region (Figure 2.4A-B and E-F, Movies S7-10). In contrast, we detected a more dynamic behavior of the endosome marker during pollen tube reception. Endosomes are membrane-bound compartments that are involved in the endocytic membrane transport pathway from the plasma membrane to the vacuole. Endosomes also transport molecules from the Golgi and either continue to vacuole or recycle back to the Golgi (Stoorvogel et al., 1991). We previously reported that mCherry-RabA1g is distributed throughout synergid cells and had some overlap with NTA-GFP in synergids of unpollinated ovules (Jones et al., 2018). Using the semi-*in vivo* system, we confirmed that before pollen tube arrival, mCherry-RabA1g distributed throughout synergid cells

(Figure 2.5A). Interestingly, as pollen tubes approached, the endosome marker started to accumulate in the filiform apparatus region of the synergid cells (Figure 2.5A and B). By the time that pollen tube reception was completed, most of the endosome signal was concentrated at or near the filiform apparatus (Figure 2.5B-D and 2.6, Movies S11 and S12). These results indicate that the RabA1g endosome compartments have a distinct response to pollen tube arrival and may play a role in facilitating the intercellular signaling pathway that occurs between the synergids and the pollen tube.

2.4.4   The CaMBD is important for NTA's function in pollen tube reception

The timing of the NTA redistribution during pollen tube arrival is similar to the start of synergid $[Ca^{2+}]_{cyto}$ oscillations that are triggered by the pollen tube in a FER-dependent manner (Iwano et al., 2012; Hamamura et al., 2014; Ngo et al., 2014). MLO proteins have the potential to bind Ca^{2+} through calmodulin binding domains (CaMBD) in their C-terminal cytoplasmic tails following the seventh transmembrane domain (Devoto et al., 1999; Kim et al., 2002; Panstruga, 2005). Like all MLO proteins, NTA has a predicted CaMBD in its C-terminal tail (Figure 2.7A). In *nta-1* mutants, pollen tube-triggered $[Ca^{2+}]_{cyto}$ oscillations occur but at a lower amplitude (Ngo et al., 2014). Domain swaps with MLO8 revealed that the C-terminal tail domain of NTA is necessary and sufficient for MLO-mediated pollen tube reception and important for NTA's subcellular distribution in synergids (Jones et al., 2017). Together, these data suggest that the subcellular distribution of NTA before and during pollen tube reception could be influenced by $[Ca^{2+}]_{cyto}$ levels sensed by the CaMBD. Previous studies have found that CaM-binding activity of the CaMBD influences MLO function in powdery mildew susceptibility (Kim et al., 2002).

We hypothesized that CaM-binding activity is also important for NTA's function during pollen tube reception. To test this, a truncation removing the C-terminal tail including the CaMBD (NTA$^{\Delta 450}$), a point mutation in a conserved tryptophan (NTA^{W458A}) necessary for CaM-binding function in other CaMBDs (Arazi et al., 1995; Yamada et al., 1995; Kim et al., 2002), and a truncation removing the tail immediately following the CaMBD (NTA$^{\Delta 481}$), all fused to GFP, were generated and expressed under the synergid-expressed MYB98 promoter in the *nta-1* background (Figure 2.7). Ovule counts in homozygous lines revealed that all three constructs had significant reductions in unfertilized ovules compared to *nta-1*. However, only NTA$^{\Delta 481}$ rescued at similar levels as full-length NTA (Figure 2.7B), indicating that the C-terminal tail after the CaMBD is dispensable for NTA function. Both NTA$^{\Delta 450}$ and NTA^{W458A} partially rescued *nta-1*, suggesting that either removal or disruption of the CaMBD have a similar impact on NTA's function.

2.4.5   A functional CaMBD facilitates NTA accumulation at the filiform apparatus during pollen tube arrival

Prior to pollen tube arrival, NTA is distributed throughout the entire synergid cell where it is localized primarily within Golgi (Figure 2.7C) (Kessler et al., 2010; Jones et al., 2017). When expressed in synergid cells, related MLO proteins that localize within Golgi can rescue *nta-1* whereas those that localize elsewhere do not function in pollen tube reception (Jones et al., 2017). The partial complementation of *nta-1* by the CaMBD-disrupted variants could be due to disrupted localization patterns before and/or after pollen tube arrival. In virgin ovules, both NTA$^{\Delta 481}$ and NTA^{W458A} were distributed throughout the synergid cell in punctate compartments and were predominantly excluded from the filiform apparatus (Figure 2.7E and F). NTA$^{\Delta 450}$ accumulated in punctate compartments throughout the synergid, but was also detected near the filiform apparatus and in the vacuole (Figure 2.7D). Although the two variants with disrupted CaMBDs (NTA$^{\Delta 450}$

and NTA^{W458A}) both partially rescued the *nta-1* unfertilized ovule phenotype at similar levels, they had different distributions in the synergid cell. This suggests that differences in localization between these two variants may not be functionally relevant to pollen tube reception. Due to this, we focused primarily on NTA^{W458A} for our downstream analyses and comparisons with wildtype NTA so as to not further complicate the interpretation of our results.

With "NTA-like" distribution in the synergid cell, we suspected that the NTA^{W458A} variant would accumulate within Golgi-associated compartments similar to wildtype NTA. NTA^{W458A} was co-expressed with fluorescent markers for Golgi (LRE$_{pro}$::Man49-mCherry, (Liu et al., 2016)) and the TGN (MYB98pro:Syp61-mCherry, (Jones et al., 2017)) in synergid cells and virgin ovules were analyzed via CLSM (Figure 2.8). The NTA^{W458A} variant partially co-localized with the Golgi maker (Figure 2.8A) and had no overlap with the TGN marker (Figure 2.8B), similar to wildtype NTA localization (Jones et al., 2017). These data demonstrate that neither NTA's distribution within the synergid cell, where it is maintained out of the filiform apparatus prior to pollen tube arrival, nor its localization within Golgi-associated compartments are dependent on a functional CaMBD.

During pollen tube reception, NTA is actively redistributed toward the filiform apparatus region. The NTA^{W458A} variant maintains a wildtype distribution and localization pattern in synergids without pollen tubes but does not fully rescue *nta-1*'s unfertilized ovule phenotype. To test whether the CaMBD is important for NTA's redistribution in response to pollen tube arrival, the semi-*in vivo* system described above was used to monitor NTA^{W458A} movement in the *nta-1* background. In this background, the partial rescue by NTA^{W458A} leads to some ovules having normal pollen

tube reception, while others exhibit pollen tube overgrowth and a failure of pollen tube rupture. In the semi-*in vivo* system, NTA^{W458A} ovules that did not attract a pollen tube, maintained distributions outside of the filiform apparatus, consistent with unpollinated flowers above (Figure 2.9A and C). In ovules with successful pollen tube reception, NTA^{W458A} redistributed to the filiform apparatus region, but in many cases this redistribution was not as complete as with the wild-type NTA-GFP protein, with some GFP signal remaining outside the filiform apparatus region (Figure 2.10 and Figure 2.9B and D). In ovules where pollen tube reception was not successful due to pollen tube overgrowth, NTA^{W458A} did not accumulate at the filiform apparatus region of the synergids (Figure 2.10C). These data suggest that an active CaMBD enhances NTA's redistribution to the filiform apparatus region during pollen tube reception and that NTA redistribution is correlated with pollen tube rupture.

2.4.6 Premature distribution of NTA to the filiform apparatus region is not toxic to synergid cells

The selective targeting of NTA-GFP from the Golgi apparatus to the filiform apparatus region of the synergid cells during pollen tube arrival (Figure 2.1-2.3) and the link between NTA^{W458A} redistribution and pollen tube reception (Figure 2.9) suggests that NTA accumulation at the pollen tube/synergid interface is important for the intercellular communication process that occurs between the pollen tube and synergids. In *nta-1* mutants, around 30% of ovules display pollen tube overgrowth and fail to complete double fertilization, but the other 70% are fertilized normally (Kessler et al., 2010). This indicates that NTA is not absolutely required for pollen tube reception, but may function as a modifier of the FER signaling pathway. Since FER signaling in the synergids leads to cell death as pollen tube reception is completed (Huck et al., 2003; Rotman et al., 2003; Escobar-Restrepo et al., 2007), NTA trafficking to the filiform apparatus from could be a

mechanism to regulate this death and would thus require sequestration of "toxic" NTA in the Golgi before pollen tube arrival. In order to test this hypothesis, we took advantage of sequence variation leading to differential subcellular localization of MLO proteins to manipulate the subcellular localization of NTA. When expressed in synergids, other proteins from the Arabidopsis MLO family have different subcellular localization patterns, indicating that specific sequences within the MLOs direct them to different parts of the secretory system (Jones and Kessler, 2017). MLO1-GFP localizes in the filiform apparatus region of the synergids when it is ectopically expressed under control of the synergid-specific MYB98 promoter and cannot complement the *nta-1* pollen tube reception phenotype (Jones et al., 2017), also see Figure 2.11C). Domain swaps between different regions of NTA and MLO1 revealed that the C-terminal cytoplasmic tail including the CaMBD of MLO1 (NTA-MLO1^{CTerm}, see diagram in Figure 2.11B) was sufficient to direct the fusion protein to the filiform apparatus region of the synergids, in a pattern very similar to MLO1-GFP (Figure 2.11A-C). Quantification of the GFP signal along the length of the synergids from the chalazal end to the filiform apparatus in the NTA-GFP, NTA-MLO1^{Cterm}-GFP, and MLO1-GFP confirmed that the MLO1 tail was sufficient to move the NTA protein to the filiform apparatus end of the cell (Figure 2.11D). In all MLO1-GFP and NTA-MLO1^{Cterm}-GFP ovules, the majority of GFP signal was detected in the lower 20-40% of the synergids and most of the signal overlapped with the diffuse FM4-64 staining in the filiform apparatus (Figure 2.11E). In contrast, NTA-GFP is excluded from the filiform apparatus (Figure 2.11A and (Jones et al., 2017).

The successful manipulation of NTA subcellular localization provided a tool for determining the functional relevance of NTA redistribution. We transformed the NTA-MLO1^{CTerm}-GFP construct into *nta-1* plants and used the percentage of unfertilized ovules as a measurement for the ability of

the fusion construct to complement the *nta-1* phenotype of unfertilized ovules caused by pollen tube overgrowth (Kessler et al., 2010).Two independent NTA-MLO1^{CTerm}-GFP insertions were able to rescue the *nta-1* phenotype when expressed in synergids (Figure 2.11F). These data indicate that premature targeting of NTA to the filiform apparatus is not toxic to synergid cells.

2.5   Discussion

2.5.1   Synergids respond to a signal from the approaching pollen tube

Successful pollination and production of seeds requires a series of signaling events between the male gametophyte (pollen tube) and both sporophytic and gametophytic cells of the female. In this study, we used live imaging to characterize dynamic subcellular changes that occur in the synergid cells of the female gametophyte in response to the arrival of the pollen tube. We showed that both the NTA protein and endosomes are actively mobilized to the filiform apparatus region where male-female communication occurs during pollen tube reception (Figure 2.12). Disruption of NTA's CaMBD partially compromised NTA redistribution and function in pollen tube reception, revealing that Ca^{2+} may play a role the synergid response to the signal from the pollen tube.

The polar accumulation of the RabA1g endosome marker near the filiform apparatus during pollen tube reception suggests a change in synergid secretory system behavior that is triggered by the approaching pollen tube. Our results with the ER, Golgi, TGN, and peroxisome markers indicate that the mobilization of the RabA1g endosomes toward the approaching pollen tube is not just a symptom of FER signaling triggering synergid cell death that leads to mass disruption of subcellular compartments. Trans-Golgi Network/Early endosomes (TGN/EEs) have been shown to be involved in the trafficking of both secretory and endocytic cargo (Viotti et al., 2010). RabA1g is present in endosomes that are highly sensitive to Brefeldin A in roots, suggesting that they could

function as recycling endosomes (Geldner et al., 2009). While the resolution of our live imaging system did not allow us to determine whether NTA completely co-localizes with this compartment, it is tempting to speculate that the RabA1g endosomes are mediating the polar movement of NTA to the filiform apparatus region. Alternatively, these endosomes could be transporting other signaling molecules either to or from the filiform apparatus.

2.5.2   Signal-mediated protein trafficking

Signal-mediated regulation of protein trafficking is an elegant mechanism to control the delivery of molecules to the precise location where they are needed for critical signaling events that occur over relatively short time frames. Selective protein targeting similar to NTA movement in response to pollen tube arrival has also been observed during cell-to-cell communication between the egg and sperm cells in Arabidopsis. After pollen tube reception and release of the sperm cells, a signal from the sperm and/or the degenerated synergid cell causes the egg cell to secrete EGG CELL 1 (EC1) peptides that have been stored in punctate compartments in the egg cytoplasm toward the sperm cells. The sperm cells perceive the EC1 signal and, in turn, mobilize the gamete fusogen HAPLESS2/GENERATIVE CELL SPECIFIC1 (HAP2/GCS1) from a cytoplasmic compartment to the cell surface (Sprunck et al., 2012). This controlled movement of proteins that have already been translated and stored allows for a quick response that allows the egg and sperm to become activated for fertilization. Likewise, NTA mobilization to the filiform apparatus region of the synergids as the pollen tube arrives could play a role in sending a signal to the pollen tube that leads to the mobilization of pollen tube proteins that allow the pollen tube to rupture and release the sperm cells. For example, proteins that regulate the integrity of the tip of the pollen tube could be quickly delivered after the "arrival" signal from the synergid is perceived. Recent work on the role of the pollen-expressed ANXUR1 and 2 and BUDDHA PAPER SEAL1 and 2 receptor-like

kinases in pollen tube tip integrity support this hypothesis. During pollen tube growth through the female tissues, RALF4 and RALF19 peptides that are secreted from pollen tubes act as ligands for ANX1/2 and BPS1/2 to promote tip growth, while RALF34 secreted from the synergids displaces RALF4 and 19 from the receptors leading to subcellular changes that result in pollen tube rupture (Ge et al., 2017).

2.5.3   Calcium and NTA movement

Our study revealed that an intact CaMBD facilitates the movement of NTA from the Golgi to the filiform apparatus in response to the stimulus from the approaching pollen tube. This result provides an intriguing link to Ca^{2+} since the polar movement of NTA-GFP to the filiform apparatus region occurs in a similar time frame to $[Ca^{2+}]_{cyto}$ spiking in the synergids during pollen tube reception (Denninger et al., 2014; Ngo et al., 2014). Subcellular Ca^{2+} spiking occurs in plant responses to both biotic and abiotic external stimuli. Notably, Ca^{2+} oscillations occur during pollen tube-synergid interactions, egg-sperm interactions, and in biotrophic interactions between plant cells and both beneficial and harmful microbes (reviewed in (Chen et al., 2015). In most cases, the mechanism for decoding Ca^{2+} spikes into a cellular response is not known, but Ca^{2+}-binding proteins such as calmodulin (CaM) and calmodulin-like proteins could play a role in relaying Ca^{2+} signals (Chin and Means, 2000). In *nta-1* mutants, the $[Ca^{2+}]_{cyto}$ oscillations still occur, but at a lower magnitude than in wild-type synergids, suggesting that NTA could be involved in modulating Ca^{2+} flux (Ngo et al., 2014). The source of Ca^{2+} during these oscillations is not known, but it is possible that NTA regulates Ca^{2+} channels to regulate the flow of Ca^{2+}ions into or out of the apoplast near the filiform apparatus.

Ca^{2+} has also been linked to regulation of endomembrane trafficking (reviewed in (Himschoot et al., 2017). In animals, calmodulin plays a role in regulating vesicle tethering and fusion (Burgoyne and Clague, 2003), and in plants calmodulin-like proteins are associated with endosomal populations (Ruge et al., 2016). Thus, it is possible that the CaMBD in NTA is critical for the precise targeting of NTA in response to pollen tube arrival. Another mechanism that has been proposed for Ca^{2+} regulation of protein targeting is that electrostatic interactions between Ca^{2+} and anionic phospholipids in specific domains of the plasma membrane regulate vesicle fusion and differential recruitment of proteins to these domains (Simon et al., 2016; Platre et al., 2018). The filiform apparatus of the synergids is distinctive from the plasma membrane in other parts of the synergid and likely has a unique phospholipid composition that could play a role in recruiting NTA to this domain. Whether NTA movement is a cause or consequence of $[Ca^{2+}]_{cyto}$ spiking requires more live imaging experiments at a higher time resolution to determine if NTA redistribution happens before or after the initiation of $[Ca^{2+}]_{cyto}$ spiking.

2.5.4 Cell death and pollen tube reception

MLOs were first discovered in barley as powdery mildew resistance genes (Buschges et al., 1997). *mlo* mutants in both monocots and dicots are resistant to powdery mildew infection, indicating that the MLO proteins are required for infection. These mutants also have ectopic cell death, indicating that one function of MLO proteins is to negatively regulate cell death (Panstruga, 2005). Pollen tube reception is catastrophic for both the pollen tube and the receptive synergid cell: both cells die as a result of successful male-female signaling and delivery of the male gametes. The timing of synergid degeneration remains under debate, with some studies suggesting that it occurs upon pollen tube arrival at the synergid and others concluding that it occurs concurrently with pollen tube rupture (Sandaklie-Nikolova et al., 2007; Hamamura et al., 2011). Our live imaging

experiments with both NTA-GFP and the subcellular compartment reporters suggest that the synergid cells are still alive and regulating their secretory systems up to the point of pollen tube rupture. Given the function of the "powdery mildew" members of the MLO gene family in preventing cell death, it is possible that one role of NTA is to prevent early degeneration of the synergids. An interesting parallel between powdery mildew infection and pollen tube reception is that, in both cases, an MLO protein gets redistributed to the site of interaction with a tip-growing cell. In the powdery mildew system, active transport of proteins and lipids to penetration site leads to membrane remodeling and establishment of the extrahaustorial membrane which separates the plant cytoplasm from the invading fungal hyphae (Huckelhoven and Panstruga, 2011). Although the relationship between the arriving pollen tube and the filiform apparatus has not been established, it is possible that similar reorganization occurs in the filiform apparatus during signaling with the pollen tube. In both cases, perhaps an MLO protein is needed in these special membrane regions to stabilize the cell and prevent precocious cell death. Our result that premature delivery of NTA (in the NTA-MLO1^{CTerm} domain swap construct) to the filiform apparatus region of the cell does not disrupt pollen tube reception is consistent with this hypothesis, since other signaling processes occurring in the synergids during communication with the arriving pollen tube would likely not be triggered by simply moving NTA to the filiform apparatus in the absence of a pollen tube.

In this study, we showed that signals from an approaching pollen tube trigger the movement of NTA out of the Golgi and to the region of the filiform apparatus and that this redistribution is correlated with pollen tube reception. However, localization of the NTA-MLO1^{CTerm} fusion protein was able to complement the *nta-1* mutant phenotype, indicating that the final localization of the

NTA protein may be more important than the active trafficking from the Golgi compartment. Future work will focus on determining the mechanism through which NTA becomes polarly redistributed and on identifying the signals from the pollen tube that lead to important subcellular changes in the synergids during pollen tube reception.

2.6   Figures, movies and tables
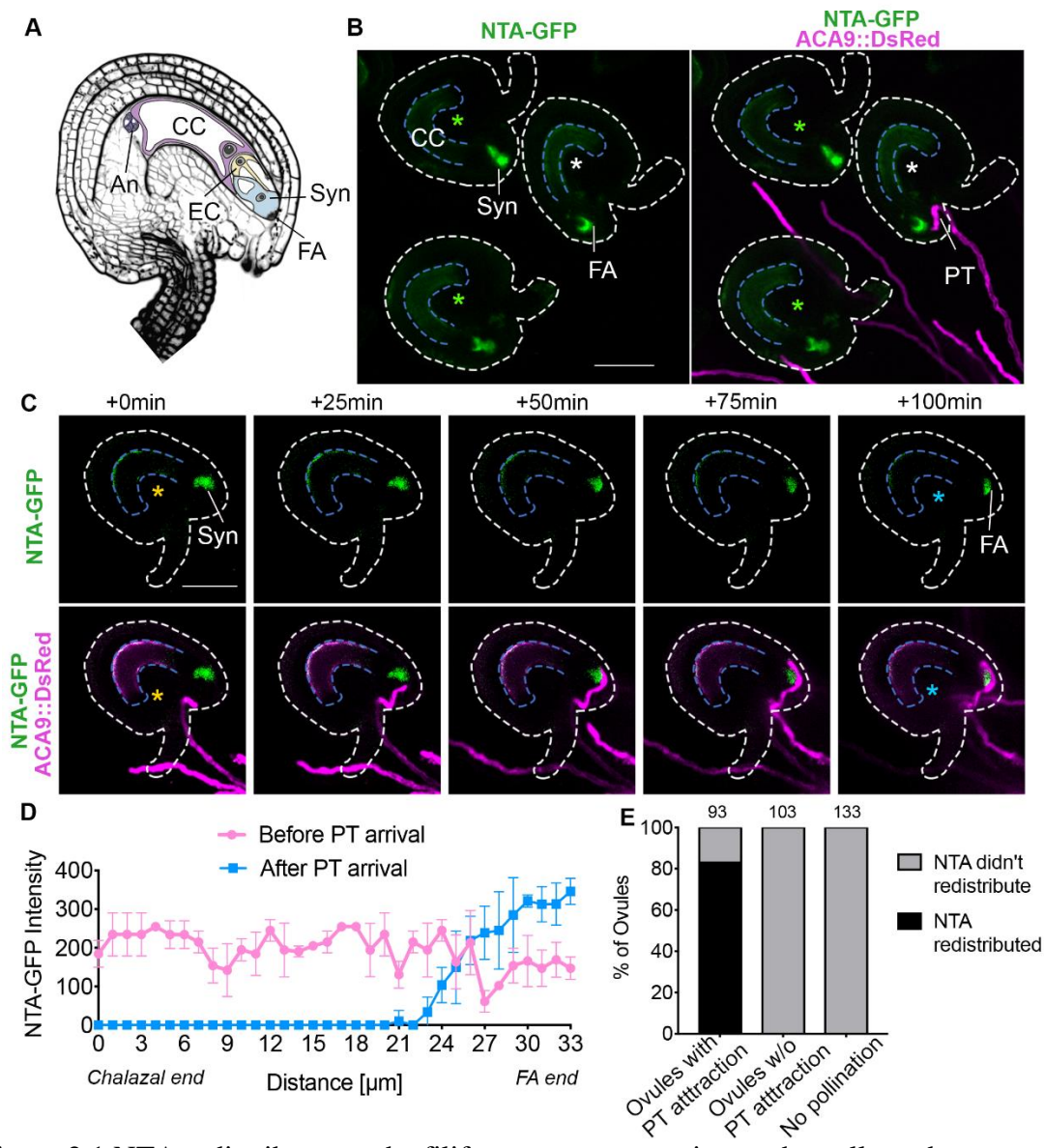
Figure 2.1 NTA redistributes to the filiform apparatus region as the pollen tube approaches.

(A) Diagram of a mature Arabidopsis thaliana ovule and embryo sac, modified from Jones et al, 2018. (B, C) Live imaging of pollen tube (PT) reception using NTA-GFP labeled synergids (green signal) and ACA9::DsRed pollen tubes (magenta signal). (B) NTA-GFP redistribution occurred in ovules that attracted a pollen tube (ovules with white stars), while NTA-GFP redistribution did not occur in ovules without pollen tube attraction (ovules with green stars). (C) Time-lapse imaging of NTA-GFP movement during pollen tube reception. NTA-GFP before (ovules with yellow stars) and after (ovules with blue stars) the PT resumes growth after initial arrival at the filiform apparatus. (D) Quantification of NTA-GFP signal before (yellow starred ovule) and after (blue starred ovule) pollen tube arrival. Synergid cell from chalazal end to filiform apparatus (FA) end was defined from 0 to 33 µm in length. (E) Quantification of the percentage of ovules with NTA redistribution under different experimental conditions.
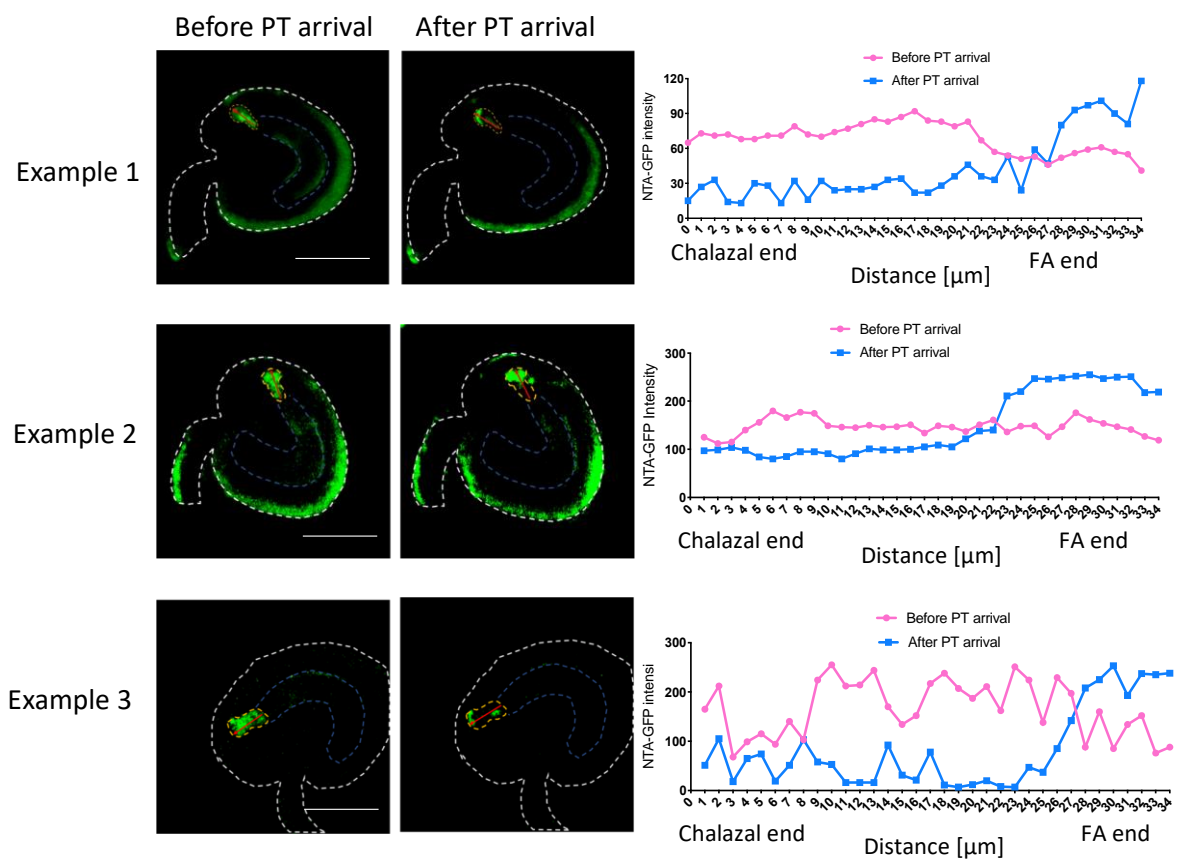
Figure 2.2 NTA consistently redistributes to the filiform apparatus region during pollen tube arrival.

Signal intensity measurement during pollen tube reception in independent imaging experiments. Bars=50µm.
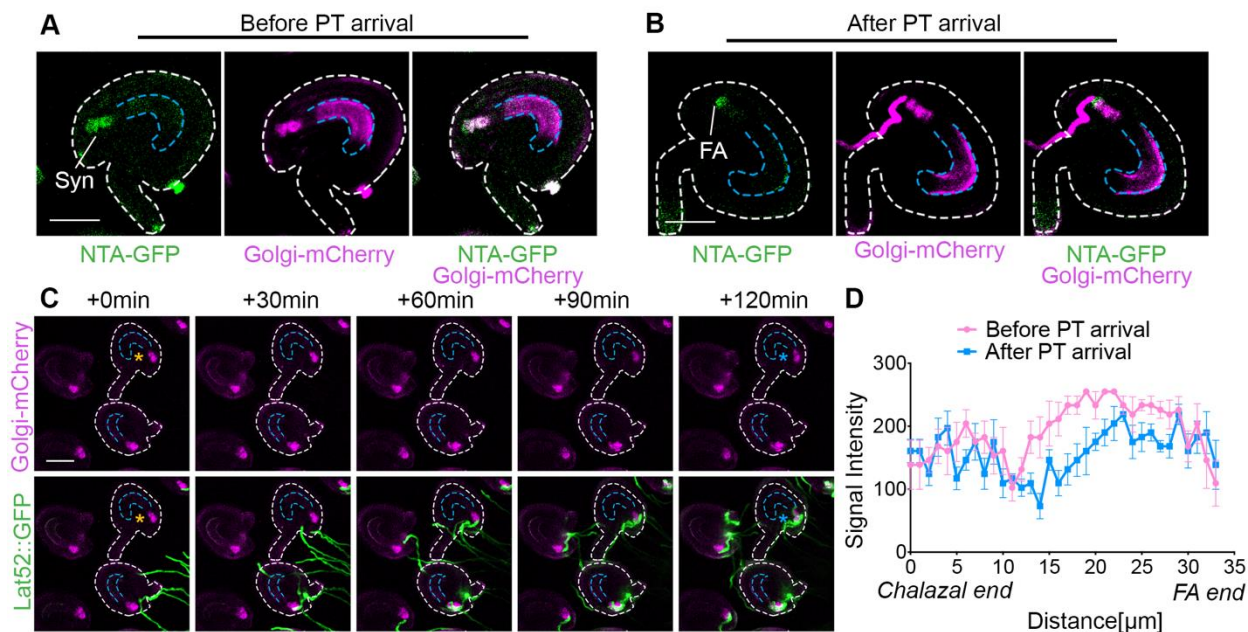
Figure 2.3 The Golgi marker is randomly distributed throughout synergids during pollen tube reception.

(A) NTA-GFP (green signal) and Golgi-mCherry signals (magenta signal) are evenly distributed along the length of the synergid and co-localized within synergid cells before pollen tube arrival. (B) After pollen tube arrival, NTA-GFP redistributed to FA region, but Golgi-mCherry did not redistribute to FA. (C) Live imaging of Golgi-mCherry during reception of Lat52::GFP labeled pollen tubes. (D) Quantification of Golgi-mCherry signal along the length of synergids before (ovule with yellow star in C) and after (ovule with blue star in C) pollen tube arrival. Bars=30µm (A-B), 50µm (C). Syn, Synergid cells, FA, Filiform Apparatus.
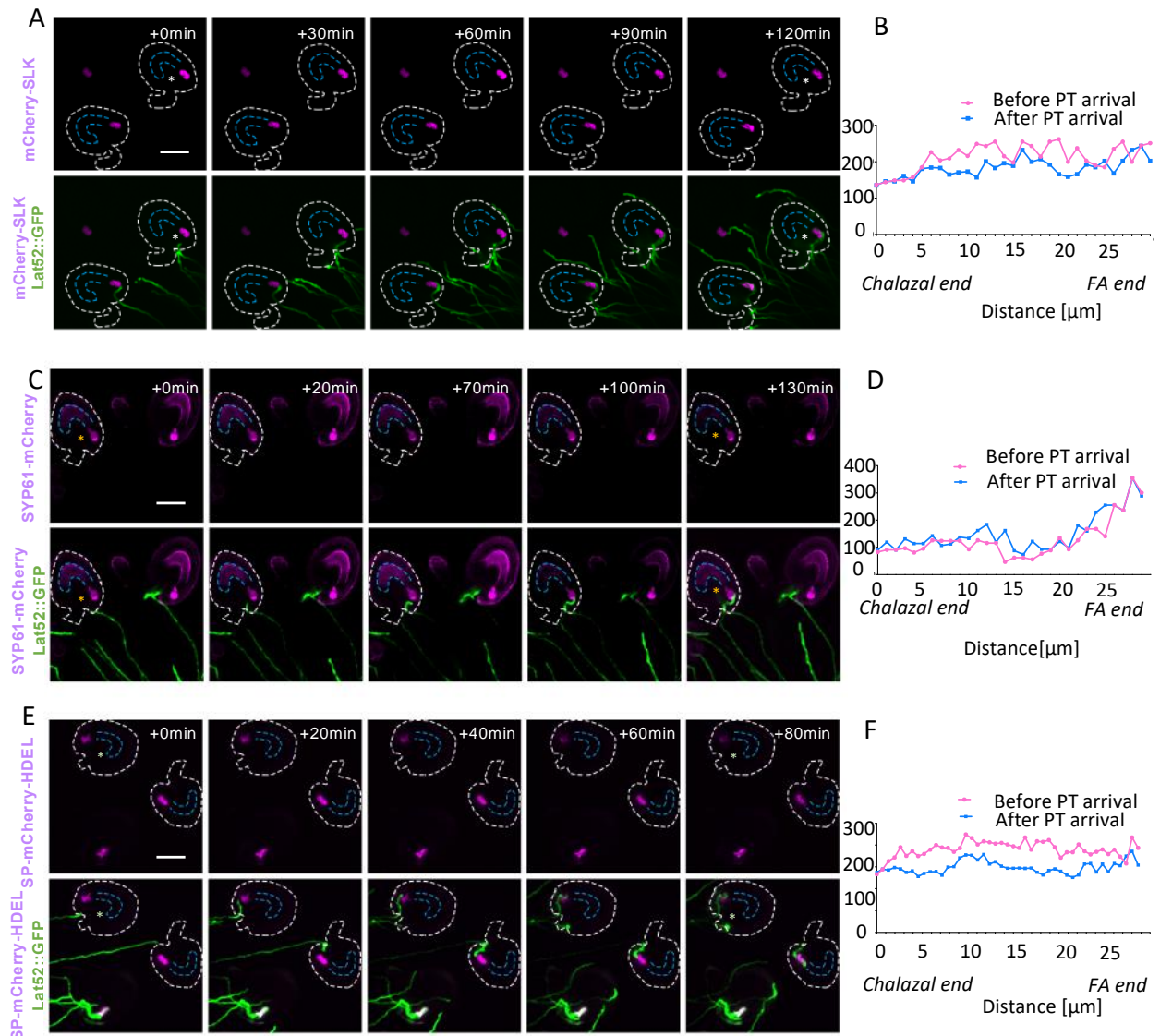
Figure 2.4 Subcellular marker behavior during reception of Lat52::GFP labeled pollen tubes.

(A) The peroxisome marker mCherry-SLK does not redistribute to the FA region after pollen tube arrival (ovules with green stars). (B) Quantification of mCherry-SLK signal before and after PT arrival. (C) The trans-Golgi marker SYP61-mCherry (magenta signal) is localizes toward the micropyle region of synergid cells both before and after pollen tube arrival (ovules with yellow stars). (D) The measurement of SYP61-mCherry signal during pollen tube reception. (E) Before and after pollen tube arrival, the ER marker SP-mCherry-HDEL (magenta signal) is distributed throughout synergid cells (ovules with white stars). (F) Quantification of SP-mCherry-HDEL signal along the length of synergids before and after pollen tube reception. Bars=50µm.
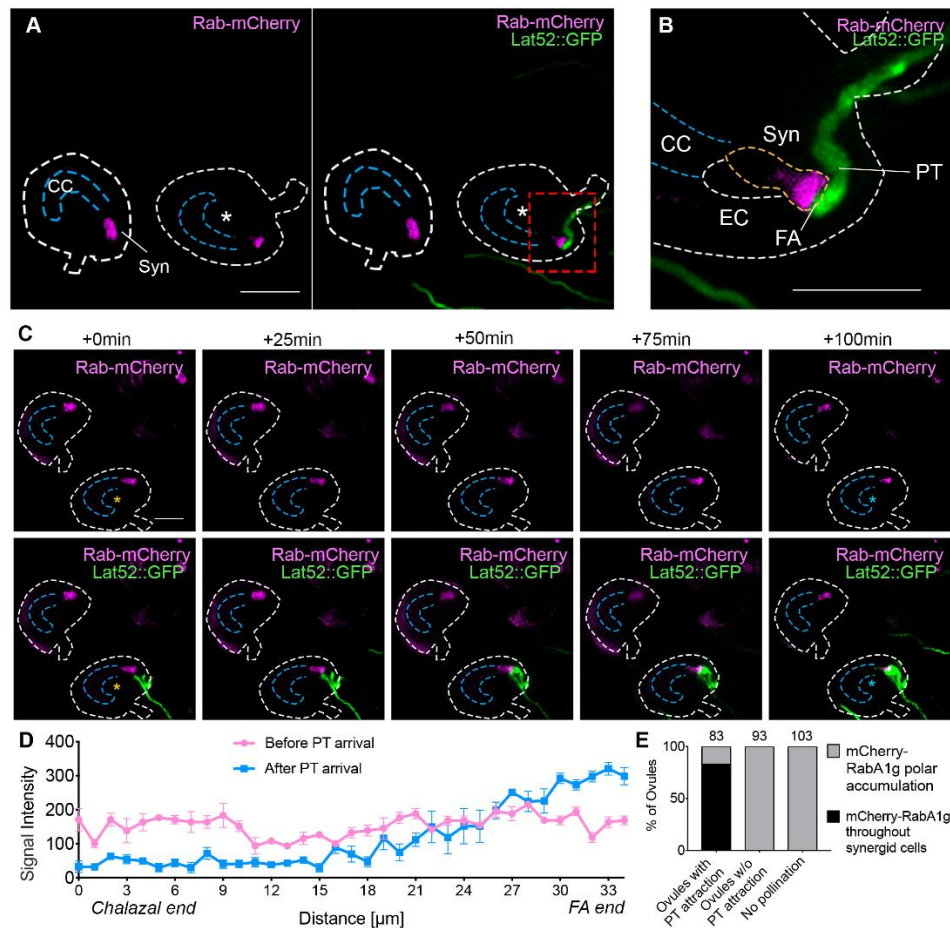
Figure 2.5 Endosome marker polarly accumulates toward filiform apparatus during pollen tube reception.

(A) Rab-mCherry endosome marker (magenta signal) accumulates at the FA region in response to pollen tube arrival (ovule with white star). (B) Higher magnification of the micropylar region of starred ovule in (red box in panel A). (C) Timing of Rab-mCherry polar accumulation during pollen tube arrival (ovules with stars). (D) Quantification of Rab-mCherry signal along the length of synergids during pollen tube reception. Bars=50µm. (E) Quantification of ovule percentage with endosome marker throughout the synergids (gray bars) or with polar accumulation near the filiform apparatus (black bars). CC, Central Cell; EC, Egg Cell; Syn, Synergid Cells; FA, Filiform Apparatus; PT, Pollen Tube.
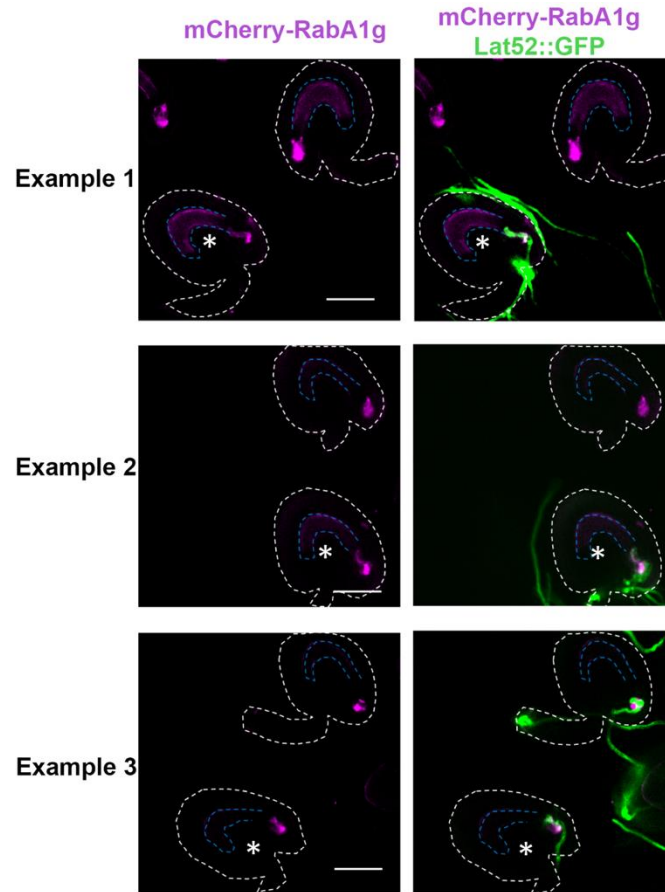
Figure 2.6 Additional examples of RabA1g endosome markers during pollen tube reception.

Endosome marker accumulates near the filiform apparatus region as pollen tube approaches (starred ovules), but no polar accumulation was found in ovules that did not attract a pollen tube. Bars=50µm.
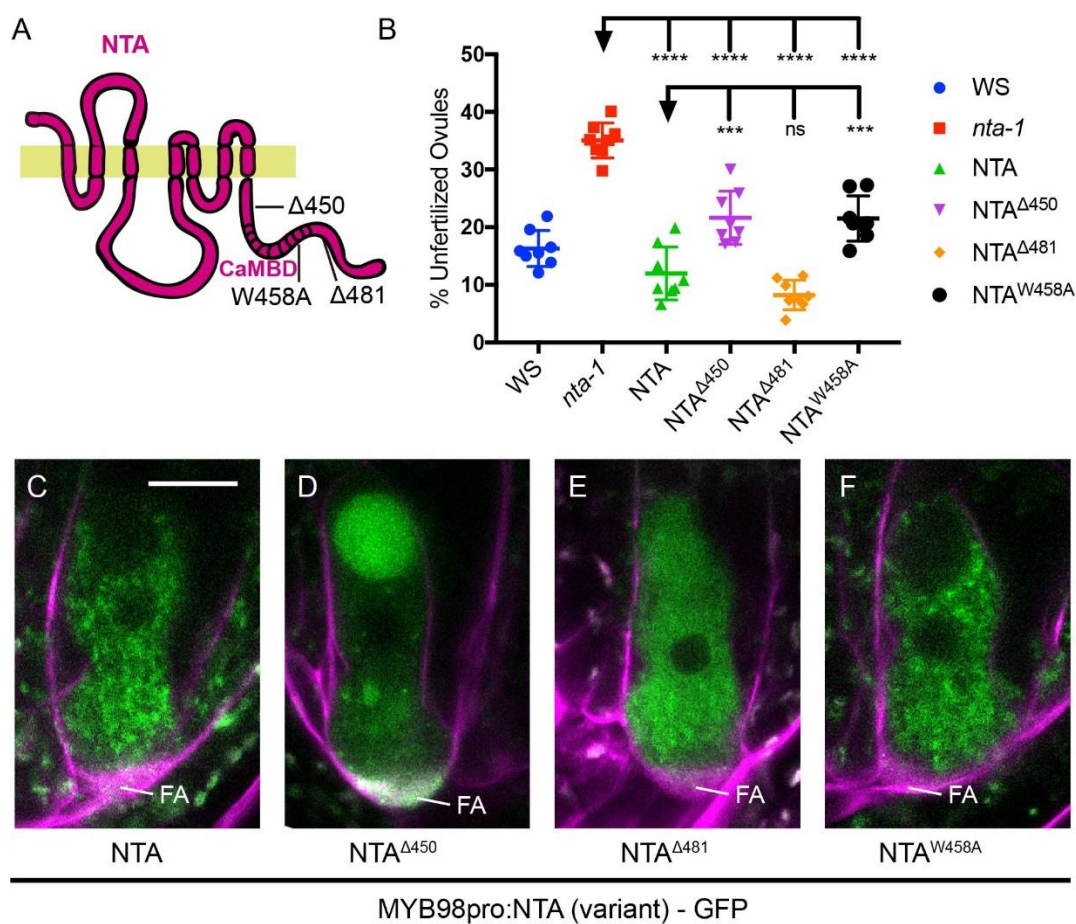
Figure 2.7 Analysis of NTA variants expressed in synergids of *nta-1*.

(A) A graph showing the NTA variant positions. (B) Complementation analysis of NTA variants in T2 plants homozygous for MYB98$_{pro}$::NTA(variant)-GFP constructs in *nta-1* mutants. (C-F) NTA (variant)-GFP (green) distribution in synergid cells of unfertilized ovules merged with FM4-64 (magenta). Bars = 10 μm. Adjusted P values from a Student's *t*-test are as follows: **** indicates $P < 0.0001$; *** indicates $P = 0.001$ to 0.0001; and ns indicates $P > 0.05$. FA, Filiform Apparatus.
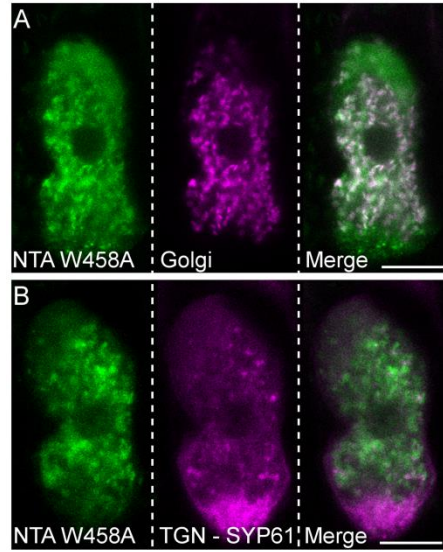
Figure 2.8 NTAW458A co-localizes with a Golgi marker in synergid cells.

Colocalization of NTAW458A-GFP (green) with: (A) Golgi (LRE:proMan49-mCherry), (B) trans-Golgi network (TGN, MYB98pro:SYP61:mCherry) markers (magenta) in the synergid cell of unpollinated ovules. Bars = 10 µm.
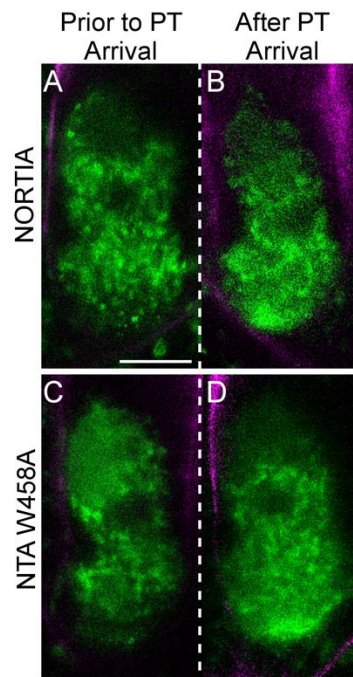
Figure 2.9 NTA and NTA W458A distribution in the synergid at PT arrival.

NTA-GFP (green) distribution in synergid cells of the same pollinated pistil prior to PT arrival (A) and at PT arrival (B). NTA^{W458A}-GFP (green) distribution in synergid cells of the same pollinated pistil prior to PT arrival (C) and at PT arrival (partial accumulation of NTA^{W458A}-GFP at the filiform apparatus region, FA) (D). Pollen from the *Lat52$_{pro}$:DsRed* PT marker line was used to pollinate emasculated flowers and imaging was done 4-6 hrs after pollination. Bar = 10 µm.
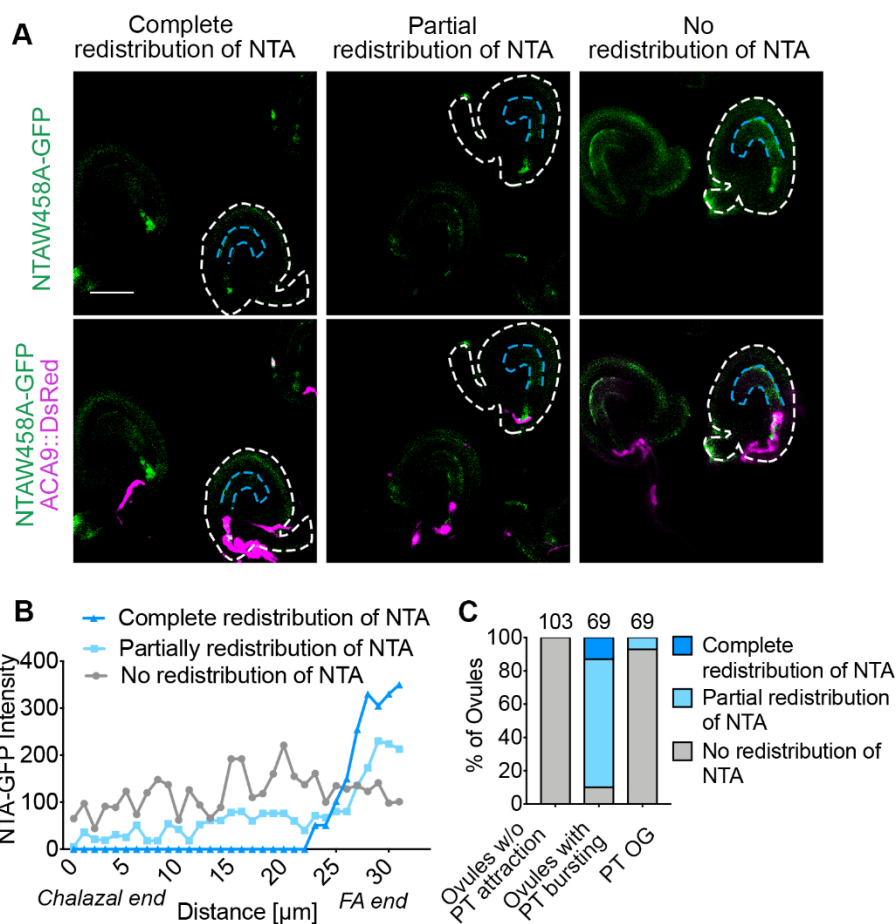
Figure 2.10 A point mutation in the CaMBD (NTAW458A) affects redistribution and pollen tube reception.

(A) NTAW458A has 3 different localization patterns in response to PT arrival under semi in-vivo conditions. (B) Quantification of GFP signal intensity in NTAW458A synergids during pollen tube reception. (C) Analysis of NTAW458A-GFP distribution patterns in ovules with successful (PT bursting) and unsuccessful (no PT or PT overgrowth (PT OG)) pollen tube reception. Bar=50 µm.
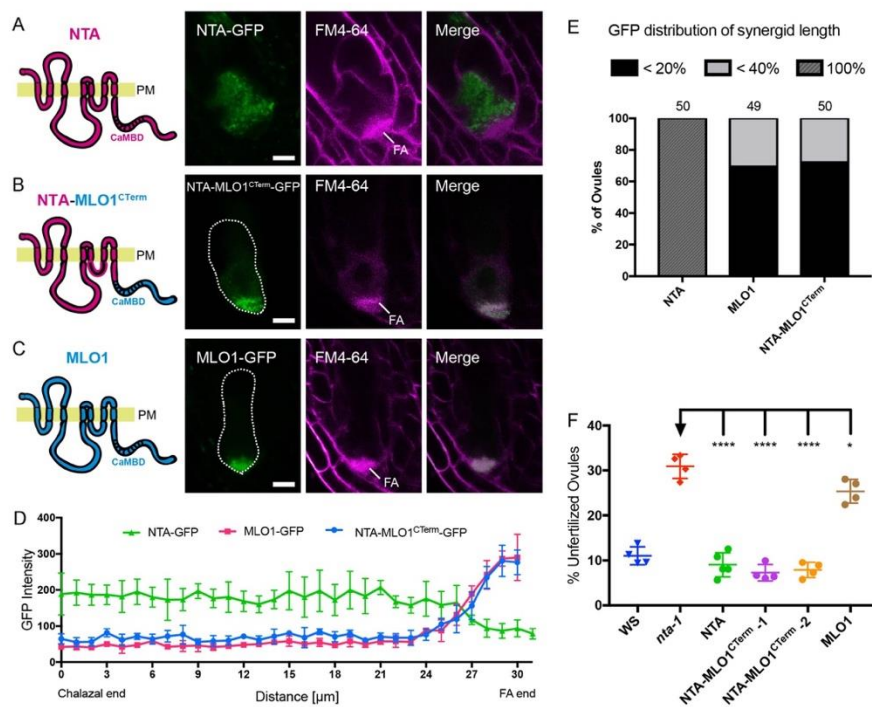
Figure 2.11 Targeting of NTA to the filiform apparatus region before pollen tube arrival is not toxic to synergid cells.

(A-C) Localization patterns of MYB98 promoter driven MLO-GFP variants (green signal) in synergids of mature virgin ovules stained with FM4-64 (magenta signal) to reveal the outline of the synergid and the filiform apparatus (FA, diffuse magenta signal). (D) Quantification of the GFP intensity of the MLO variants in A-C along the length of the synergids. (E) Percentage of ovules showing MLO-GFP signal throughout the synergids (100% of length), in the FA only (20% of length) and the region surrounding and including the FA (40% of length). (F) Scatter plot of unfertilized ovule percentages in homozygous plants of pMYB98::MLO-GFP in nta-1 mutants to assess the ability of the MLO-GFP constructs to complement nta-1. WS, Wassilewskija. Significance was determined by a Student's t-test (****, $P < 0.0001$; *, $P = 0.05$ to 0.01). Bars = 10 μm.
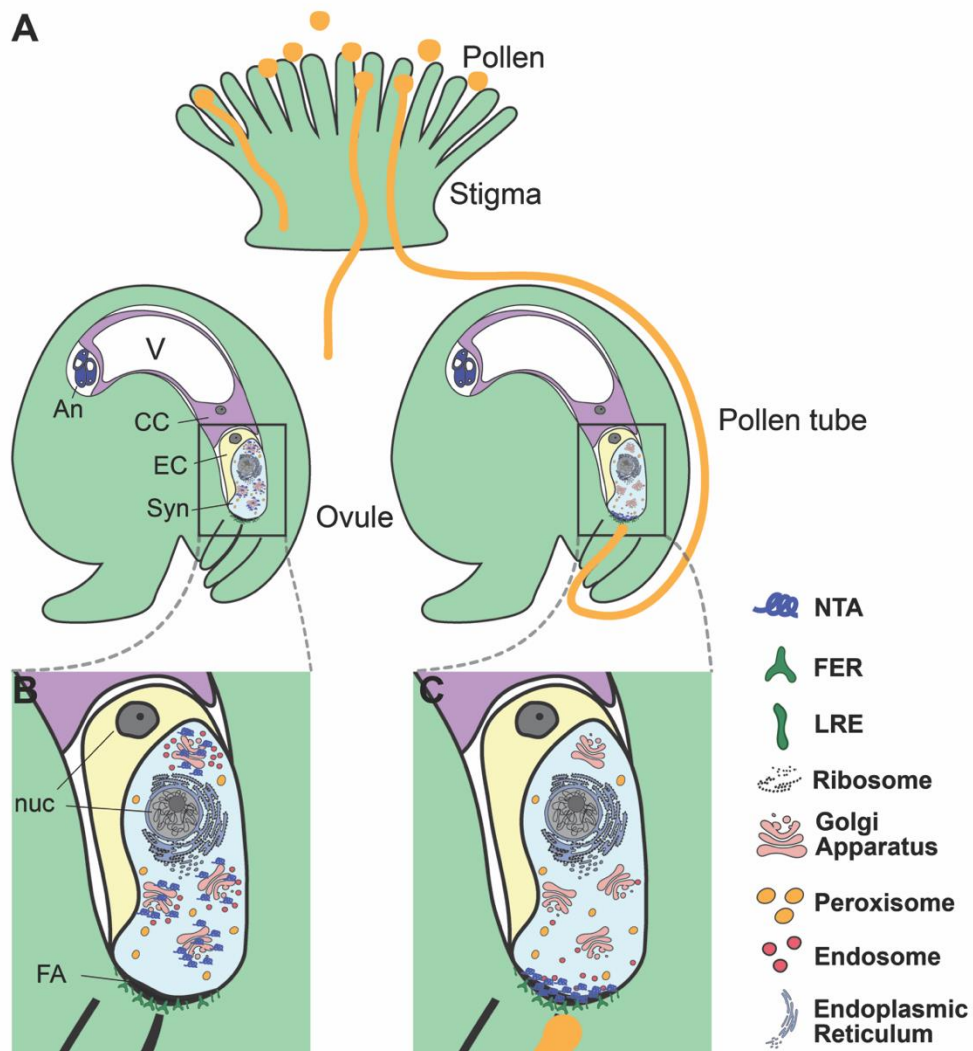
Figure 2.12 Subcellular dynamics in synergids during pollen tube reception.

(A) Pollination using a semi-*in vivo* pollen tube guidance assay. (B) Before pollen tube arrival, NTA is in a Golgi-associated compartment and endosomes are distributed throughout the synergids. (C) As a pollen tube arrives, NTA and endosomes move toward the filiform apparatus (FA). NTA redistribution is dependent on signaling from the FER receptor like kinase, which acts in a complex with LRE. Abbreviations: CC, Central Cell; Syn, Synergid cells; EC, Egg Cell; An, Antipodal cells; nuc, Nucleus; FA, Filiform Apparatus.

Movie 2.1 NTA-GFP (green signal) redistributes to filiform apparatus region as ACA9::DsRed labeled pollen tube (magenta signal) approaches.
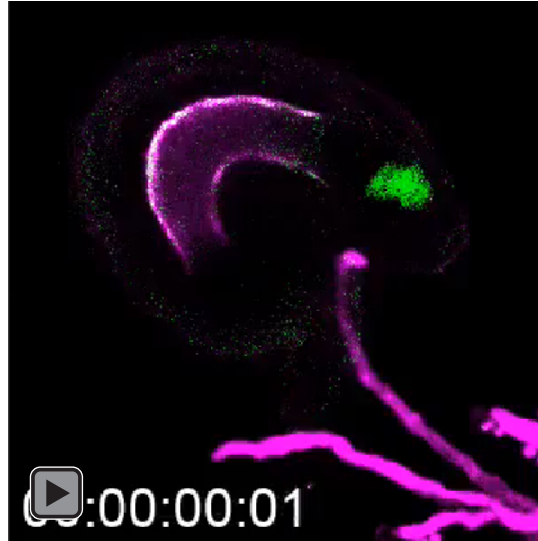
Movie 2.2 NTA-GFP (green signal) redistributes to filiform apparatus region during pollen tube reception (GFP channel only, same movie as 2.1)
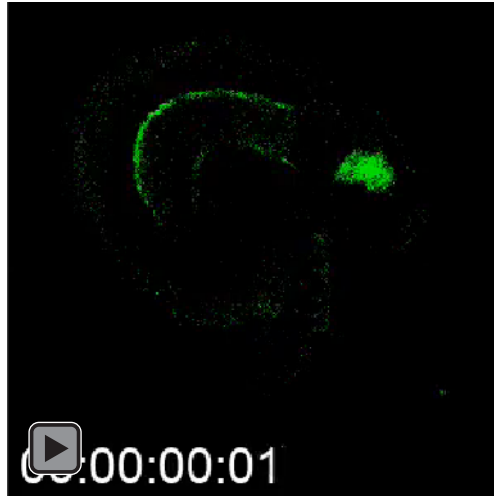
Movie 2.3 Golgi-mCherry signals (magenta signal) are evenly distributed along the length of the synergid as Lat52::GFP labeled pollen tube (green signal) approaches.
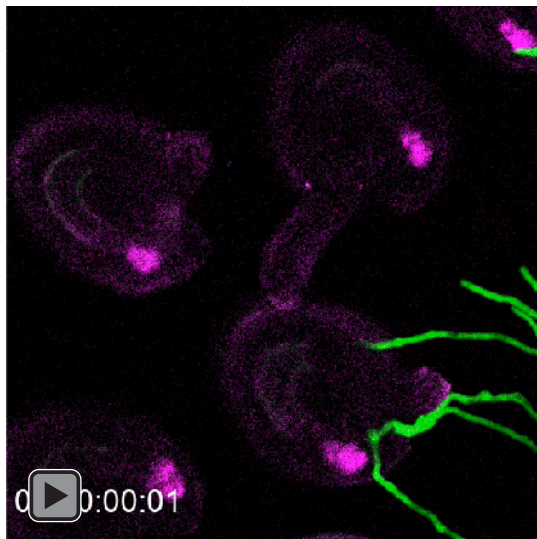
Movie 2.4 Golgi-mCherry signals (magenta signal) are evenly distributed along the length of the synergid during pollen tube reception (mCherry channel only, same movie as 2.3).
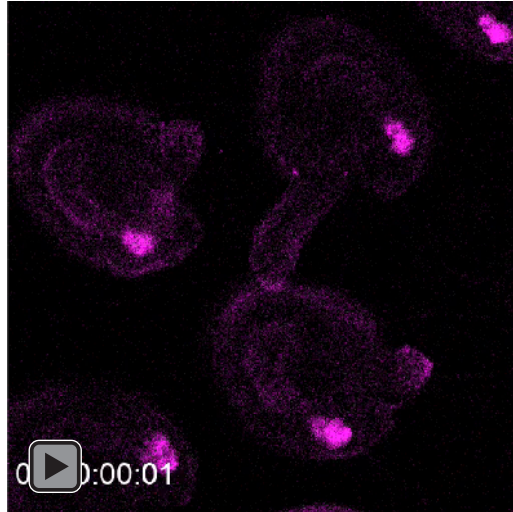
Movie 2.5 The trans-Golgi marker SYP61-mCherry (magenta signal) is localized toward the micropyle region of synergid cells both before and after pollen tube (green signal) arrival.
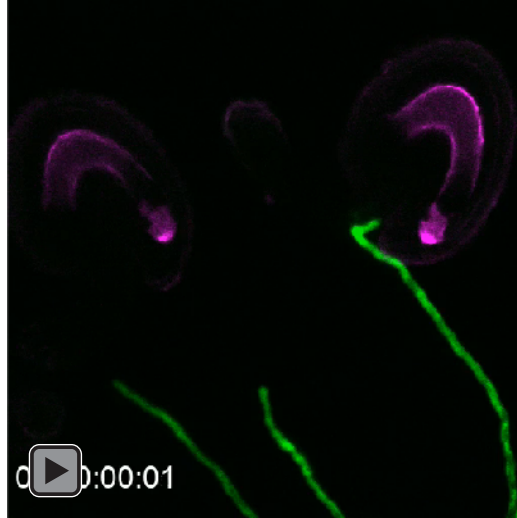
Movie 2.6 The trans-Golgi marker SYP61-mCherry (magenta signal) is localized toward the micropyle region of synergid cells during pollen tube reception (mCherry channel only, same movie as 2.5).
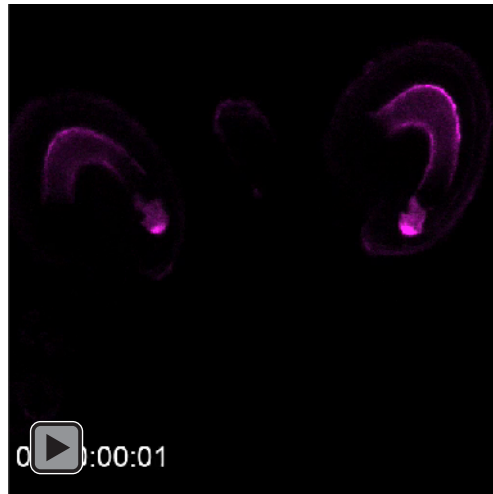
Movie 2.7 Before and after pollen tube (green signal) arrival, the ER marker SP-mCherry-HDEL (magenta signal) is distributed throughout synergid cells.
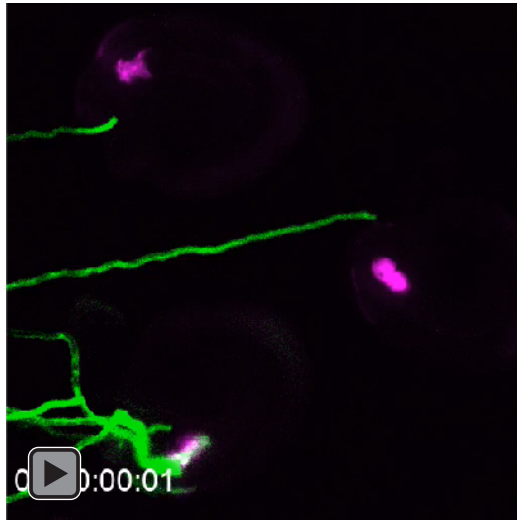
Movie 2.8 The ER marker SP-mCherry-HDEL (magenta signal) is distributed throughout synergid cells (mCherry channel only, same movie as 2.7).
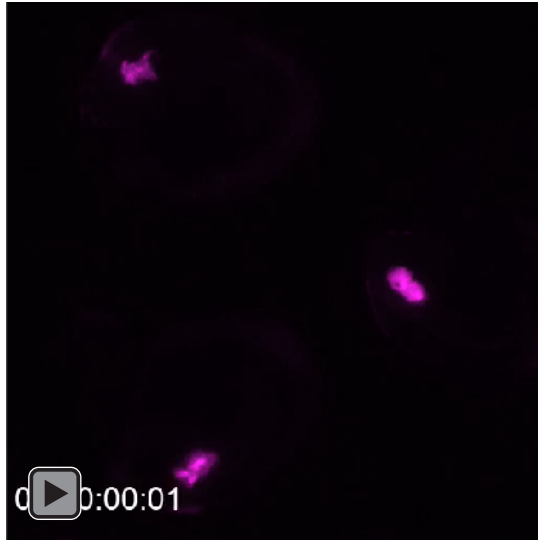
Movie 2.9 The peroxisome marker mCherry-SLK (magenta signal) does not redistribute to the filiform apparatus region after pollen tube (green signal) arrival.
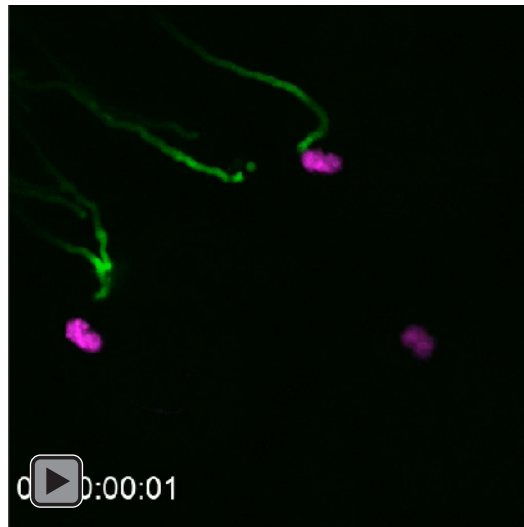
Movie 2.10 The peroxisome marker mCherry-SLK (magenta signal) does not redistribute to the filiform apparatus region during pollen tube reception (mCherry channel only, same movie as 2.9).
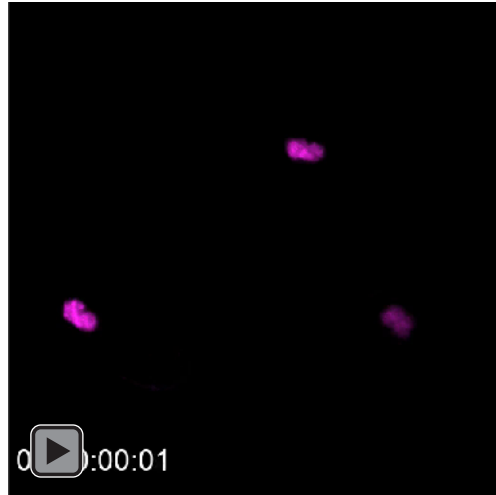
Movie 2.11 RabA1g-mCherry endosome marker (magenta signal) accumulates at the filiform apparatus region in response to pollen tube (green signal) arrival.
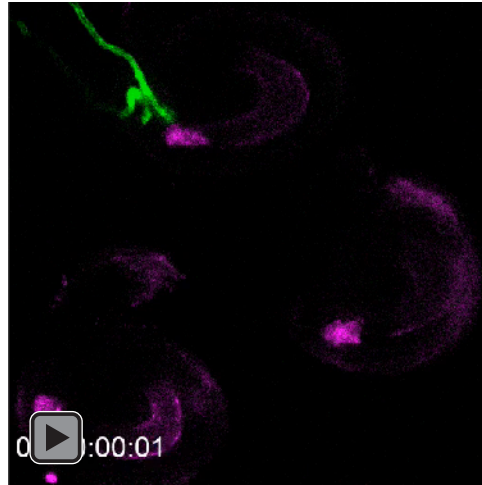
Movie 2.12 RabA1g-mCherry endosome marker (magenta signal) accumulates at the filiform apparatus region during pollen tube reception (mCherry channel only, same movie as 2.11).
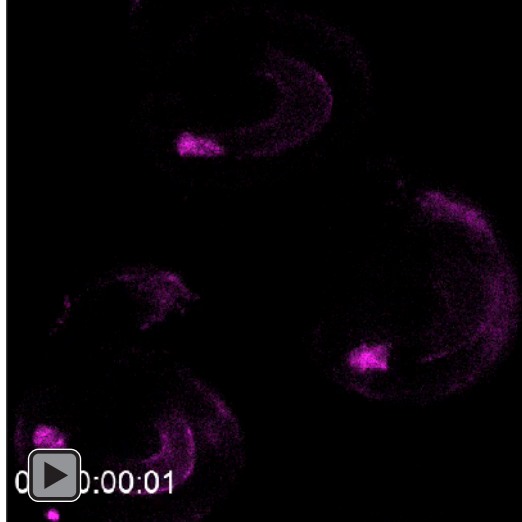
Table 2.1 List of primers used for cloning

Primer Name	Primer Sequences (5' to 3')
NTA450-RattB2	GGGGACCACTTTGTACAAGAAAGCTGGGTGCTCATCAAACACTGCTTTCTTC
NTA481-RattB2	GGGGACCACTTTGTACAAGAAAGCTGGGTGTGAAACACCAAGTGTCTTGCT
NTAW458A-F	GCATTGAAGAAGGCGCACAAAGACATCAAATTGAAGAAAG
NTA-RattB2	GGGGACCACTTTGTACAAGAAAGCTGGGTGAGAGTTGTGGAATTGCATCTC
NTA-FattB1	GGGGACAAGTTTGTACAAAAAAGCAGGCTTCACCATGATCACAAGAAGCAGGTGT
NTAW458A-R	CGCCTTCTTCAATGCCTTTGCCAT
NTA-R19	CTCATCAAACACTGCTTTCTTCATG
MLO1-F	GCAGTGTTTGATGAGAATGTGCAGGTTGGTCTTGTTG
MLO1-RattB2	GGGGACCACTTTGTACAAGAAAGCTGGGTGGTTGTTATGATCAGGTGTAATCTCA

CHAPTER 3.   A GENOME-WIDE ASSOCIATION STUDY REVEALS A NOVEL REGULATOR OF OVULE NUMBER AND FERTILITY IN *ARABIDOPSIS THALIANA*

3.1   Abstract

Ovules contain the female gametophytes which are fertilized during pollination to initiate seed development. Thus, the number of ovules that are produced during flower development is an important determinant of seed crop yield and plant fitness. Mutants with pleiotropic effects on development often alter the number of ovules, but specific regulators of ovule number have been difficult to identify in traditional mutant screens. We used natural variation in Arabidopsis accessions to identify new genes involved in the regulation of ovule number. The ovule numbers per flower of 189 Arabidopsis accessions were determined and found to have broad phenotypic variation that ranged from 39 ovules to 84 ovules per pistil. Genome-Wide Association tests revealed several genomic regions that are associated with ovule number. T-DNA insertion lines in candidate genes from the most significantly associated loci were screened for ovule number phenotypes. The *NEW ENHANCER of ROOT DWARFISM (NERD1)* gene was found to have pleiotropic effects on plant fertility that include regulation of ovule number and both male and female gametophyte development. Overexpression of NERD1 increased ovule number per fruit in a background-dependent manner and more than doubled the total number of flowers produced in all backgrounds tested, indicating that manipulation of NERD1 levels can be used to increase plant productivity.

3.2   Introduction

During plant reproduction, pollen tubes deliver two sperm cells to female gametophytes contained within ovules. This allows double fertilization to occur in order to produce the embryo and endosperm in the developing seed. Angiosperms with all kinds of pollination syndromes (insect-, wind-, and self-pollinated) produce much more pollen than ovules in order to ensure successful pollination. For example, most soybean varieties produce only 2 ovules per flower, but more than 3,000 pollen grains, a 1,500-fold difference (Palmer et al., 1978). Wind-pollinated plants such as maize have an even more extreme difference in pollen production vs. ovule production per plant, with more than 1 million pollen grains versus an average of 250 ovules per plant (a 4000-fold difference (Uribelarrea et al., 2002)). *Arabidopsis thaliana*, which is a self-pollinating plant, also produces an excess of pollen, with at least 2000 pollen grains per flower compared to an average of 60 ovules per flower (Yan et al., 2017). Since pollen is produced in excess, in self-pollinated plants the number of ovules (i.e. female gametes) sets the maximum seed number per flower.

The ability to manipulate ovule number to increase the reproductive potential of plants requires an understanding of the molecular pathways that control ovule initiation. The model plant *Arabidopsis thaliana* produces flowers with four whorls of organs: sepals, petals, stamens, and carpels. The inner whorls (3 and 4) are responsible for sexual reproduction, with pollen (the male gametophytes) produced in the whorl 3 stamens and the female gametophytes (also known as the embryo sacs), produced in ovules contained within the whorl 4 carpels. Specification of the 4 whorls is controlled by the "ABC" genes, with the C-class gene *AGAMOUS (AG)* a major regulator of carpel development (Coen and Meyerowitz, 1991).

In Arabidopsis, ovules are initiated from the carpel margin meristem (CMM) at stage 9 of floral development (Smyth et al., 1990). The Arabidopsis gynoecium comprises two carpels that are fused vertically at their margins (Reyes-Olalde et al., 2013). The CMM develops on the adaxial face of the carpels (inside the fused carpel cylinder) and will give rise to the placenta, ovules, septum, transmitting tract, style, and stigma. Once the placenta is specified, all of the ovule primordia are initiated at the same time (Robinson-Beers et al., 1992). Subsequently, each primordium will be patterned into three different regions: the funiculus, which connects the ovule to the septum; the chalaza, which gives rise to the integuments; and the nucellus, which gives rise to the embryo sac. Ovule development concludes with the specification of the megaspore mother cell within the nucellus which undergoes meiosis followed by three rounds of mitosis to form the mature haploid embryo sac (reviewed in (Drews and Koltunow, 2011)).

In Arabidopsis, CMM development requires coordination of transcriptional regulators involved in meristem function with hormone signaling (reviewed in (Reyes-Olalde et al., 2013)). Most mutants that have been reported to affect ovule number have pleiotropic effects related to the establishment of polarity and boundaries during gynoecial development (reviewed in (Cucinotta et al., 2014)). For example, the *AINTEGUMENTA* (*ANT*) transcription factor regulates organ initiation and cell divisions during flower development (Klucher et al., 1996). *ANT* acts redundantly with the related gene *AINTEGUMENTA-LIKE6/PLETHORA3* to regulate carpel margin development and fusion which leads to a modest reduction in ovule number. This phenotype is exacerbated when *ant* is combined with mutations in other carpel development transcriptional regulators, such as *SEUSS* (*SEU*), *LEUNIG* (*LUG*), *SHATTERPROOF1* and *2* (*SHP1* and *SHP2*), *CRABSCLAW* (*CRC*), *FILAMENTOUS FLOWER* (*FIL*), and *YABBY3* (*YAB3*). Mutant combinations between *ant* and

these mutants leads to severe defects in carpel fusion coupled with severe reductions in the marginal tissues that give rise to the CMM (summarized in (Reyes-Olalde et al., 2013)). An extreme example is the double mutant *seu-3 ant-1* which results in a complete loss of ovule initiation due to defects in CMM development (Azhakanandam et al., 2008). The organ boundary genes, *CUP-SHAPED COTYLEDON1* and *2* (*CUC1* and *CUC2*), are also required for CMM development and subsequent ovule initiation. *ant cuc2* mutants with *cuc1* levels decreased specifically in the CMM by an RNAi construct driven by the *SEEDSTICK* promoter show an 80% reduction in ovule number, indicating that *ANT* controls cell proliferation while *CUC1/2* are necessary to set up the boundaries that allow ovule primordia to be initiated (Galbiati et al., 2013). Plant hormones are also involved in gynoecium development and can have both indirect and direct effects on ovule number. Auxin biosynthesis, transport, signaling, and transport mutants have varying effects on gynoecium development and patterning, many of which lead to pleiotropic effects on tissues and organs derived from the CMM (Nemhauser et al., 2000). Treatment of developing flowers with the auxin polar transport inhibitor NPA showed that an apical-basal auxin gradient in the developing gynoecium is necessary for patterning events that lead to ovule initiation (Nemhauser et al., 2000). Cytokinin has also been implicated in ovule initiation and development in Arabidopsis. Notably, triple mutants in the *ARABIDOPSIS HISTIDINE KINASE* (*AHK*) cytokinin receptors, *AHK2*, *AHK3*, and *AHK4/CRE1*, displayed a 90% reduction in ovule number due to decreased cytokinin signaling (Bencivenga et al., 2012). Conversely, double mutants in the cytokinin degrading cytokinin oxidases/dehydrogenases (CKXs) displayed higher cytokinin levels in inflorescences and produced more than double the number of ovules as in wild-type controls (Bartrina et al., 2011). Brassinosteroids (BR) may also be positive regulators of ovule initiation. Gain-of-function mutants in the BR-induced transcription factor *BZR1* had increased ovule number

per flower while BR-deficient and insensitive mutants had decreased ovule number compared to wild-type controls. Upregulation of the ovule regulators *ANT* and *HUELLENLOS* (*HLL*) was correlated with *BZR1* activity, indicating the BR signaling positively regulates ovule development (Huang et al., 2013). Recently, gibberellins were shown to negatively regulate ovule number independently of auxin transport and signaling. A gain-of-function mutation in the DELLA gene, GA-INSENSITVE (GAI) and loss-of-function mutations in GA receptors all led to increased ovule number in Arabidopsis (Gomez et al., 2018).

To date, research on the factors controlling ovule number has been dominated by the analyses of mutants that have been identified based on pleiotropic effects on gynoecium development. In an attempt to identify loci that regulate ovule number without affecting other aspects of flower morphology, we took advantage of natural variation in ovule number in Arabidopsis accessions from diverse geographical locations. Over 7,000 natural accessions are now available with intraspecific variation, and next generation sequencing has been used to generate data on single nucleotide polymorphisms (SNPs) from over 1,000 of these accessions as part of the 1001 genomes project (Weigel, 2012). 100s of different phenotypes have been analyzed in this collection such as flowering time, leaf shape and size, the ability to resist to pathogens (Atwell et al., 2010). In this study, we identified variation in ovule number per flower in a screen of 189 Arabidopsis accessions and conducted a Genome Wide Association Study (GWAS) to identify loci associated with the ovule number trait. Further analysis of two loci identified in our GWAS revealed that the *NEW ENHANCER of ROOT DWARFISM* (*NERD1*) and *OVULE NUMBER ASSOCIATED 2* (*ONA2*) genes participate in the determination of ovule number during Arabidopsis flower development.

The discovery of new ovule number regulators in Arabidopsis has the potential to provide targets for the development of crop varieties with greater yield.

3.3 Materials and Methods

3.3.1 Plant Material and Growth Conditions

Arabidopsis thaliana accessions and insertion mutants were ordered from the Arabidopsis Biological Resource Center at Ohio State University (ABRC). ABRC stock numbers for the accessions and insertion mutants used in our study are listed in tables 3.3 and 3.4. Seeds were sterilized and plated on ½ Murashige and Skoog (MS) plates. All plates were sealed and stratified at 4 ˚C for two days, and then transferred to the growth chamber (long day conditions, 16h of light and 8 h of dark at 22˚C) for germination and growth. After one-week, seedlings were transplanted to soil. Many of the Arabidopsis accessions require vernalization for flowering (Lempe et al., 2005), we therefore chose to vernalize all of the accessions in our study for 4 weeks at 4 ˚C. After vernalization, the plants were returned to the growth chamber and grown under the long day conditions described above. Seeds from transformed lines were sterilized and plated on ½ MS plate with 20mg/L hygromycin for selection of transgenic seedlings, which were then transplanted to soil and grown in long days.

3.3.2 Ovule Number Phenotyping

For determination of ovule number per flower, we counted four to five siliques per plant and five plants per accession. Carpel walls were removed with a dissecting needle and total ovule number (including unfertilized and aborted ovules) was counted with the aid of a Leica dissecting microscope. To minimize age-related variation in ovule number, we counted siliques from flowers 6-10 on the primary shoot for all accessions.

3.3.3   Genome-Wide Association Study

GWAS was performed using GWAPP, which is a GWAS web application for Genome-Wide Association Mapping in *Arabidopsis* (http://gwas.gmi.oeaw.ac.at) (Seren et al., 2012). In our study, 148 accessions had single nucleotide polymorphisms (SNPs) data available on the 1001 Full-sequence dataset; TAIR 9. Logarithmic transformation was applied to make the results more reliable for parametric tests. A simple linear regression (LM) was used to generate the Manhattan plot by using GWAPP (Seren et al., 2012). SNPs with P values $\leq 1 \times 10^{-6}$ were further considered as candidate loci linked to alleles that regulate ovule number (a horizontal dashed line in Figure 3.3 shows the 5% FDR threshold $-\log_{10}p$ value $= 6.2$, which was computed by the Benjamini-Hochberg-Yekutieli method). SNPs with < 15 minor allele count (MAC) were not considered to help control false positive rates. 10 genes flanking the highest SNP for each locus were tabulated as candidate genes for each significant association.

3.3.4   Cloning and Generation of Transgenic Lines

For complementation and overexpression experiments, Gateway Technology was used to make all the constructs. Genomic DNA fragments corresponding to the coding regions of candidate genes were amplified from either beginning of the promoter (defined by the end of the upstream gene) or the start codon to the end of the CDS (without stop codon) by PCR with primers that had attB1 and attB2 sites from Col-0 genomic DNA (see table 3.5 for primer sequences). For amplifying At3g60660 and At3g51050, PHUSION High-Fidelity Polymerase (NEB, M0535S) was used. All the PCR products were put into entry vector pDONR207 by BP reactions and then were recombined into destination vector pMDC83 (GFP) by LR reaction (Curtis and Grossniklaus, 2003). Native promoter constructs were amplified from ~2KB promoter region to the end (without stop codon) by PCR with primers that had attB1 and attB2 sites from Col-0 genomic DNA. The

PCR products were put into entry vector pDONR207 by BP reactions and then were recombined into destination vector pMDC32 (tdTomato) and pMDC163 (GUS) by LR reaction. All constructs were transformed into *Agrobacterium tumefaciens* strain GV3101 and then used for plant transformation by the floral-dip method (Clough and Bent, 1998).

3.3.5   GUS Staining

GUS staining was performed as previously described (Davis et al., 2017). Samples were imaged with Differential Interference Contrast (DIC) on a Nikon Eclipse Ti2-E microscope. 12 independent T1 NERD-GUS transformants were analyzed and showed similar GUS patterns.

3.3.6   Transient Expression in *N. benthamiana*

Leaves from 3-4 week old *N. benthamiana* were co-infiltrated with 35S::NERD1-GFP and Golgi-mCherry, ER-mCherry, PM-mCherry, Plastid- mCherry and Peroxisome-mCherry markers from (Nelson et al., 2007) as previously described (Jones et al., 2017). Leaves were imaged 2-3 days after infiltration with a Nikon A1Rsi inverted confocal microscope under 20x dry and 40x water objectives with GFP excited by a 488nm laser and mCherry excited by a 561nm laser in normal mode.

3.3.7   Analysis of embryo sac and pollen development

Analysis of embryo sac development was conducted using confocal microscopy based on (Christensen et al., 1997). Pistils were dissected from FG2, FG3, FG4 and mature stages of flowers from Col-0, *nerd1-2* and *nerd1-4* and fixed in 4% glutaraldehyde and 12.5mM cocadylate, PH=6.9 for two hours at room temperature. Pistils were dehydrated in 20%, 40%, 60%, 80% and 100% ethanol for 10 min each. Samples were then cleared in a 2:1 mixture of benzyl benzonate: benzyl alcohol for 2-4 hours and mounted in immersion oil for imaging. Images were captures using a

Nikon A1Rsi inverted confocal microscope under 60x oil objectives and excitation with a 561nm laser.

Pollen was released from tetrad, microspore, bi-cellular, tri-cellular and mature stage anthers from Col-0, *nerd1-2* and *nerd1-4*. Samples were incubated in 1ug/ml DAPI (4′,6-diamidino-2-phenylindole) staining solution for 2hrs and imaged using a Nikon A1Rsi inverted confocal microscope under 60x oil objectives with DAPI excited by a 405nm laser.

3.3.8   Alexander Staining of Mature Pollen

Mature anthers from Col-0 and *nerd1-2/nerd1-2* were dissected under the Leica dissecting microscope and placed into a drop (20 μl) of Alexander staining solution on a microscope slide (Alexander, 1969). After several minutes of staining, samples were imaged with a Nikon Eclipse Ti2-E microscope.

3.3.9   Aniline blue staining of pollen tube behavior

Flowers that two days after emasculation from *nerd1-2* plants were cross-pollinated with wild-type Col-0. The pollinated pistils were then collected at 36 h after hand pollination and fixed immediately in ethanol-acetic acid (3:1 v/v) overnight. Pistils were rehydrated in 70%, 50%, 30% ethanol for 5 min each at room temperature. After clearing in 5 N NaOH at 60 ˚C for 5 min and washing $2 \times$ in 0.1M phosphate buffer (pH-8), they were stained using aniline blue (0.1% aniline blue in K3PO4) for 15mins. Five pistils per sample were analyzed and images were captured with a Nikon Eclipse Ti2-E microscope (Nikon Instruments Inc, Melville, NY).

3.3.10 Phylogenetic Analysis

The cladogram tree was generated in MEGA7, which nucleotide distance and neighbor-join tree

file were calculated by PHYlogeny Inference Package (PHYLIP, version 3.696).

The phylogenetic tree of NERD1 was inferred using neighbor-joining method in MEGA7 (Kumar

et al., 2016). The associated taxa clustered together with the bootstrap test (1000

replicates)(Felsenstein, 1985). All the branch lengths are in the same units as those of the

evolutionary distances used to generate the phylogenetic tree.

3.3.11 Quantitative Real-time RT-PCR

For qRT-PCR, leaves and young flowers were collected from mature plants of Col-0 and Altai-5.

Samples were immediately frozen in liquid nitrogen, ground, and total RNA was extracted using

the E.Z.N.A Plant RNA kit (OMEGA, USA). Oligo-dT primers and Superscript II reverse

transcriptase (Invitrogen) was used for cDNA synthesis. qRT-PCR reactions were prepared using

SYBR Green PCR Master Mix and PCR was conducted with a StepOnePlus RT-PCR system.

Relative quantifications were performed for all genes with the Actin11 used as an internal

reference. The primers used for qRT-PCR shown in table 3.5.

3.4   Results

3.4.1   Natural Variation in Ovule Number

We set out to identify new regulators of ovule number in Arabidopsis by taking advantage of

phenotypic variation in naturally occurring accessions. We obtained 189 Arabidopsis accessions

from the ABRC and assayed them for variation in ovule number (Table 3.3). Since ovule number

can vary throughout the life cycle of the plant (Wetzsteini et al., 2013), we determined the average

number of ovules from flowers 6-10 on the main stem of plants that were vernalized for 4 weeks

and then grown in long days at 22˚C. Under these growth conditions, accessions displayed a remarkable diversity in ovule number per flower, with a range of 39-82 ovules per flower (Figure 3.1A-B). The commonly used reference accession, Col-0, falls in the middle of the range with an average ovule number of 63±3 ovules.

In contrast to flowering time variation which has been shown to correlate with latitude of origin in Arabidopsis accessions (Stinchcombe et al., 2004), ovule number was not strongly correlated with location of origin in the accessions analyzed (Figure 3.1C and 3.2). Mapping ovule number data onto a cladogram of the accessions used in our study revealed a cluster of low ovule number accessions in one specific clade, indicating that these closely-related accessions may have similar genetic control of ovule number Figure 3.1D). Interestingly, several clades were made up of accessions with high, medium, and low ovule numbers. This suggests that the ovule number trait may be regulated by different loci that have been selected for in some lineages.

3.4.2 GWAS reveals SNPs linked to natural variation in ovule number

In order to identify genomic regions linked to variation in ovule number, we assessed whether the average ovule number per flower from 148 accessions was predicted by Single Nucleotide Polymorphisms (SNP) available in the 1001 Full-sequence dataset; TAIR 9. Logarithmic transformation was applied to the ovule number data to make the results more reliable for parametric tests. Associations were tested for each SNP using a linear regression model (LM) and the results were analyzed using GWAPP (Seren et al., 2012) (Figure 3.3A). A significance cutoff value of $-\log_{10}(p$ values$) \geq 6.2$ identified at least 9 genomic regions that are associated with variation in ovule number, while a higher cutoff of $-\log_{10}(p$ values$) \geq 7.5$ identifies only four significant genomic regions.

We next determined if known ovule number regulators (Alonso-Blanco et al., 1999; Bartrina et al., 2011; Gomez et al., 2018) colocalized with our GWAS loci. Of the previously described loci, only BIN2 mapped close to a significant association (Figure 3.4). This indicates that our GWAS has identified novel functions for loci in the regulation of ovule number. For further analysis, we focused on the two loci with the lowest p-values which are both located on the long arm of chromosome 3 (Figure 3.3B-C). Genes containing the most significantly associated SNPs as well as the 10 surrounding genes around the highest peak were considered as candidates for regulating ovule number. These genes were further prioritized based on whether they are expressed in developing pistils, by examining publicly available transcriptome data in ePlant (Waese et al., 2017) (Figure 3.5). Based on this prioritization, 35 candidate genes were selected, and of these 26 insertion mutants were available from the Arabidopsis Biological Resource Center. All 26 mutants were evaluated for changes in ovule number compared to the wild-type background, Col-0 (Table 3.4). Of these, two had significantly reduced ovule number compared to the Col-0 control (Figure 3.6 and 3.7A). The strongest ovule number phenotype was found in insertion mutants in At3g51050, a gene that was recently identified in a screen for enhancers of exocyst-mediated root phenotypes and named *NEW ENHANCER OF ROOT DWARFISM 1* (*NERD1*) (Cole et al., 2018). The second locus with T-DNA insertions affecting ovule number identified in our screen was At3g60660, which we call *OVULE NUMBER ASSOCIATED 2* (*ONA2). ONA2* encodes an unknown protein containing a DUF1395 domain (TAIR) (Figure 3.3C).

3.4.3   *NERD1* is a positive regulator of ovule number

We focused our analysis on *NERD1* since it had the strongest effect on ovule number. The fruits of homozygous mutants in two T-DNA insertion alleles, *nerd1-2* (described in (Cole et al., 2018) and *nerd1-4,* had fewer ovules than wild-type plants (Figure 3.7A). To confirm that this resulted

from the disruption of NERD1, we generated transgenic plants expressing a translational fusion of the *NERD1* protein with the red-fluorescent protein tdTomato under the control of the native *NERD1* promoter. In *nerd1-2* and *nerd1-4* mutants, this transgene fully rescued the reduced ovule phenotype and resulted in plants with ovule numbers indistinguishable from Col-0 (Figure 3.7A). This demonstrates that *NERD1* is a positive regulator of ovule number.

In addition to reduced ovule number per flower, homozygous *nerd1* mutants had fertility defects. Homozygous *nerd1-2* mutants had 100% unfertilized ovules and homozygotes of the less severe *nerd1-4* allele had 75% unfertilized ovules (Figure 3.7B-C and 3.8A). *nerd1* mutants displayed both male and female defects. Homozygous *nerd1-2* mutants pollinated with Col-0 pollen displayed around 40% unfertilized ovules, indicating a female defect (Figure 3.8A). A developmental analysis of embryo sac development in homozygous *nerd1-2* mutants revealed that 38% embryo sacs were abnormal, with defects visible as early as the first mitosis (stage FG2) and mature ovules having a range of defects from only having 2 nuclei to complete collapse of the embryo sac (Figure 3.7D-E, 3.8A and 3.9A). Pollen tube attraction to ovules requires proper differentiation of the embryo sac since the synergid cells secrete the LURE pollen tube attractants (Higashiyama et al., 2001; Okuda et al., 2009). The defective embryo sacs in *nerd1-2* mutants do not appear to differentiate the synergid, egg, and central cells necessary for double fertilization. Consistent with the defects in embryo sac development, only 41% of ovules attracted pollen tubes in *nerd1-2* pistils pollinated with Col-0 pollen (Figure 3.8B-C). Homozygous *nerd1-4* mutants displayed similar defects in embryo sac development, but a higher percentage of embryo sacs differentiated normally (Figure 3.10A-B).

Pollen development is also defective in *nerd1* mutants. During pollen development, the microspore mother cell undergoes meiosis to form a tetrad of four microspores. Tetrads were produced in *nerd1-2/nerd1-2* anthers, but 3 out of the four microspores collapsed and appeared to be aborted in mutant tetrads (Figure 3.7F). In the *nerd1-2* allele, later stages of pollen development were also defective and no viable pollen grains could be detected in mature anthers (Figure 3.7G-H, 3.9B). The less severe *nerd1-4* allele displayed similar defects in pollen development, but, similar to embryo sac development in both alleles, some normal pollen grains were produced (Figure 3.10C-D).

Both *nerd1-2* and *nerd1-4* segregate as recessive mutations in a 1:2:1 ratio in F2 populations (Table 3.1). This suggests that the male and female reproductive defects are sporophytic rather than gametophytic. To test this, we performed reciprocal crosses between heterozygous *nerd1-2* mutants and Col-0 wild-type plants (Table 3.2). When heterozygous *nerd1-2/NERD1* was used as the female, there was no transmission defect, demonstrating that the reduced female fertility in *nerd1-2* mutants was not female gametophytic. When *nerd1-2/NERD1* was used as the pollen donor, the transmission efficiency of the mutant allele was reduced to 45%, indicating a partial male gametophytic transmission defect (Table 3.2). Even though the *nerd1* F2 segregation ratios fit a 1:2:1 segregation by a *Chi*-squared test, it should be noted that the number of homozygous *nerd1* individuals is lower than wild-type individuals in both alleles (Table 3.1), consistent with a mild male gametophytic transmission defect.

3.4.4   *NERD1* encodes an integral membrane protein

Phylogenetic analyses indicate that *NERD1* is a member of a low-copy number, highly conserved gene family that is found throughout the plant kingdom and in cyanobacteria (Figure 3.11A-B and

(Cole et al., 2018)). The NERD1 protein is predicted to be an integral membrane protein with a signal peptide and one transmembrane domain (Figure 3.12A). The majority of the protein is predicted to be extracellular, with the transmembrane domain located near the C-terminus and a 17 amino acid cytoplasmic extension. Transient expression of a NERD1-GFP fusion in *Nicotiana benthamiana* with subcellular markers confirmed that NERD1 puncta colocalize with the Golgi marker and partially overlap with a plasma membrane marker (Figure 3.12B and D). NERD1 does not co-localize with ER, peroxisome, and plastid markers Figure 3.12C, 3.13). Consistent with NERD1-GFP localization reported in (Cole et al., 2018), our Arabidopsis plants complemented with the NERD1-tdTomato fusion protein driven by the native NERD1 promoter had NERD1-tdTomato signal in a punctate pattern consistent with Golgi in roots and early stages of ovule development, but it was not detected in plasma membrane (Figure 3.14).

3.4.5   *NERD1* is expressed throughout Arabidopsis development

The *nerd1* ovule number and fertility phenotypes suggest that *NERD1* should be expressed in developing flowers. We used a *NERD1$_{pro}$::gNERD1-GUS* fusion to examine *NERD1* expression throughout Arabidopsis development. In *NERD1$_{pro}$::gNERD1-GUS* inflorescences, GUS activity was detected throughout flower development, including inflorescences, developing and mature anthers, and in the stigma, ovules, and carpel walls of mature pistils (Figure 3.15). NERD1-GUS activity was present in the carpel margin meristem (CMM) in stage 9 flowers, where ovule initiation occurs (Figure 3.15C and E). *NERD1* reporter expression in the CMM during pistil development is consistent with a role for *NERD1* during ovule initiation. During seedling development, the *NERD1-GUS* reporter was detected in shoot and root apical meristems (SAM and RAM) and in the vasculature (Figure 3.15I). Our GUS reporter results are consistent with tissue-specific transcriptome data from ePlant (Figure 3.16), suggesting that NERD1 is

ubiquitously expressed throughout the plant and that the NERD1 promoter used in our experiment accurately reflects endogenous transcription.

3.4.6   Overexpression of NERD1 increases plant productivity

We examined *NERD1* transcript levels in the low ovule number accession Altai-5 compared to Col-0. *NERD1* transcript accumulation was reduced in Altai-5 and Kas-2 buds as compared to Col-0 but similar in Altai-5 and Col-0 leaves (Figure 3.17A-B). We hypothesized that the low ovule number in Altai-5 may be linked to reduced *NERD1* expression in developing flowers. In order to determine whether increasing *NERD1* expression is sufficient to increase ovule number, we transformed Col-0 and the low ovule number accession Altai-5, with a *NERD1-GFP* fusion construct driven by the constitutively expressed Cauliflower Mosaic Virus 35S promoter (*35S::NERD1-GFP*). Overexpression of *NERD1* had no effect on ovule number in the Col-0 background, but significantly increased ovule number in the Altai-5 background (Figure 3.18A-C), indicating that the *NERD1* effect on ovule number is background-dependent. The *35S::NERD1-GFP* plants displayed an even more striking phenotype when overall plant architecture was examined (Figure 3.18A). In both the Altai-5 and Col-0 backgrounds, *NERD1* overexpression led to increased branching (Figure 3.18D) and shortened internode lengths between flowers, leading to an overall increase in flower number in the overexpression plants compared to untransformed controls (Figure 3.18E-H). Thus, *NERD1* overexpression leads to increased biomass and reproductive capacity, with up to a 2.5-fold increase in total flower number over the lifespan of the plant. While all independent transformants displayed increased branching and flower number, some of the *35S::NERD1* plants were male sterile (Figure 3.19). This male sterility correlated with *NERD1* expression levels and plants with higher *NERD1* transcript levels had more severe male sterility (Figure 3.19). The sterility effect was more severe in Col-0 than in Altai-5

(Figure 3.19). The lower endogenous *NERD1* expression in Altai-5 inflorescences might explain the lower sensitivity of Altai-5 to *NERD1* overexpression with respect to male fertility, demonstrating background-dependent sensitivity to *NERD1* levels for both ovule number and male sterility.

NERD1 was recently identified in enhancer screen performed on exocyst mutants with weakly dwarfed roots. *nerd1* mutants have reduced root growth as a result of impaired cell expansion, indicating that NERD1 may be a positive regulator of exocyst-dependent root growth (Cole et al., 2018). Consistently, the *35S::NERD1-GFP* plants had longer roots compared to the Col-0 control, indicating that root development is also sensitive to *NERD1* expression levels (Figure 3.20).

Four SNPs in *NERD1* exons showed significant correlation with ovule number in our GWAS (Figure 3.21A-B). Three of them are synonymous SNPs that are not predicted to change the amino acid sequence, but the fourth is a non-synonymous SNP (C to A change in comparison to Col-0 reference) causing a Serine to Tyrosine change at amino acid 230 of NERD1 (Figure 3.21A-B). This non-synonymous SNP was present in 10 out of the 16 lowest ovule number accessions and not present in the 16 highest ovule number accessions (Figure 3.21A). Across all of the accessions in our GWAS panel, the "A" allele at this position was significantly associated with lower ovule numbers (Figure 3.21C). However, some accessions with the "C" allele of *NERD1* have low ovule numbers (Figure 3.21A), including the Altai-5 accession described above. We examined *NERD1* transcript levels in additional low ovule number accessions to determine if *NERD1* expression correlated with ovule number in other accessions. Like Altai-5, the "C" allele accession Kas-1 had reduced *NERD1* transcript levels in flowers when compared to Col-0 (Figure 3.17A-B).

However, four "A"-containing accessions with the S230Y amino acid change had similar or higher expression levels of *NERD1* in developing flowers (Figure 3.17C-D), indicating that reduced *NERD1* expression in flowers is not the explanation for reduced ovule number in these accessions. A second possibility is that the S230Y amino acid change affects the protein function of NERD1 in these accessions. To test this hypothesis, we transformed *nerd1-2* mutants with *NERD1* from both Gre-0 and Hh-0 expressed as td-Tomato fusions driven by their native promoters. Both of these *NERD1* genes could complement the *nerd1-2* ovule number phenotype (Figure 3.22), indicating that some other mechanism influences ovule number in these accessions.

3.5 Discussion

Our experiments revealed that Arabidopsis displays a wide variation in the number of ovules per flower, a key component of plant fitness and crop yield. Association genetics linked this natural variation to the plant-specific gene, *NERD1*, that regulates the number of ovules produced in Arabidopsis flowers and gametophyte development (Figure 3.7) and was previously found to alter root growth (Cole et al., 2018). Overexpression of *NERD1* led to dramatic effects on plant architecture, indicating that *NERD1* may be involved in regulating meristem activity during Arabidopsis development.

3.5.1 GWAS reveals new ovule number-associated loci in Arabidopsis

A quantitative trait locus (QTL) mapping study utilizing variation between L*er* and Cvi identified QTL residing on chromosomes 1, 2 (near the *ERECTA* gene), and two QTL on chromosome 5 (Alonso-Blanco et al., 1999). No follow-up study has identified the genes underlying these QTL. Our population displayed a much larger range of ovule numbers per flower (39-84) than that seen in Cvi vs L*er* (66 and 56, respectively). We identified 9 significant associations in our GWAS, but

only one potentially overlaps with a known ovule number QTL (see chromosome 5 in Figure 3.4). Of the genes with an identified effect on ovule number, only BIN2 overlapped with a GWAS peak, indicating that our study has revealed at least seven novel regulators of ovule number in Arabidopsis. We molecularly identified two new genes that control ovule number that were linked to two GWAS peaks on chromosome 3. This expands that number of known ovule number determinants and confirms the value of GWAS as a forward genetics tool.

3.5.2 NERD1 may play a role in the secretory system

NERD1 is a plant-specific, low copy number gene that is found throughout the plant kingdom. *NERD1* was recently identified as an enhancer of root development phenotypes in weak mutants of the exocyst subunits SEC8 and EXO70A1 (Cole et al., 2018). While a direct interaction with the exocyst could not be identified, the authors identified Golgi localization of NERD1 and hypothesized that NERD1 could be involved in synthesizing or modifying pectins or other polysaccharide components of the cell wall that are synthesized in the Golgi and transported to the cell wall (Cole et al., 2018). Changes in cell wall elasticity mediated by pectin modifications have been correlated with lateral organ initiation at the shoot apical meristem (Peaucelle et al., 2008; Peaucelle et al., 2011). The decreased ovule number in *nerd1* mutants and increased lateral branching and flower initiation in *35S::NERD1* transformants could be consistent with alterations in Golgi-synthesized cell wall components affecting cell wall mechanics and organ initiation.

3.5.3 *NERD1* and fertility

Homozygous *nerd1* mutants are completely male sterile and partially female sterile. This sterility is due to a lack of pollen production and problems in female gametophyte development leading to aborted embryo sacs. Transmission efficiency tests using heterozygous loss-of-function mutants

revealed that *nerd1* could be transmitted through the egg at near 100% efficiency, indicating a sporophytic effect on female gametophyte development. Ovule development mutants that have defective integument development such as *short integuments 1* (*sin1*), *bell 1* (*bel1*) and *ant* fail to produce functional female gametophytes, indicating that female gametophyte development is dependent on properly differentiated sporophytic cells in the ovule (Modrusan et al., 1994; Elliott et al., 1996; Schneitz et al., 1997). Sporophytic development in ovules seem to be normal in *nerd1* mutants, yet embryo sacs abort. As a membrane protein, NERD1 could transmit some unknown signal between sporophytic and gametophytic cells during embryo sac development.

The male fertility defect in *nerd1* plants is more severe than the female defect. Homozygous *nerd1* anthers have severe reductions in pollen production resulting from defects in early stages of pollen development. Transmission efficiency tests using pollen from heterozygous *nerd1* plants crossed to wild-type females revealed that *nerd1* also has gametophytic effects on pollen function. The sporophytic effects could be related to early stages of anther development. In particular, specification of the tapetum is critical for pollen development (reviewed in (Wilson and Zhang, 2009)). In our *35S::NERD1* experiment, transformants that accumulated the most *NERD1* transcripts were male sterile. Together these results indicate that pollen development is sensitive to *NERD1* levels, i.e. either too much or too little *NERD1* is detrimental to pollen development. Future experiments should focus on determining the stage of anther and/or pollen development that is affected in *nerd1* mutants and the specific cell types that express *NERD1* in developing anthers.

Even though *NERD1* is expressed broadly throughout the plant, above ground vegetative development appears to be normal in *nerd1* loss-of-function mutants. However, *nerd1* roots are shorter than normal and have root hair defects that include bulging and rupture (Cole et al., 2018). *NERD1* could have distinct or related developmental functions in roots and flowers, as is seen for many of the genes involved in hormonal regulation of development (Schaller et al., 2015).

3.5.4   *NERD1* and lateral organ formation

NERD1 overexpression under control of the constitutive 35S promoter dramatically changed plant architecture in both the Col-0 and Altai-5 backgrounds. Overexpression phenotypes can be difficult to interpret since the 35S promoter could be active in cells where NERD1 is not normally expressed, causing NERD1 to interfere with pathways specific to those cell types. Alternatively, the increase in lateral organ formation seen in *35S::NERD1* plants could be related to increased root capacity that changes source/sink relationships within the plant and leads to higher plant productivity. This hypothesis is consistent with the smaller roots reported in *nerd1* mutants and could be related to the secretory machinery and trafficking (Cole et al., 2018). A third possibility is that NERD1 is a positive regulator of meristem activity. *NERD1* overexpression plants produced significantly more branches than wild-type controls and produced significantly more flowers that were produced at closer intervals along the stem. Like branches and flowers, ovules are lateral organs produced from meristematic cells. Lateral meristem activation and subsequent branching have been shown to be affected by several different hormones (reviewed in (Rameau et al., 2014)). Classic experiments in *Vicia faba* showed that auxin produced in the shoot apex inhibits axillary meristems (Thimann and Skoog, 1933), and more recently strigolactones were identified as graft-transmissible suppressors of branching (reviewed in (Domagalska and Leyser, 2011)). Gibberellins also repress shoot branching in Arabidopsis, maize, and rice, with GA-deficient

mutants displaying increased branching compared to wild-type controls (Silverstone et al., 1997; Lo et al., 2008; Best et al., 2016; Best et al., 2017). In contrast, cytokinins and brassinosteroids are both positive regulators of branching (Wickson and Thimann, 1958; Sachs and Thimann, 1967; Yin et al., 2002; Best et al., 2016; Best et al., 2017). The mechanism through which these plant hormones work together to regulate branching is unknown, but auxin has been proposed to control cytokinin and strigolactone biosynthesis (Foo et al., 2005; Shimizu-Sato et al., 2009), while the brassinosteroid signaling regulator *BES1* may inhibit strigolactone signaling to promote branching (Wang et al., 2013). The promotion of branching in *35S::NERD1* plants could be related to regulation of one or more of these hormonal pathways. Like *NERD1*, upregulation of both cytokinin and brassinosteroid signaling pathways have been shown to positively regulate branching and ovule number (Yin et al., 2002; Bartrina et al., 2011; Wang et al., 2013), suggesting that *NERD1* may be intimately connected to these pathways. Future research is needed to explore the intersection between *NERD1* and hormonal pathways.

3.5.5   *NERD1*-induced increases in ovule number are background-dependent

Overexpression of *NERD1* in the Col-0 and Altai-5 backgrounds led to increased branching and flower number, but ovule number was only increased in the Altai-5 background, suggesting a background-dependence on the ovule number trait. In Arabidopsis, natural accessions were shown to respond differently in their ability to buffer GA perturbations caused by overexpressing GA20 oxidase 1, which encodes a rate-limiting enzyme for GA biosynthesis (Nam et al., 2017). Genetic background dependence has been shown to be a wide-spread phenomenon in *C. elegans*, with approximately 20% of RNAi-induced mutations (out of 1400 genes tested) displaying different phenotypic severity in two different genetic backgrounds (Vu et al., 2015). Similar to our results with *NERD1*, where Altai-5 has lower endogenous levels of the *NERD1* transcript in developing

flowers compared to Col-0, the severity of the *C. elegans* phenotypes could be linked to gene expression levels of either the target gene itself or other genes in the same pathway (Vu et al., 2015).

Our GWAS revealed multiple novel loci that control ovule number in Arabidopsis. It remains to be seen if exocyst function is linked to NERD1's role in ovule number determination. Identification of NERD1 interacting proteins will provide candidates for other players in the NERD1 pathway. Some of the other novel loci identified in our GWAS may well participate in the same signaling pathway as *NERD1*. While *NERD1* is a promising candidate for engineering plants with increased ovule number, the differential responses to *NERD1* overexpression seen in Altai-5 and Col-0 suggest that specific alleles at other loci may be necessary for achieving maximum effect of *NERD1* overexpression.

3.6   Figures and tables
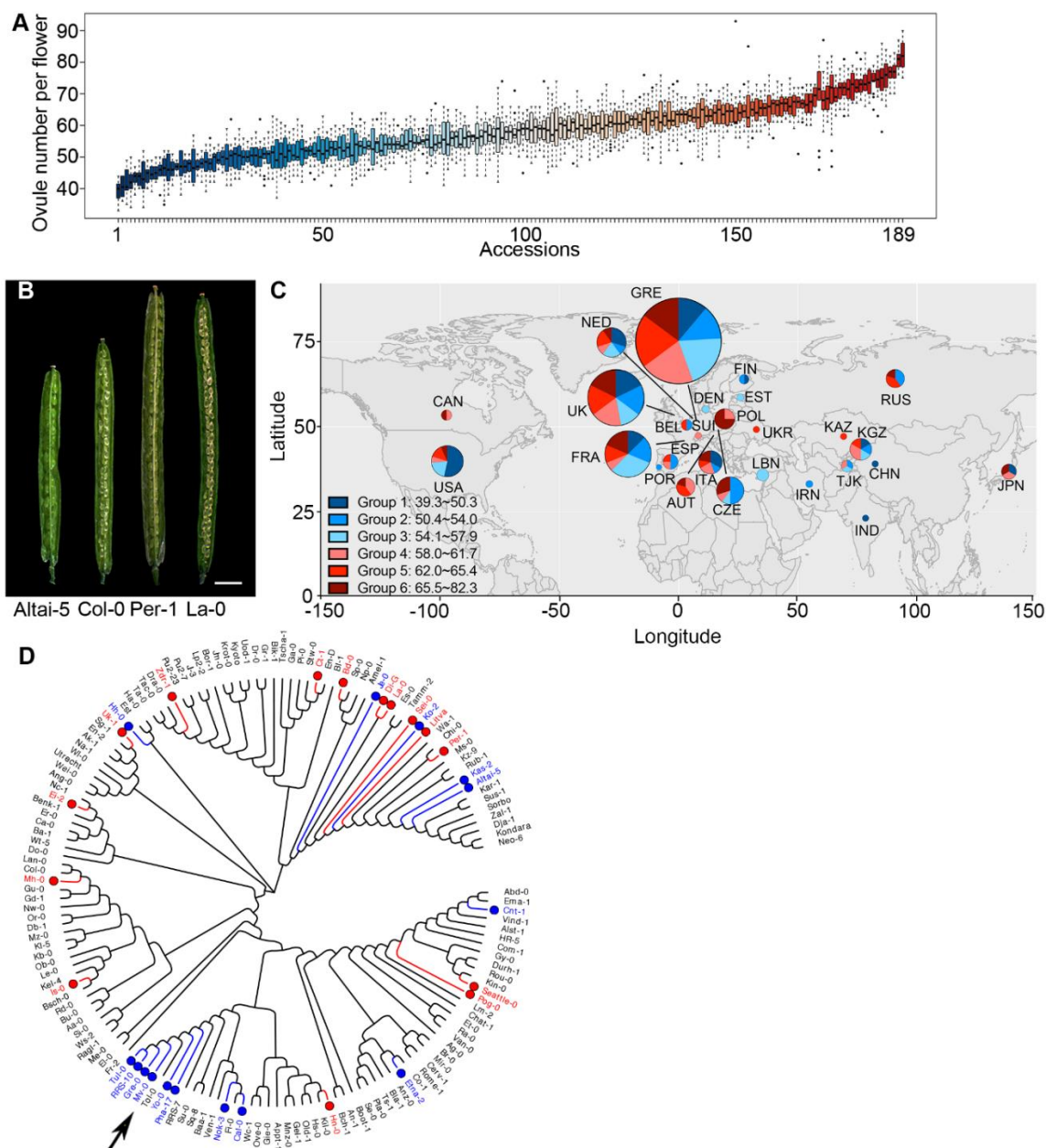
Figure 3.1 Arabidopsis accessions display natural variation in ovule number per flower.

(A) Boxplot of ovule number in 189 Arabidopsis accessions. The detailed names of these accessions are in Table 3.3. (B) Dissected siliques of low, medium, and high ovule number accessions (Bar=2.0mm). (C) Geographic distribution of accessions. Groups 1 to 6 correspond to ovule number ranking (from low to high), with the colors corresponding to panel A. The pie chart indicates the percentage of accessions in each country in each ovule number group, while the size of the pie chart corresponds to the total number of accessions per country. (D) Cladogram of accessions used in this study (generated in MEGA7). The 15 accessions labeled in blue had the lowest ovule numbers, and the 15 accessions labeled with red had the highest ovule numbers. The arrow points to a clade with clustered low ovule number accessions.
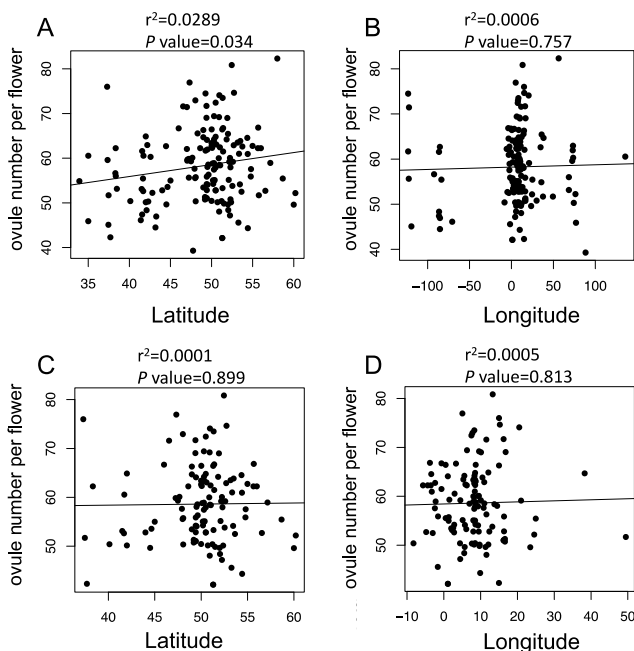
Figure 3.2 Statistical analysis of the relationship between ovule number per flower and geographical origin of the accessions used in the GWAS.

(A-B) A weakly positive correlation was detected between latitude and ovule number when all accessions were considered. (C-D) No correlation between ovule number and latitude or longitude was identified when only European accessions were tested. A Pearson correlation coefficient was computed to assess the relationship between the ovule number per flower and their geographic distribution of latitude or longitude, respectively. There was a slight correlation between the ovule number per flower and latitude distribution when accessions from all locations were tested [r2 = 0.0289, p value = 0.034]. There was no correlation between the ovule number per flower and longitude when accessions from all locations were tested [r2 = 0.0006, p value = 0.757]. There was no correlation between the ovule number per flower and latitude or longitude of the accessions' origin when only European accessions were tested [r2 = 0.0001 or 0.0005, p value = 0.899 or 0.813], respectively.
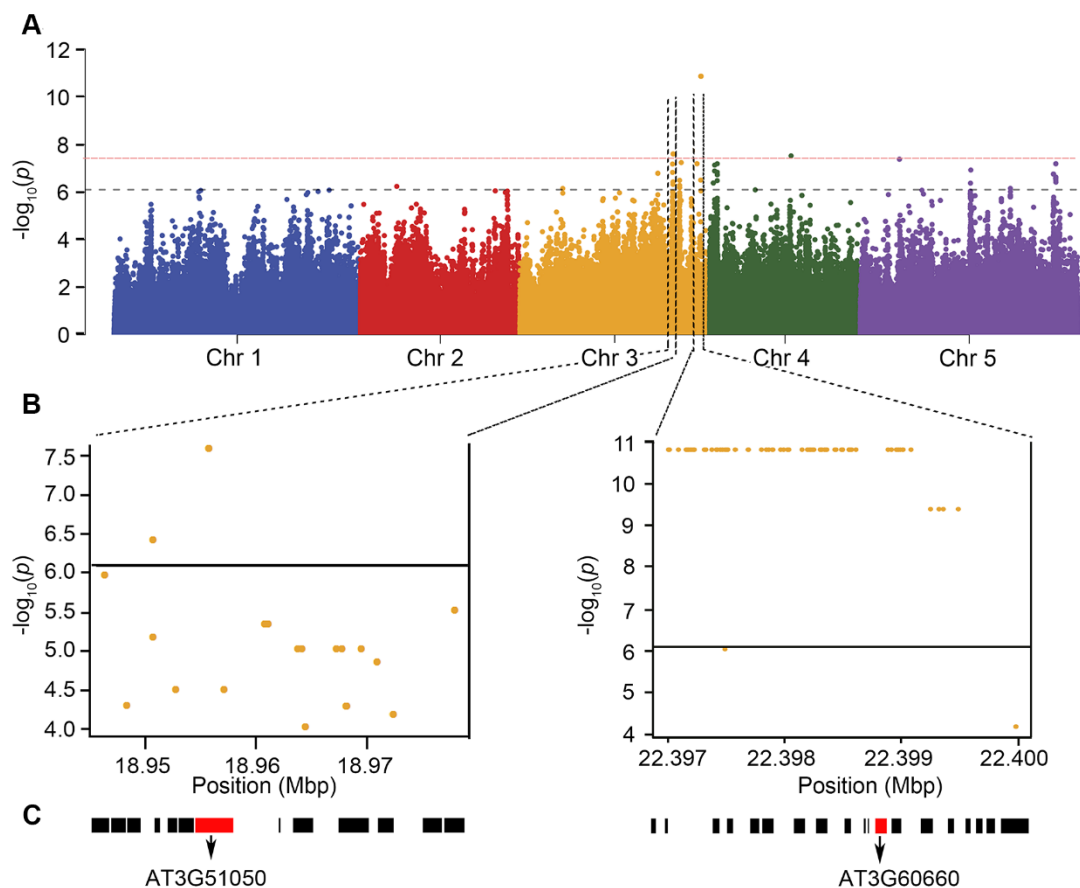
Figure 3.3 GWAS identifies candidate loci associated with ovule number per flower. (A) Manhattan plot for the SNPs associated with ovule number per flower.

(A) Manhattan plot for the SNPs associated with ovule number per flower. Chromosomes are depicted in different colors. The horizontal blue dashed line corresponds to a $-\log_{10}(p$ values) $\geq$ 6.2 and the red dashed line corresponds to $-\log_{10}(p$ values) $\geq$ 7.5 after Benjamini Hochberg (False Discovery Rate) correction. (B) The genomic region surrounding the two most significant GWA peaks on Chromosome 3. (C) Genes in the genomic region surrounding the two significant GWA peaks in (B). The red boxes are AT3G51050 (*NERD1*) and AT3T60660 (*ONA2*).
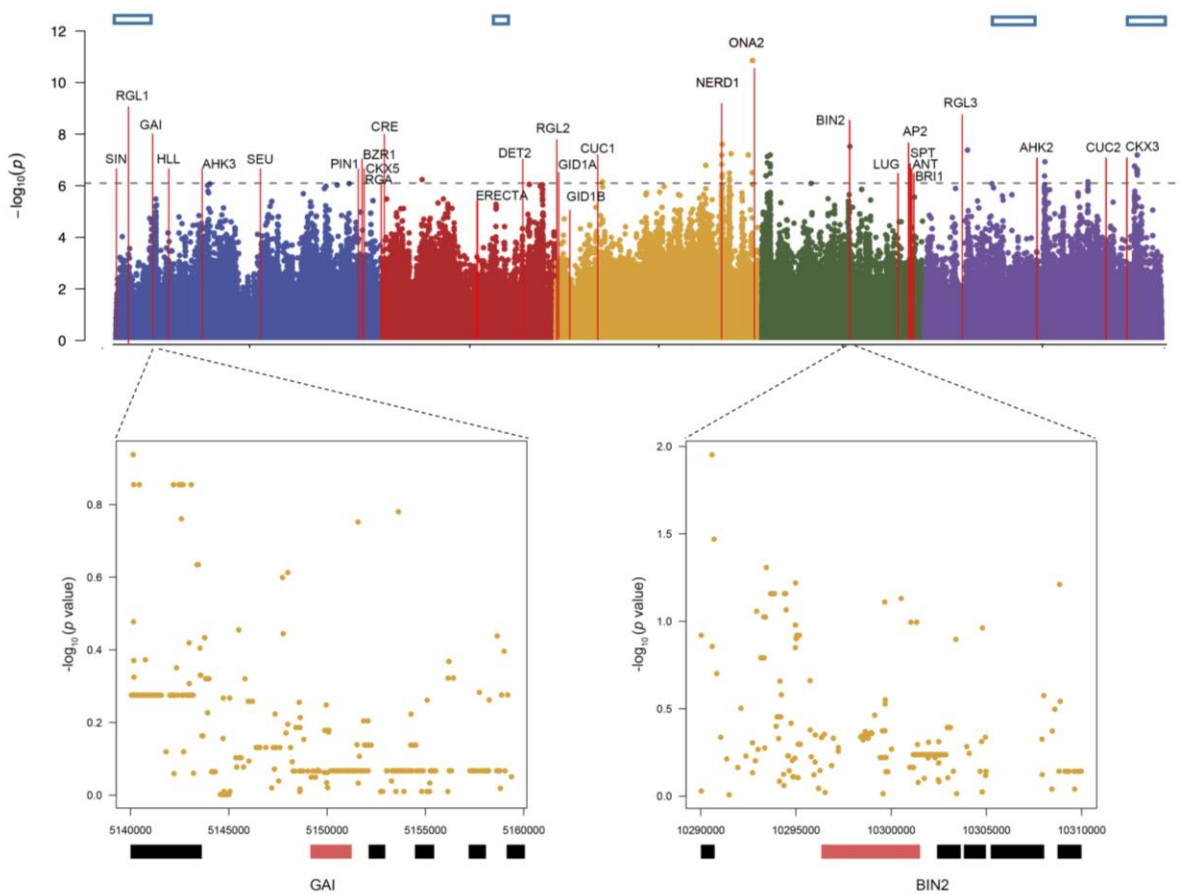
Figure 3.4 Previously identified ovule number related genes' positions in relation to the Manhattan plot from the ovule number GWAS.

The Manhattan plot is the same as in Figure 2. Red lines indicate the known ovule number related genes. Blue boxes indicate the genomic regions underlying 4 ovule number QTL identified by Alonso et al, 1999.
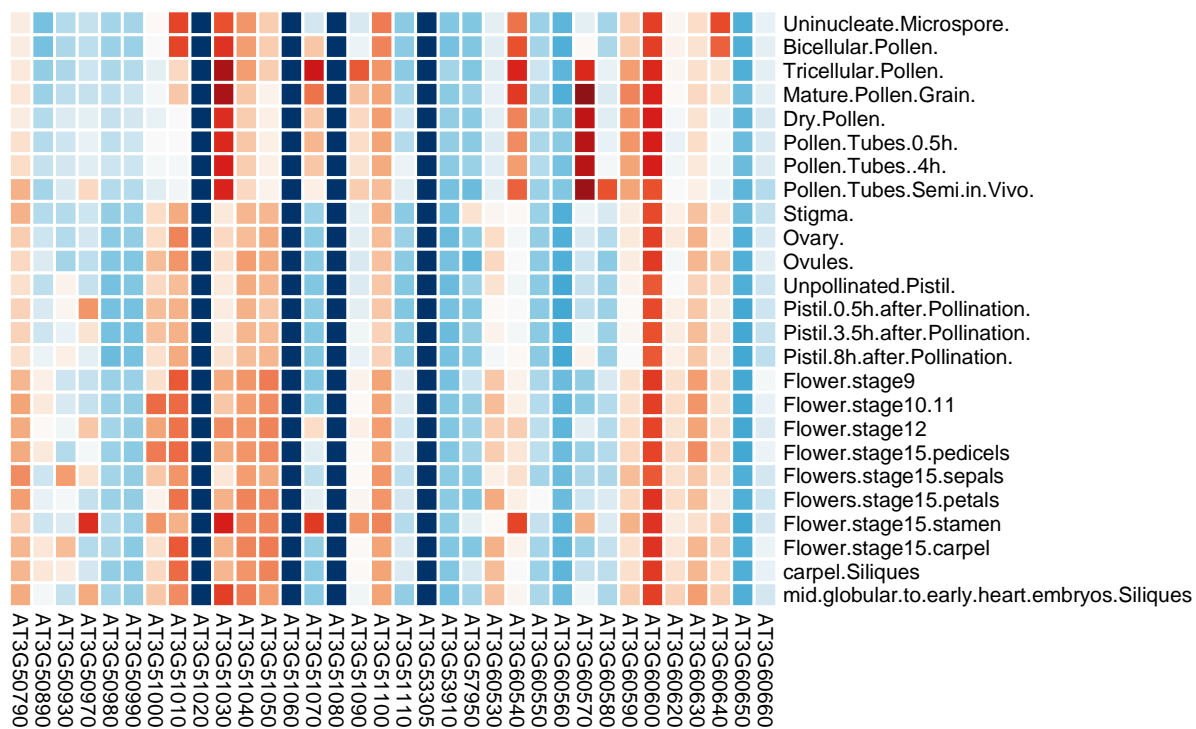
Figure 3.5 Heat map of candidate gene expression patterns in reproductive tissues. Colors from blue to red indicate the gene expression level from low to high.
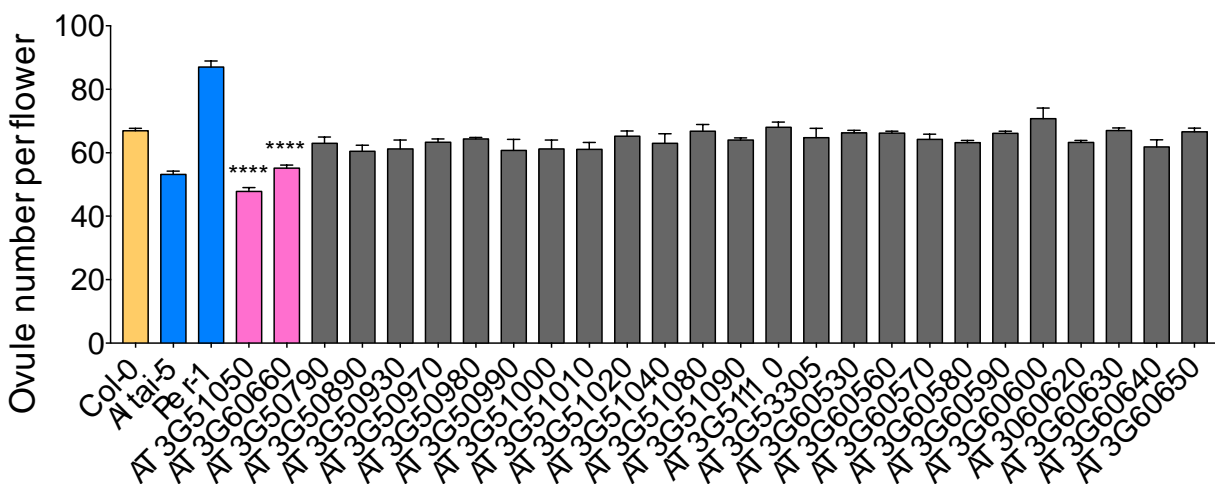
Figure 3.6 Total ovule number per flower of all available T-DNA insertion mutants in ovule number-associated genomic regions on chromosome 3.

"****" indicates statistical significance (*p* value < 0.0001 determined by Student's t-test).
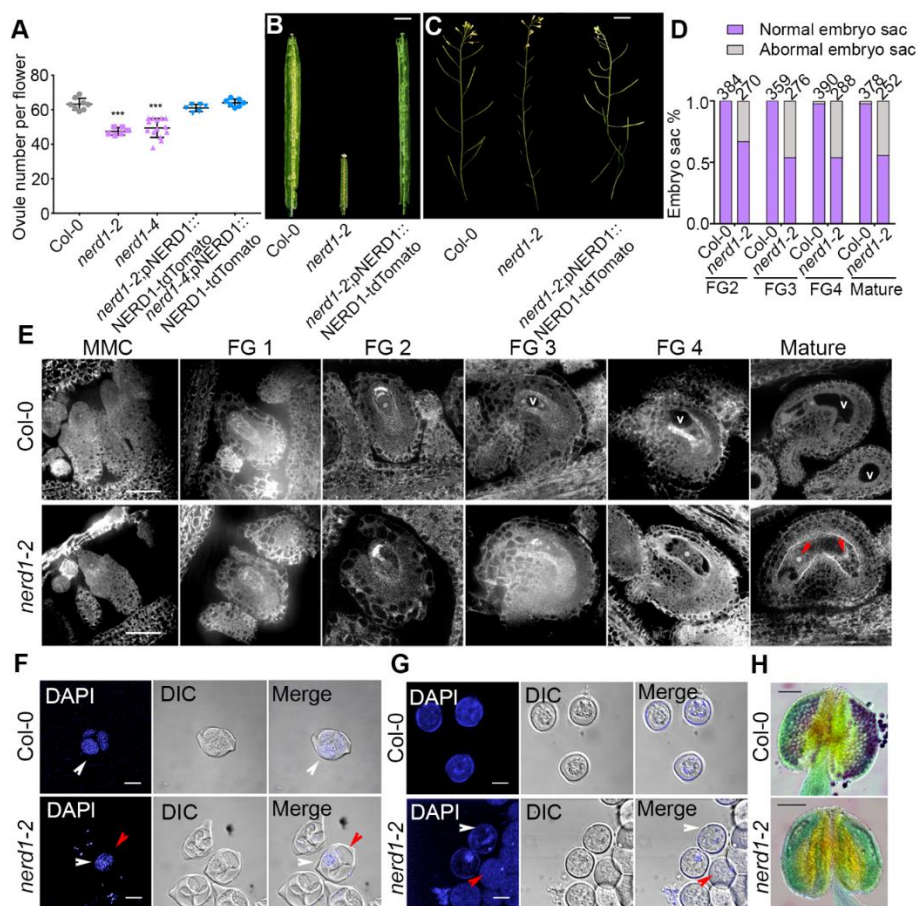
Figure 3.7 *nerd1* mutants have reduced ovule number and fertility.

 (A) Scatter plot of ovule number per flower in Col-0, *nerd1-2*, *nerd1-4* and their complementation lines. "***" indicates statistical significance (*p* value<0.001 determined by Student's t-test). (B-C) *nerd1-2/nerd1-2* displays lower ovule number, infertile ovules, and short siliques compared to Col-0 and complemented lines. (D) Quantification of normal vs abnormal embryo sacs from developmental stages FG2 to mature ovule in Col-0 vs *nerd1-2/nerd1-2*. (E) During female gametophyte development, instead of the functional megaspore developing into female gametophyte by sequential mitotic divisions as seen in Col-0, *nerd1-2/nerd1-2* displays defective embryo sacs from stages FG2 to mature ovule. The central vacuole (V) is absent in FG3 and FG4 *nerd1* embryo sacs and mature ovules often have only 2 nuclei (red arrows) (F-G) DAPI staining of early stages of pollen development. (F) At tetrad stage in pollen development, *nerd1-2/nerd1-2* only has one developed haploid microspore instead of four microspores in Col-0 (white arrowheads indicate normal microspores and red arrowheads indicate aborted microspores). (G) After separation of the microspores, Col-0 has microspores with decondensed chromosomes, while most *nerd1-2/nerd1-2* microspores appear empty (white arrow heads indicate some normal chromosomes and red arrow head indicate empty microspores). (H) Alexander-stained Col-0 anthers have viable pollen grains (red indicates viable pollen while the green is non-viable). Alexander-stained *nerd1-2/nerd1-2* anthers have no viable pollen. Bars=2.5mm (B-C), 30μm (E), 10μm (F-G), 100μm (H).
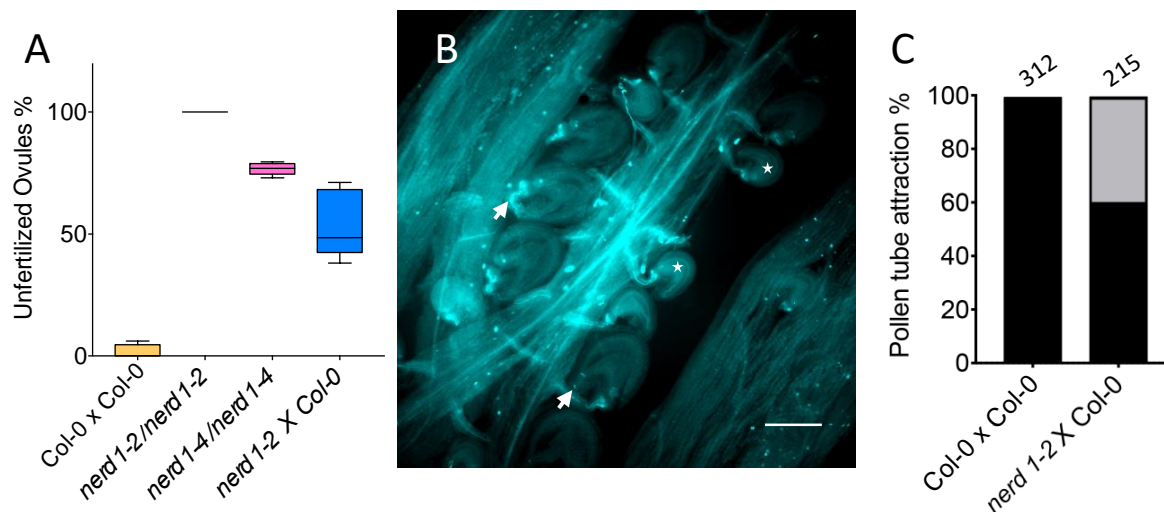
Figure 3.8 Pollen tube guidance in nerd1-2 mutants.

(A) Homozygous nerd1 mutants have high levels of infertility that can be partially rescued by pollinating with Col-0 wild-type pollen. (B) Aniline blue staining for nerd1-2/nerd1-2 pollinated with Col-0 pollen. Arrows indicate fertilized ovules with normal pollen tube attraction and stars indicate unfertilized ovules without pollen tube attraction. Bar = 100 µm. (C) Quantification of pollen tube attraction percentage for nerd1-2/nerd1-2 plants pollinated with Col-0 pollen (black indicates fertilized ovules with pollen tubes and gray indicates unfertilized ovules with no pollen tubes). 5 pistils were analyzed for each cross.

A

nerd1-2 *nerd1-2*

B Microspore Early Bi-cellular Tri-cellular Mature pollen

Col-0

nerd1-2
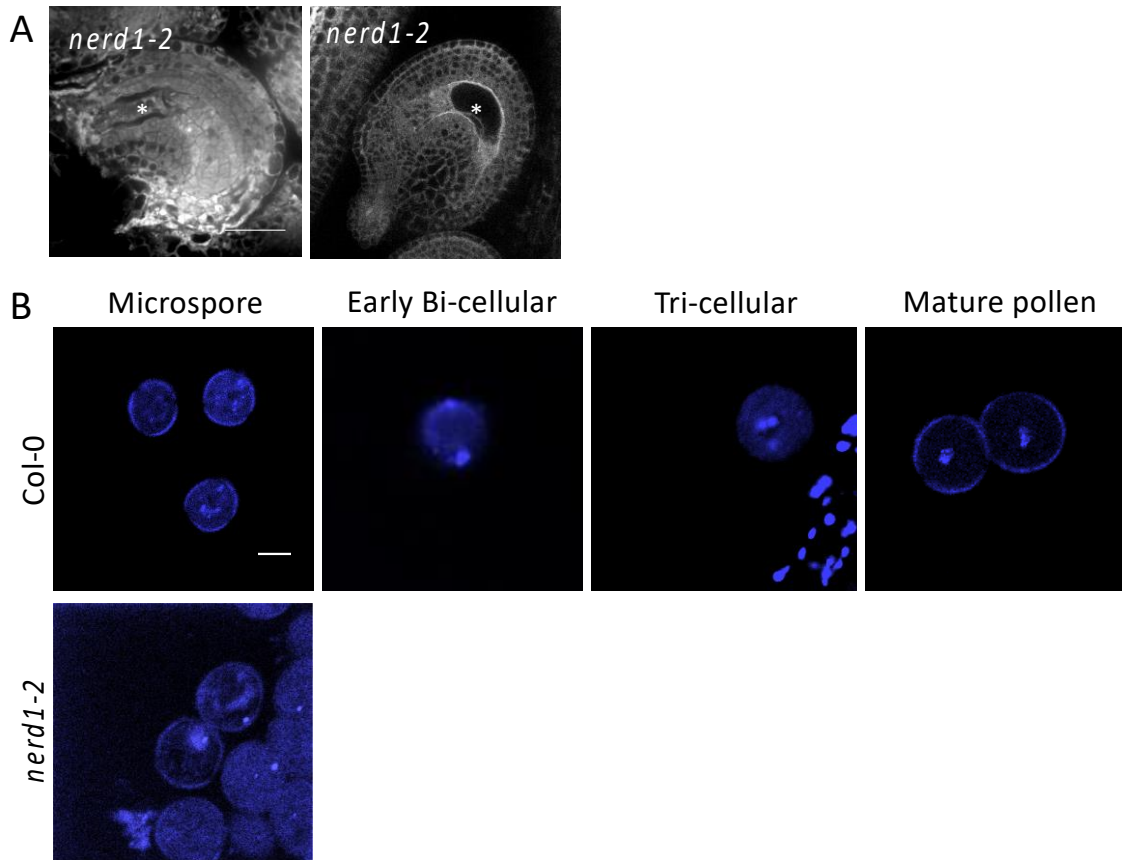
Figure 3.9 *nerd1-2* has both male and female defects.

 (A) Examples of defective embryo sacs in *nerd1-2/nerd1-2* mature ovules. Bar = 50 µm. (B) In comparison to Col-0, *nerd1-2/nerd1-2* has defective microspores and an absence of later pollen stages. Bar = 15 µm.
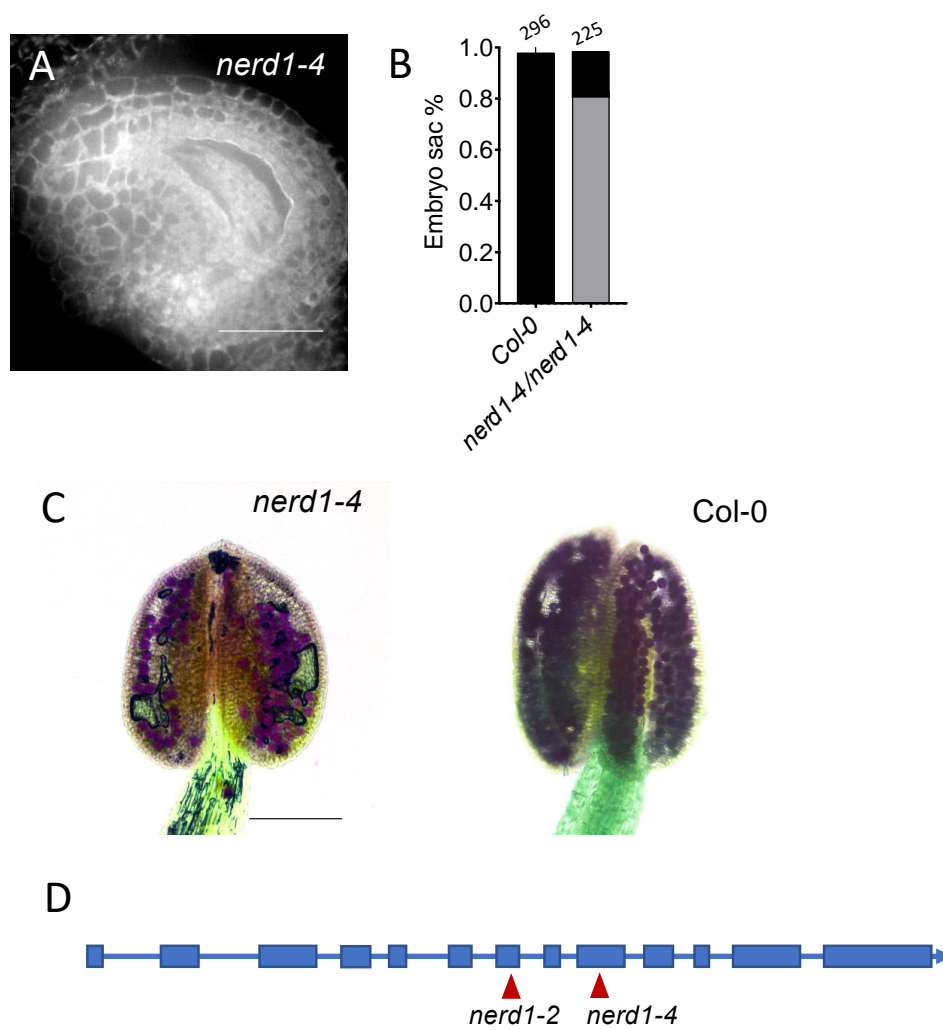
Figure 3.10 *nerd1-4* has defective embryo sacs and reduced pollen production.

(A) Aborted embryo sac in a mature *nerd1-4* ovule. Bar = 50 µm. (B) Comparison of normal (black) vs. defective (gray) embryo sac percentages in Col-0 and *nerd1-4* pistils. (C) Fewer viable pollen grains are present in Alexander stained anthers of *nerd1-4/nerd1-4* compared to Col-0. Bar = 100 µm. (D) T-DNA insertion sites in the NERD1 gene (boxes indicate exons and lines indicate introns).
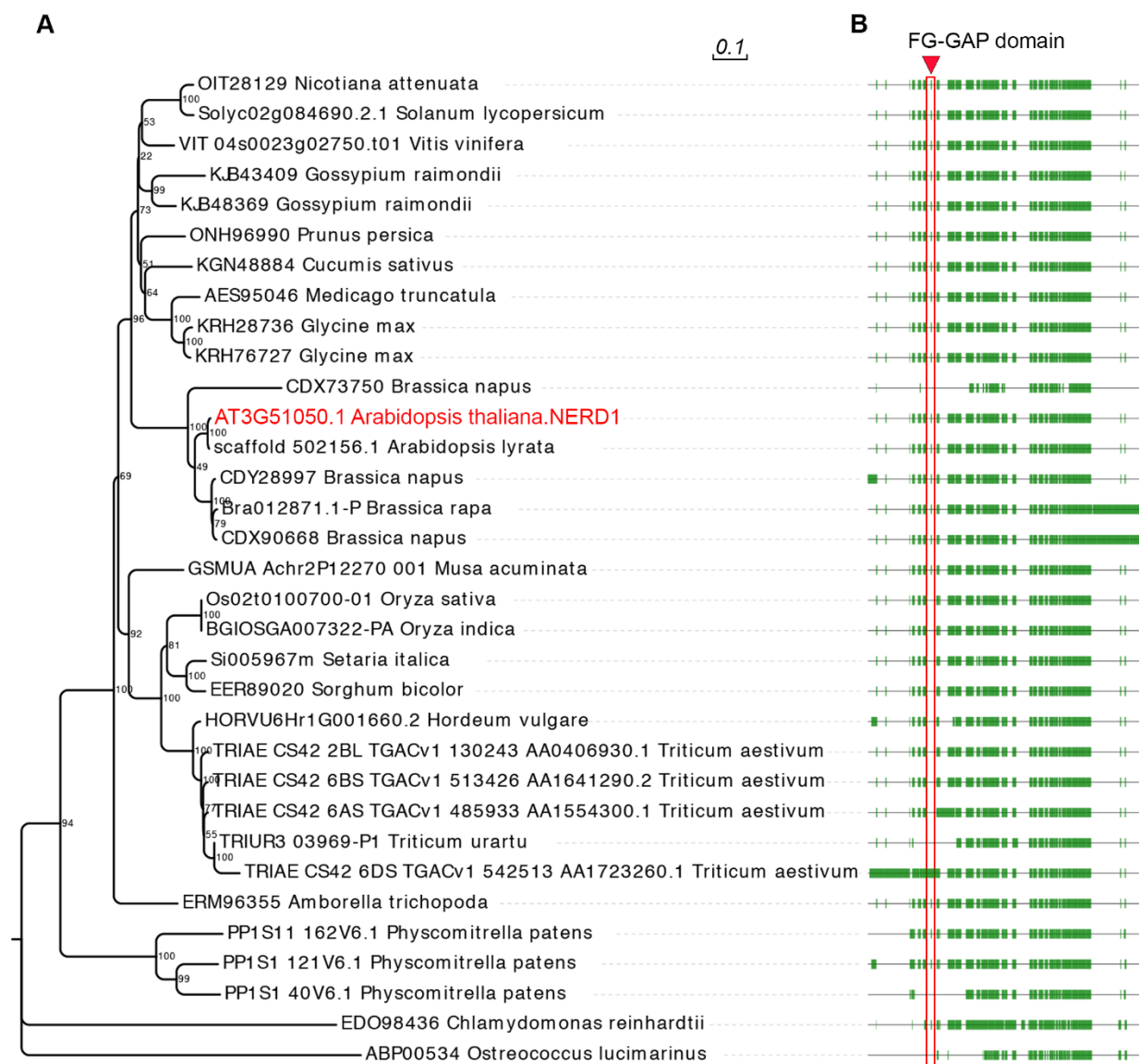
Figure 3.11 NERD1 is conserved across plant lineages.

(A) Phylogenetic tree from amino acid alignment of NERD1 generated using the Neighbor-joining method in MEGA7. (B) NERD1 alignment showing sequence conservation among species. The green boxes correspond to conserved regions of NERD1 and the lines represent gaps in the alignment. The red box indicates the FG-GAP domain annotated in NERD1 by Langhans, et al., 2017.
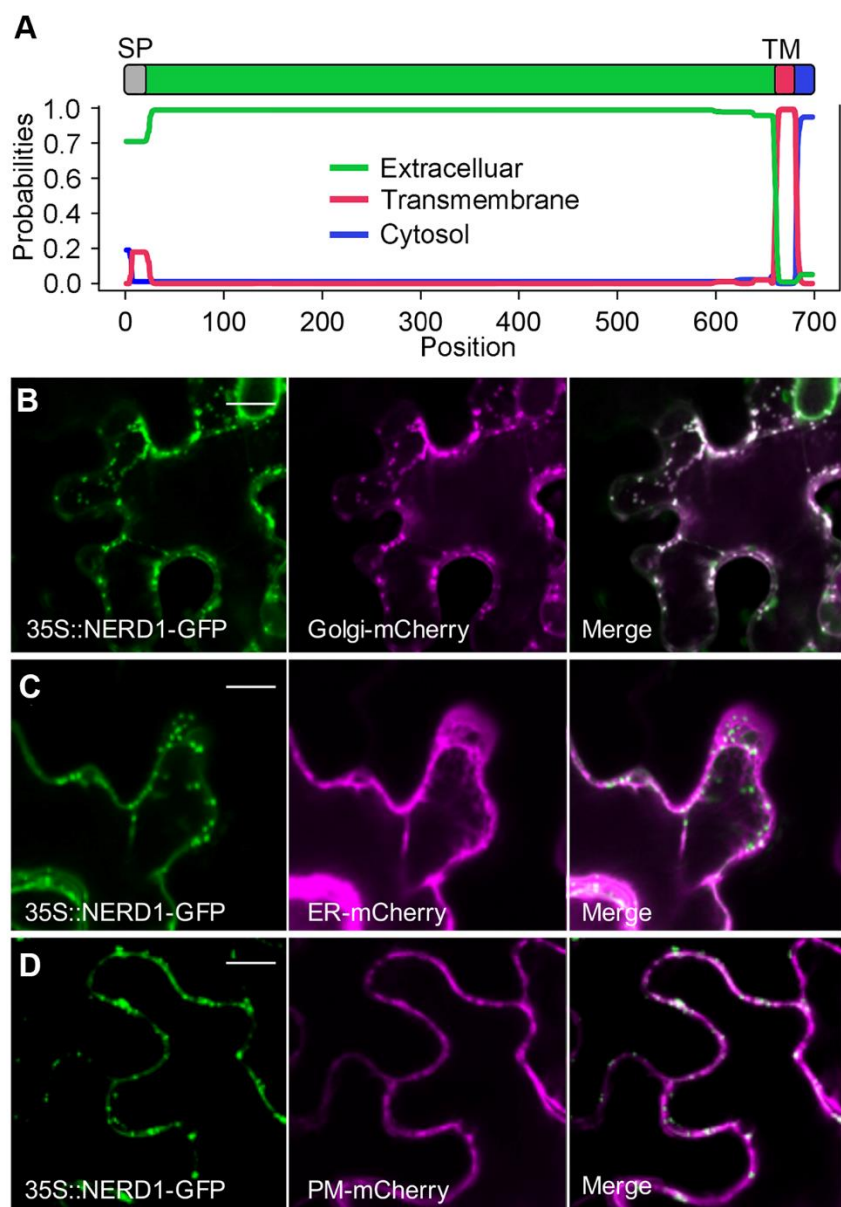
Figure 3.12 NERD1 co-localizes with a Golgi marker in *N. benthamiana* epidermal cells.

(A) NERD1 protein domains determined by TMHMM 2.0. (B) NERD1-GFP (green signal) co-localizes with Golgi-mCherry (magenta signal) in *N. benthamiana* epidermal cells. (C) NERD1-GFP (green signal) does not co-localize with ER-mCherry (magenta signal). (D) NERD1-GFP (green signal) partially overlaps with PM-mCherry (magenta signal). Bars=15 µm.
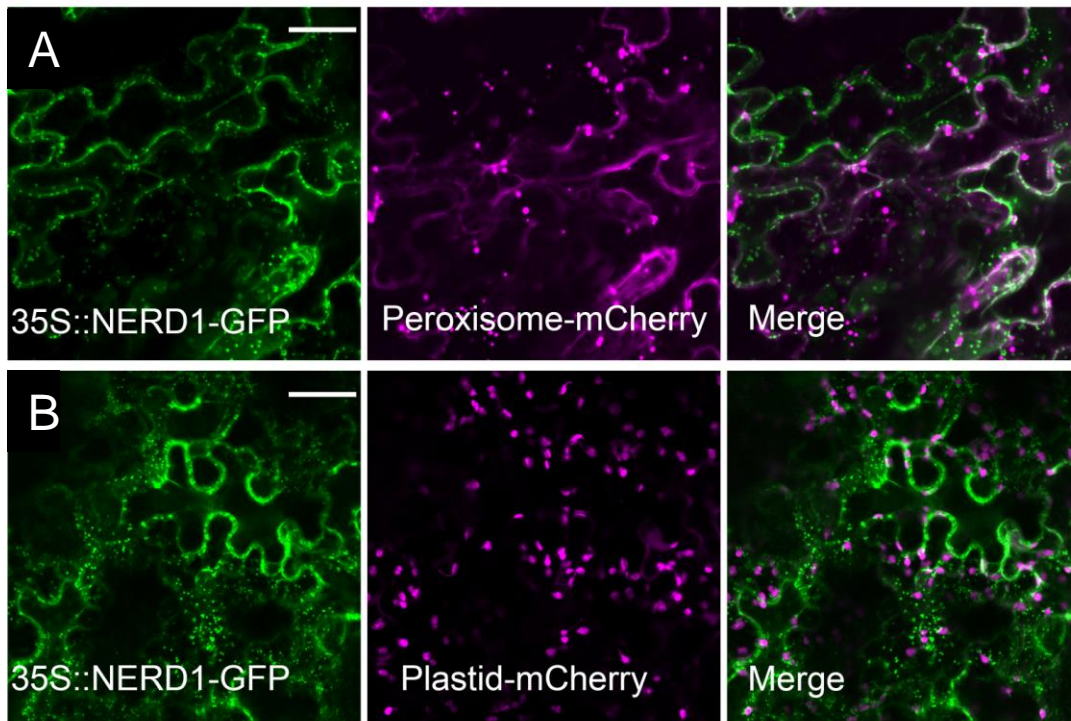
Figure 3.13 Co-localization of 35S::NERD1-GFP with subcellular markers.

(A) 35S::NERD1-GFP (green signal) does not co-localize with Peroxisome-mCherry and (B) Plastid-mCherry (magenta) markers in *N. benthamiana* epidermal cells. Scale bar = 25 µm.
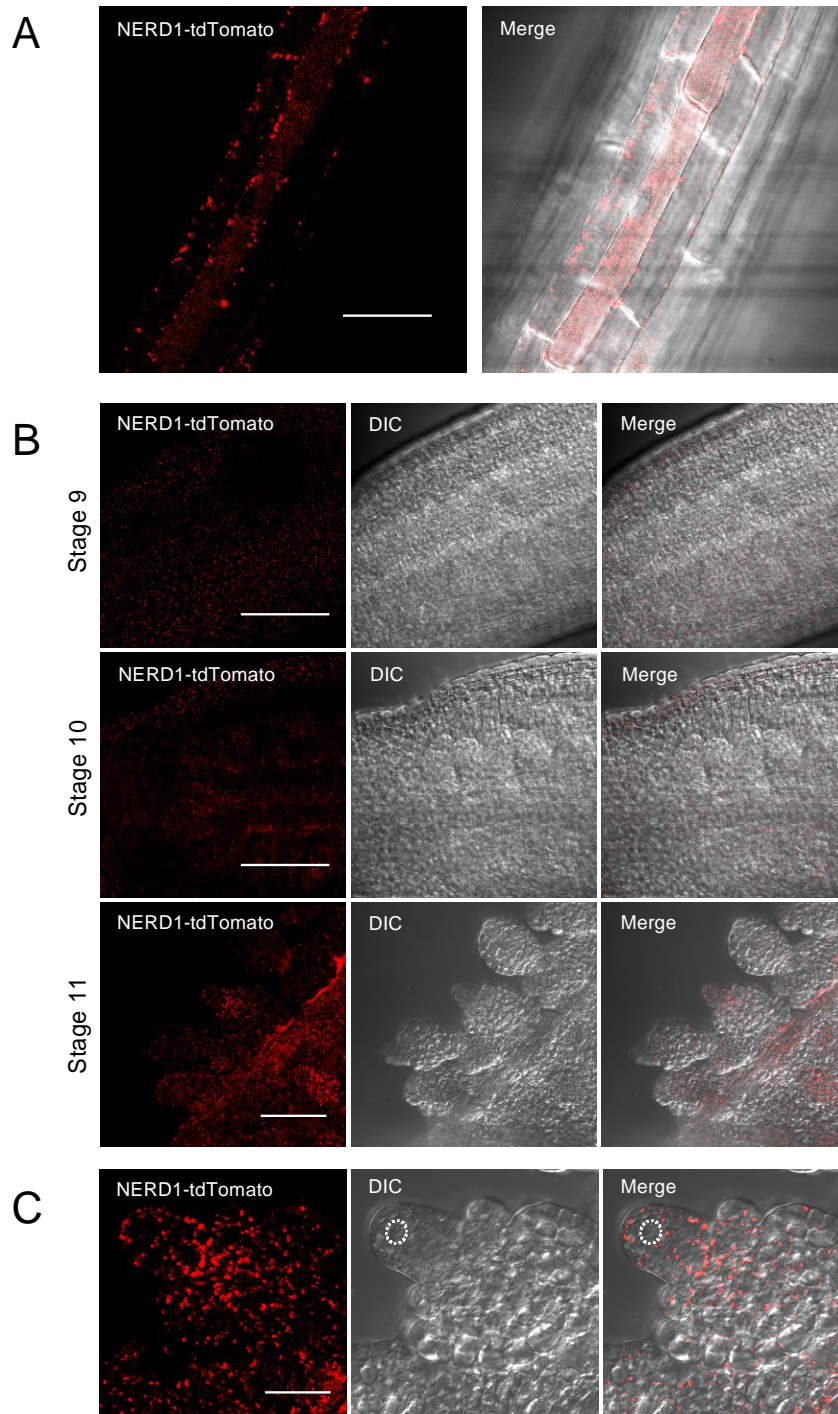
Figure 3.14 NERD1 localization in Arabidopsis transgenic lines expressing pNERD1::NERD1-TdTomato.

 (A) NERD1-TdTomato is present in a punctate compartment in root epidermal cells. (B) NERD1 localization in ovules at flower developmental stages 9, 10 and 11. (C) Magnification of stage 11 from panel B showing punctate NERD1 accumulation in the nucellus around the megaspore mother cell (dashed circle). Bars = 30 µm (A), 20 µm (B), 10 µm (C).
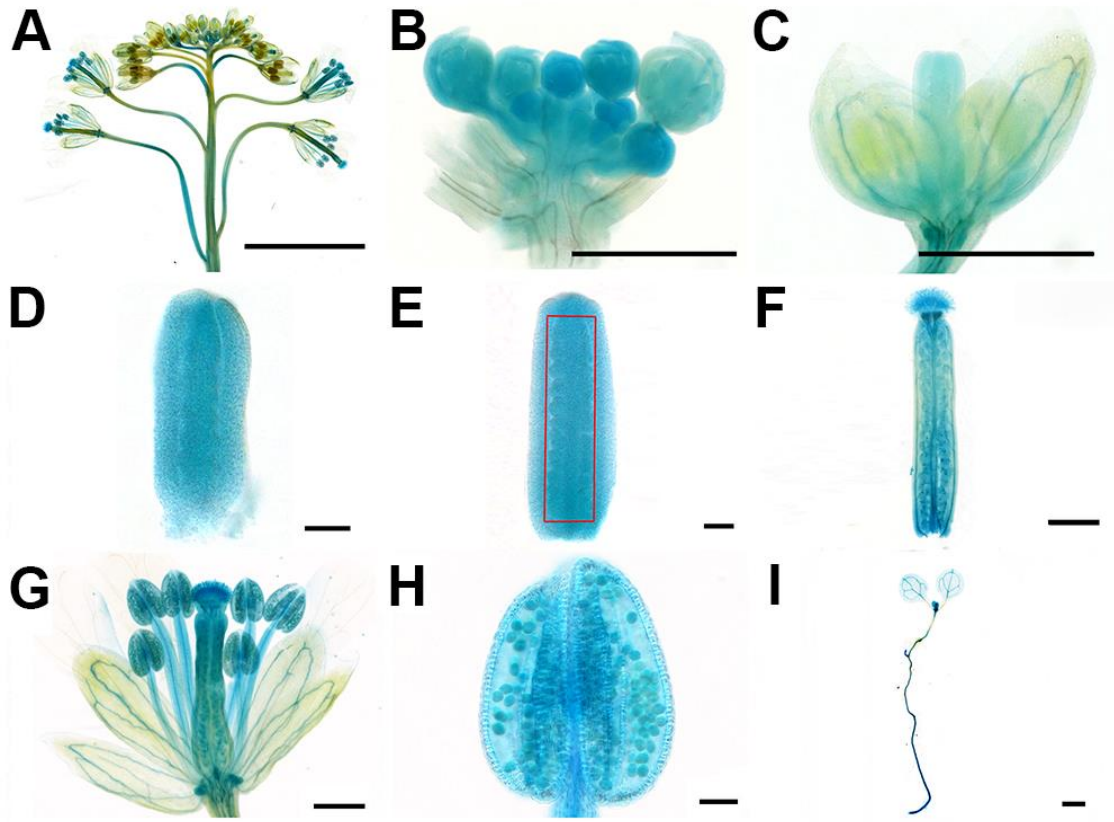
Figure 3.15 NERD1 expression in plant development.

The NERD1pro::NERD1-GUS reporter (blue signal) is detected in inflorescence (A-B), the flower in stage 9 (C), the pistil in stage 8 (D), the pistil in stage 9 (E), mature pistil (F), mature flower (G), mature anther (H), and SAM and RAM of seedlings (I). Bars=25 µm.

A

Expression level

Stigma
Ovary
Ovules
Root, 7 days
Hypocotyl, 7 days
Internode, 21+ days
Leaf
Seedling, green parts, 7 days
Shoot apex, vegetative, 7 days
Flower, stage 9, 21+ days
Flower, stage 10-11, 21+ days
Flower, stage 12, 21+ days
Flower, 28 days

B NERD1_{pro}::NERD1-GUS
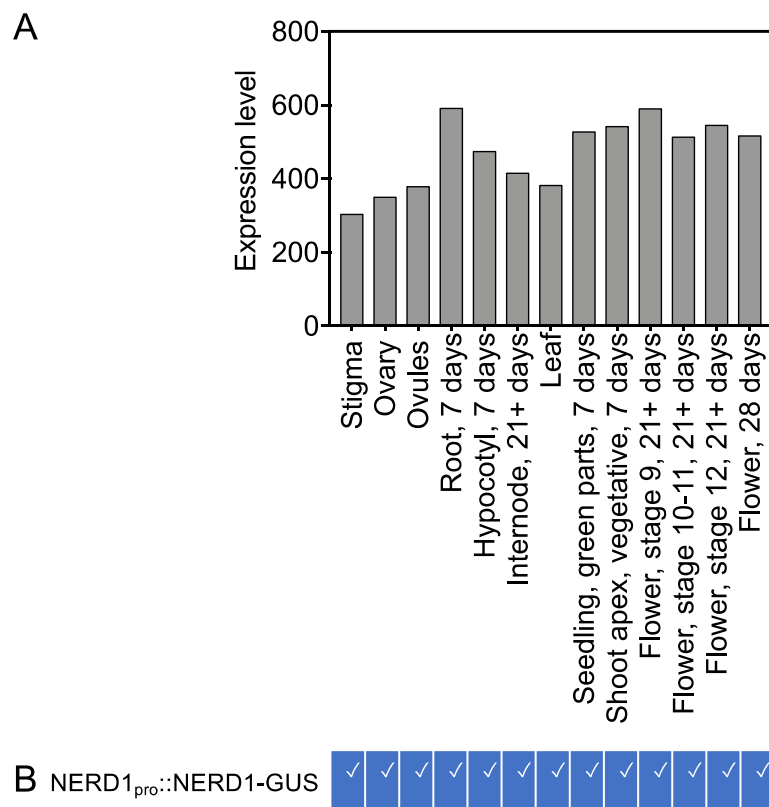
Figure 3.16 NERD1 is constitutively expressed throughout Arabidopsis development.

(A) NERD1 expression level in different tissues from publicly available transcriptome data in ePlant. (B) NERD1_{pro}::gNERD1-GUS fusion construct data (see Figure 3.15) matches the ePlant transcriptome data.
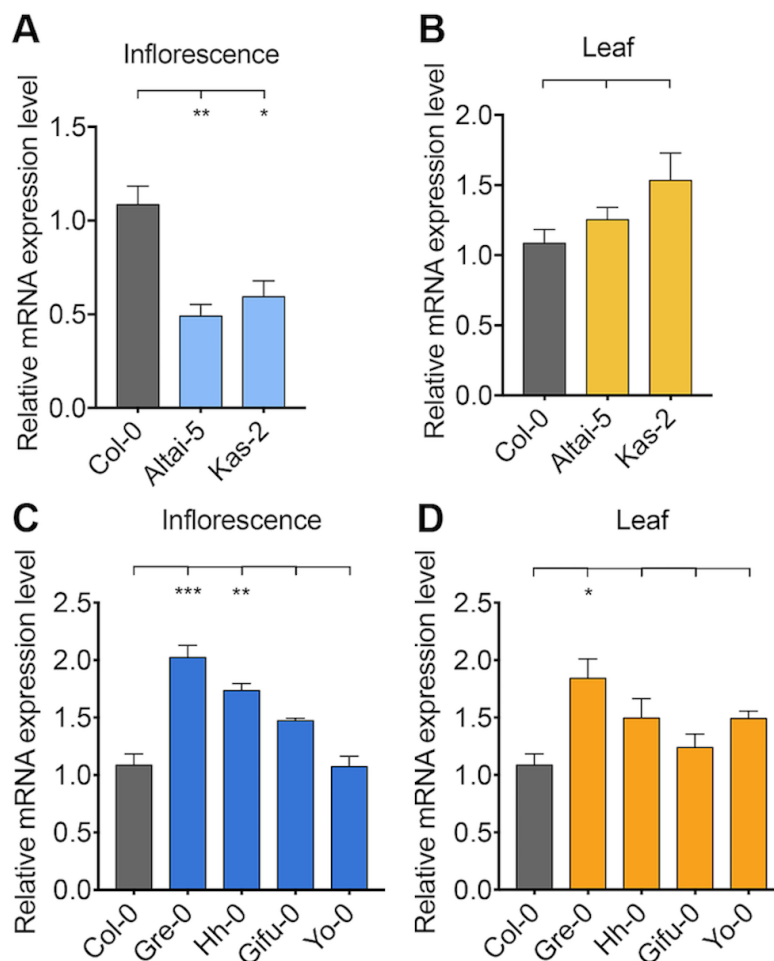
Figure 3.17 NERD1 expression is reduced in developing flowers of some specific low ovule number accessions.

(A) qRT-PCR of NERD1 in Col-0, Altai-5 and Kas-2 inflorescences. (B) qRT-PCR of NERD1 in Col-0, Altai-5 and Kas-2 leaves. (C) qRT-PCR of NERD1 in Col-0, Gre-0, Hh-0, Gifu-0 and Yo-0 inflorescences. (D) qRT-PCR of NERD1 in Col-0, Gre-0, Hh-0, Gifu-0 and Yo-0 leaves. "***" indicates statistical significance at p value<0.001, "**" indicates statistical significance at p value<0.01, "*" indicates statistical significance at p value<0.05 determined by Student's t-test.
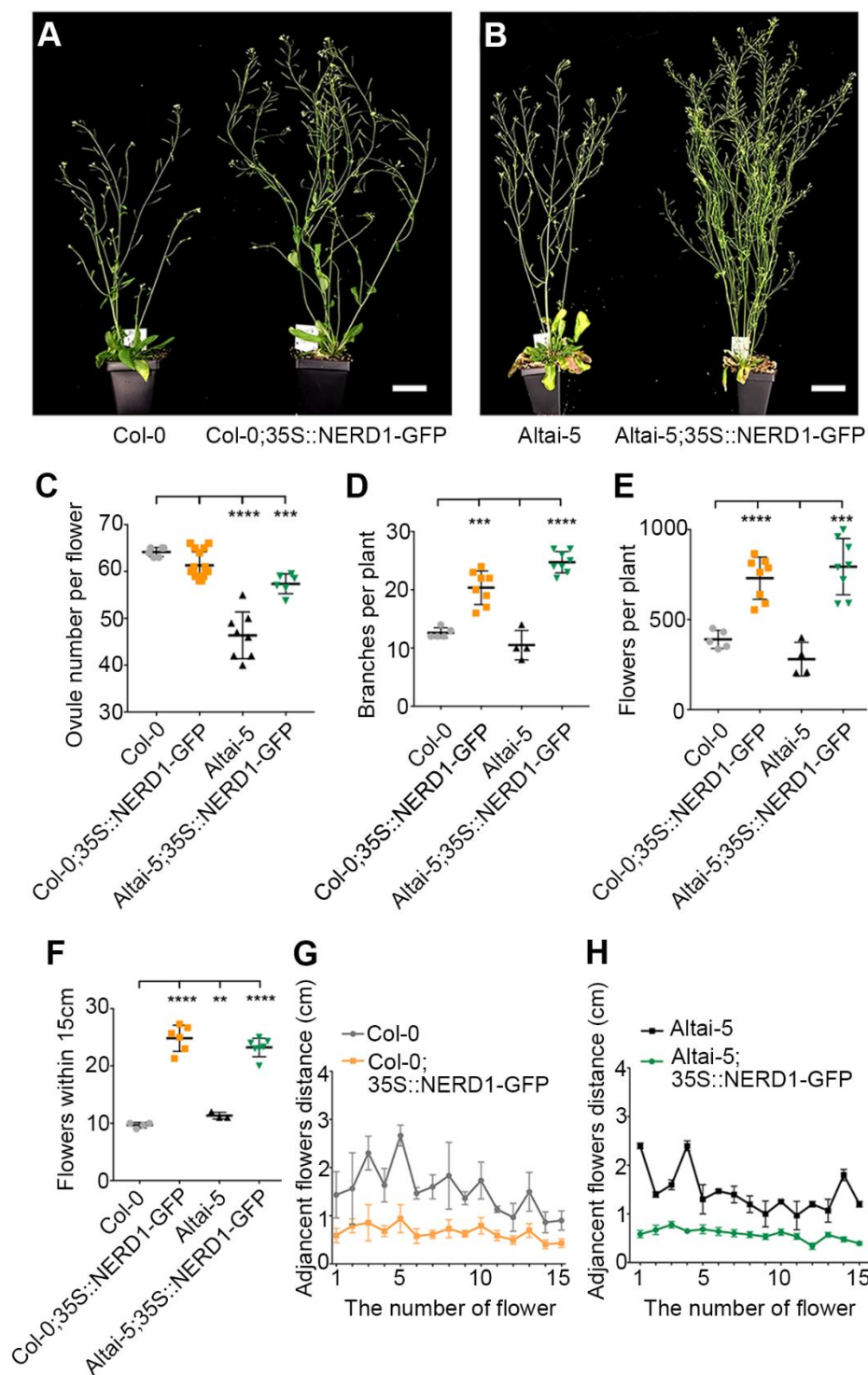
Figure 3.18 Overexpression of NERD1 affects plant architecture and fertility.

(A-B) 35S::NERD1-GFP expressed in Col-0 and Altai-5 backgrounds. Bars=5cm. Scatter plots of total ovule number per flower (C), total branch number (D), total flower number per plant (E), number of flowers within 15 cm of the main shoot (F), and distance between adjacent flowers (G-H) in 35S::NERD1-GFP transformants in the Col-0 and Altai-5 backgrounds compared to untransformed controls.

A

Accessions	Sterile plants	Normal plants
Col-0	4	6
Altai-5	1	9

B
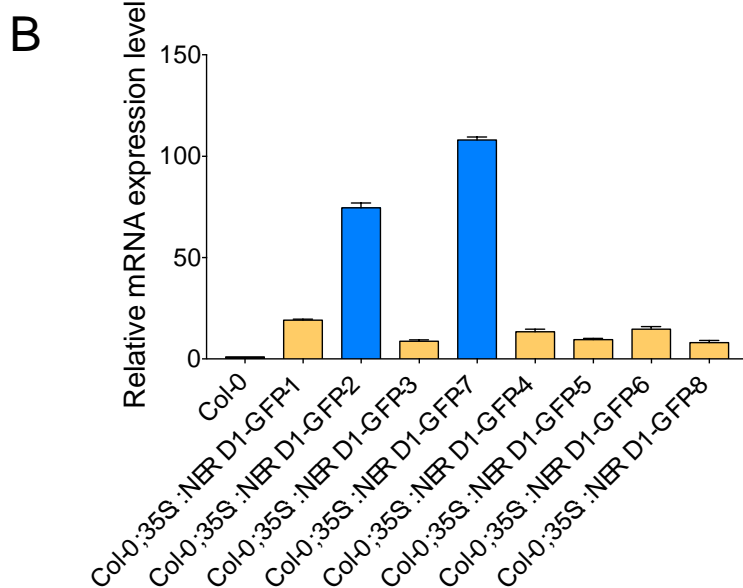
Figure 3.19 35S::NERD1 plants have variable fertility.

(A) The number of sterile plants and normal T1 plants in Col-0 and Altai-5. (B) qRT-PCR of NERD1 in *35S::NERD1* plants in Col-0 background. Yellow bars represent plants with normal fertility and blue bars indicate male sterile plants.
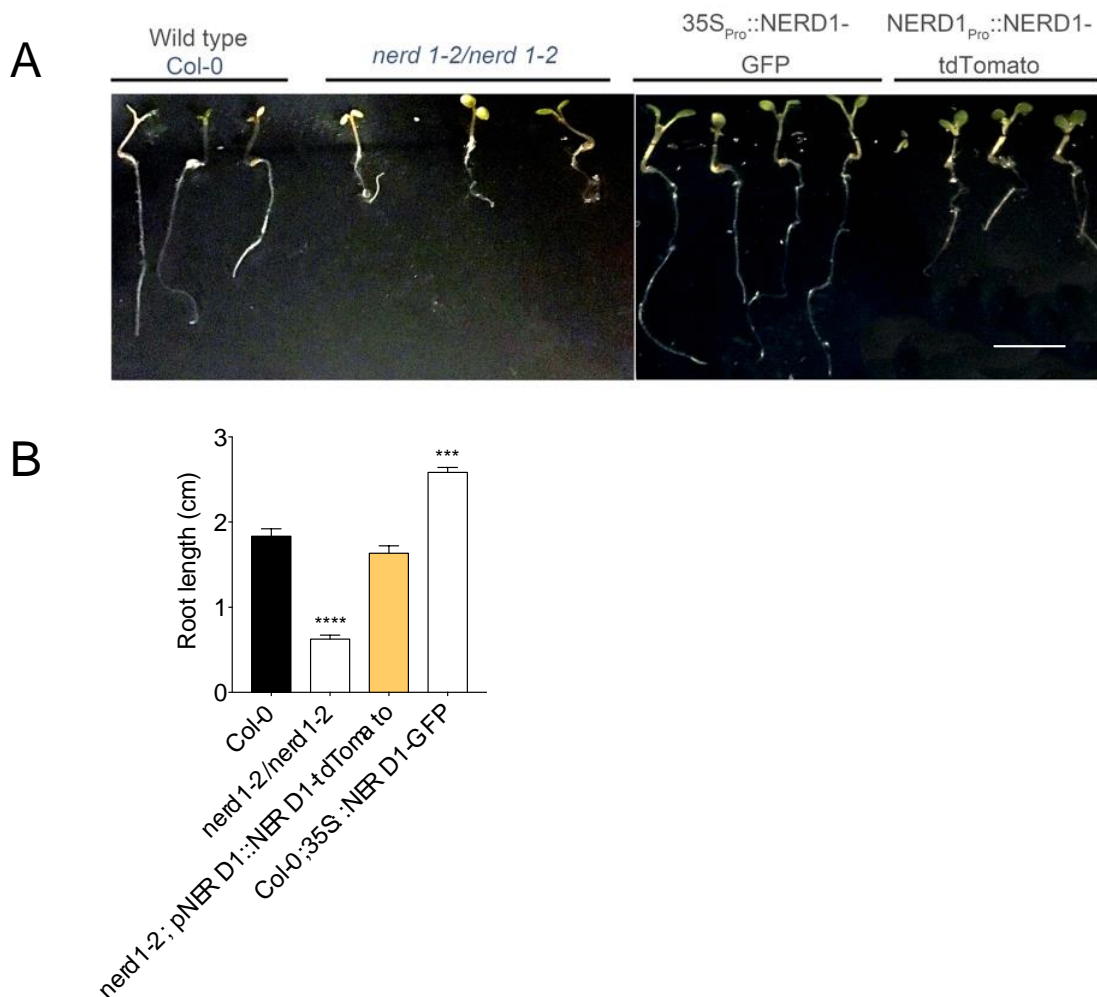
Figure 3.20 *NERD1* is involved in in root growth.

 (A) Root phenotype in Col-0, *nerd1-2/nerd1-2*, *35S::NERD1,* and the *NERD1* complementation line. *nerd1* mutants have significantly shorter roots while overexpression of *NERD1* leads to longer roots than the Col-0 control. Bar = 0.7 cm. (B) Bar graph of the quantification of the root length. "****" indicates statistical significance (*p* value < 0.0001 determined by Student's t-test). "***" indicates statistical significance (*p* value < 0.001 determined by Student's t-test, n = at least 9 individuals for each genotype).

A Arabidopsis 1,001 Genomes Chr3 : 18953000 -18962999 (TAIR10)

B

	Position	p value	Alleles	Amino	LOCN
1	18954034	9.55E-07	C-T	R4	Exon
2	18955603	2.45E-08	C-A	S230Y	Exon
3	18955604	2.45E-08	T-C	S230	Exon
4	18956947	3.09E-05	G-C	S480	Exon

I=A
I=G
I=T
I=C
I=A,C
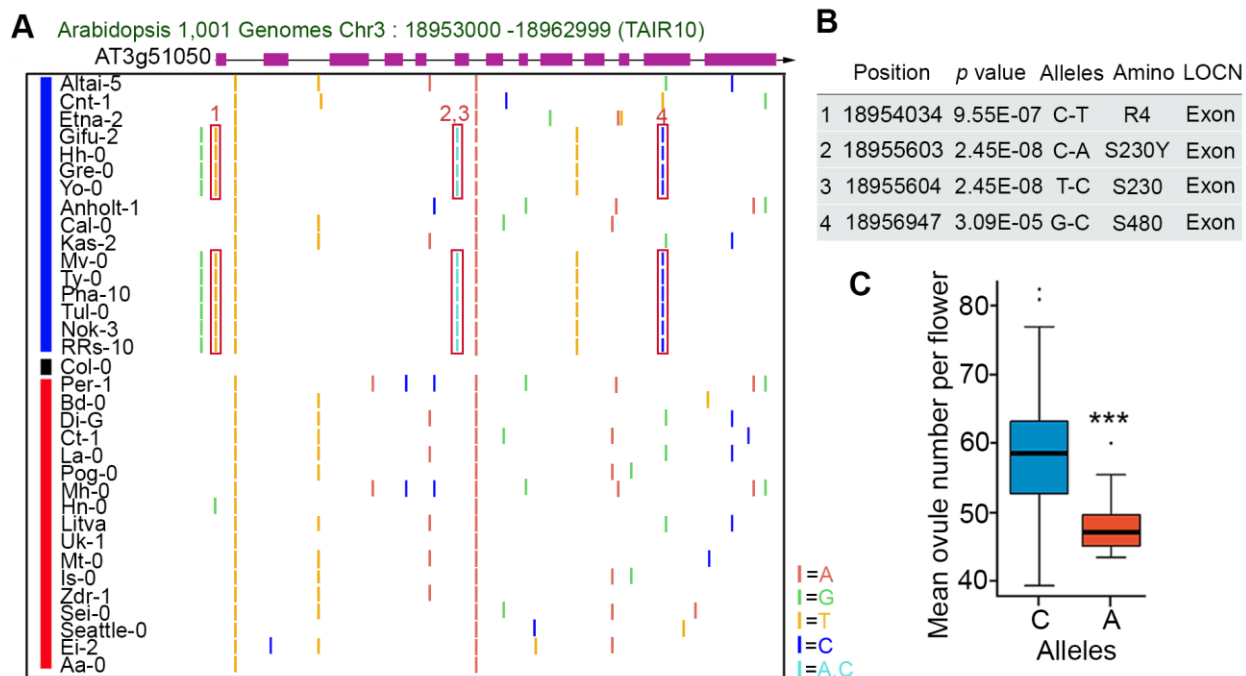
Figure 3.21 Sequence variation in the *NERD1* locus correlates with ovule number.

(A) SNPs in and around the *NERD1* gene. The blue line indicates the 16 lowest ovule number accessions and the red line indicates the 16 highest ovule number accessions. SNPs are identified based on comparison to the Col-0 reference genome. The red boxes highlight low-ovule number associated SNPs (the turquoise bar indicates two SNPs in adjacent nucleotides, a non-synonymous C-A SNP and a synonymous C-G SNP). Only genomes that were available on the SALK 1,001 genomes browser (http://signal.salk.edu/atg1001/3.0/gebrowser.php) were considered. (B) One of the ovule number-associated SNPs in NERD1 causes a serine-tyrosine substitution in low ovule number accessions. (C) Average ovule number in *NERD1* "A" and "C" allele-containing accessions. The "A" allele is significantly associated with lower ovule numbers. "***" indicates statistical significance at *p* value<0.001 determined by Student's t-test.
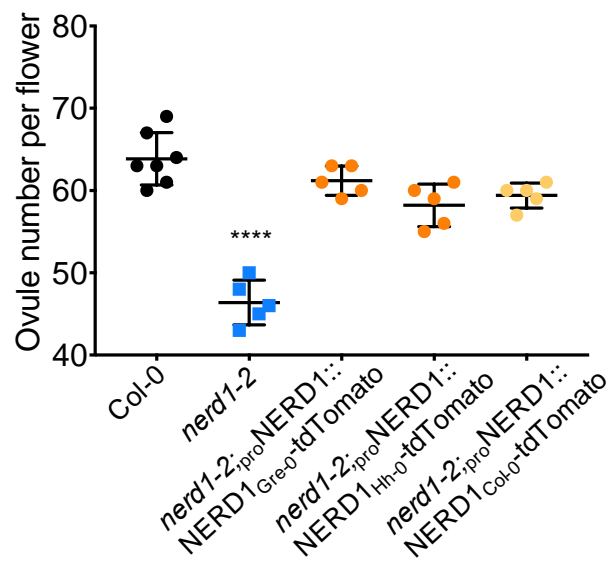
Figure 3.22 *nerd1-2* reduced ovule number phenotype can be rescued by NERD1 complementation constructs derived from Col-0, Gre-0 and Hh-0.

p value < 0.0001 determined by Student's t-test.

Table 3.1 *nerd1* segregation in F2 populations

Female	Male	*NERD1/ NERD1*	*nerd1-2/ NERD1*	Female TE%	Male TE%	Chi-square test (*p* value)
nerd1-2/ NERD1	Col-0	43	42	97.67	NA	0.91
Col-0	*nerd1-2/* NERD1	92	41	NA	44.57	9.767e^{-06} *

Table 3.2 Transmission efficiency of the *nerd1-2* allele determined by reciprocal crosses with wild-type Col-0.

Allele	n	*NERD1/ NERD1*	*nerd1/ NERD1*	*nerd1/ nerd1*	Expected ratio	χ^2	*p* value
nerd1-2	107	35	49	23	1:2:1	3.4486	0.1783
nerd1-4	86	25	42	19	1:2:1	0.8837	0.6428

* Chi-square is significant at the *p* value< 0.01 level.

Table 3.3 List of Arabidopsis accessions used in the study and their ovule number data.

Accession	Average ovule number per flower	Ovule number ranking	Ecotype. ID	CS. Number	Countries	Lat.	Long.
Aa_0	69.20	171	7000	CS76428	GER	50.91 67	9.570 73
Abd_0	58.94	105	6986	CS76429	UK	57.15 39	-2.220 7
Ag_0	55.00	75	6897	CS76430	FRA	45	1.3
Ak_1	50.35	34	6987	CS76431	GER	48.06 83	7.625 51
Alst_1	57.56	93	6989	CS76432	UK	54.8	-2.433 3
Altai_5	39.30	1	9758	CS76433	CHN	47.75	88.4
Amel_1	54.15	66	6990	CS76434	NED	53.44 8	5.73
An_1	50.40	35	6898	CS76435	BEL	51.21 67	4.4
Ang_0	63.45	145	6992	CS76436	BEL	50.3	5.3
Anholt_1	43.50	6	6680	CS76437	GER	51.85	6.433 3
Ann_1	49.69	28	6994	CS76438	FRA	45.9	6.130 28
Anz_0	51.70	47	9759	CS76439	IRN	37.47	49.47
Appt_1	64.20	149	6997	CS76440	NED	51.83 33	5.583 3
Ba_1	52.70	53	7014	CS76441	UK	56.54 59	-4.798 21
Baa_1	53.30	60	7002	CS76442	NED	51.33 33	6.1
Baz_0	51.63	44	9760	CS76443	FRA	48.81	1.66
Bch_1	54.07	65	7028	CS76444	GER	49.51 66	9.316 6
Bd_0	80.85	188	7013	CS76445	GER	52.45 84	13.28 7
Be_0	56.75	91	7010	CS76446	GER	49.68 03	8.616 1
Benk_1	49.65	26	7008	CS76447	NED	52	5.675
Ber	56.53	89	7458	CS76448	DEN	55.67 5	12.56 87

Accession	Average ovule number per flower	Ovule number ranking	Ecotype. ID	CS. Number	Countries	Lat.	Long.
Bik_1	54.88	73	9761	CS76449	LBN	33.92	35.7
Bl_1	49.65	27	7025	CS76450	ITA	44.5041	11.3396
Bla_1	52.63	52	8264	CS76451	ESP	41.6833	2.8
Bla_5	44.00	7	NA	NA	NA	NA	NA
Boot_1	60.95	122	7026	CS76452	UK	54.4	-3.2667
Bor_1	51.00	41	5837	CS76453	CZE	49.4013	16.2326
Br_0	50.75	38	6904	CS76455	CZE	49.2	16.6166
Bsch_0	66.45	162	7031	CS76457	GER	50.0167	8.6667
Bu_0	52.80	54	7036	CS76458	GER	50.5	9.5
Ca_0	57.45	92	7062	CS76459	GER	50.2981	8.26607
Cal_0	45.58	11	7061	CS76460	UK	53.2699	-1.64293
Cen_0	54.81	72	8275	CS76461	FRA	49	0.5
Cerv_1	50.15	31	7068	CS76462	ITA	42	12.1
Chat_1	55.75	83	7071	CS76463	FRA	48.0717	1.33867
Chi_0	62.63	134	7072	CS76464	RUS	53.7502	34.7361
Cit_0	40.42	2	7075	CS76466	FRA	43.3779	2.54038
Cnt_1	42.13	3	7064	CS76467	UK	51.3	1.1
Co_1	50.40	36	7077	CS76468	POR	40.12	-8.25
Col_0	56.65	90	6909	CS76778	USA	38.3	-92.3
Com_1	54.20	67	7092	CS76469	FRA	49.416	2.823
Ct_1	76.00	185	7067	CS76786	ITA	37.3	15
Da(1)-12	51.65	45	7460	CS76470	CZE	NA	NA
Db_1	64.20	150	7419	CS76471	GER	50.3058	8.32213
Di_G	76.94	186	7096	CS76472	FRA	47.3239	5.04278

Accession	Average ovule number per flower	Ovule number ranking	Ecotype. ID	CS. Number	Countries	Lat.	Long.
Dja_1	60.30	119	766	CS76473	KGZ	42.58 33	73.63 33
Do_0	50.15	32	7102	CS76474	GER	50.72 24	8.237 2
Dr_0	58.40	99	7106	CS76475	GER	51.05 1	13.73 36
Dra_0	51.05	42	7103	CS76476	CZE	49.41 67	16.26 67
Dra_1	76.95	187	NA	NA	NA	NA	NA
Durh_1	55.90	85	7107	CS76477	UK	54.77 61	-1.573 3
Ei_2	69.42	173	6915	CS76478	GER	50.3	6.3
El_0	49.85	29	7117	CS76479	GER	51.51 05	9.682 53
Ema_1	66.44	161	7109	CS76480	UK	51.3	0.5
En_2	50.44	37	7119	CS76481	GER	50	8.5
En_D	63.40	144	7120	CS76482	GER	50	8.5
Er_0	58.56	101	7125	CS76483	GER	49.59 55	11.00 87
Es_0	52.19	49	7126	CS76484	FIN	60.19 97	24.56 82
Est	55.45	79	7127	CS76485	EST	58.66 56	24.98 71
Et_0	53.56	62	7130	CS76486	FRA	44.64 47	2.564 81
Etna_2	42.30	4	9762	CS76487	ITA	37.69	14.98
Fi_0	52.81	55	7138	CS76488	GER	50.5	8.016 7
Fr_2	58.81	103	7133	CS76489	GER	50.11 02	8.682 2
Ga_0	58.90	104	6919	CS76490	GER	50.3	8
Gd_1	63.85	147	7161	CS76491	GER	53.5	10.5
Gel_1	62.44	133	7143	CS76492	NED	51.01 67	5.866 67
Gie_0	63.06	141	7147	CS76493	GER	50.58 4	8.678 25
Gifu_2	43.45	5	7148	CS76494	JPN	35.45	137.4 2
Gr_1	62.06	128	430	CS76496	AUT	47	15.5

Accession	Average ovule number per flower	Ovule number ranking	Ecotype. ID	CS. Number	Countries	Lat.	Long.
Gre_0	44.50	9	7160	CS76497	USA	43.178	-85.2532
Gu_0	63.35	143	6922	CS76498	GER	50.3	8
Gy_0	53.45	61	8214	CS76499	FRA	49	2
Ha_0	50.13	30	7163	CS76500	GER	52.3721	9.73569
Had_1b	54.70	70	9767	CS76509	LBN	34.25	35.92
Hey_1	69.06	170	7166	CS76511	NED	51.25	5.9
Hh_0	44.33	8	7169	CS76512	GER	54.4175	9.88682
Hn_0	73.50	181	7165	CS76513	GER	51.3472	8.28844
HR_5	61.50	124	6924	CS76514	UK	51.4083	-0.6383
Hs_0	60.06	117	7162	CS76515	GER	52.24	9.44
Is_0	72.44	177	8312	CS76517	GER	50.5	7.5
Je_0	48.05	21	7181	CS76518	GER	50.927	11.587
Jl_3	51.30	43	7424	CS76519	CZE	49.2	16.6166
Jm_0	66.30	160	7177	CS76520	CZE	49	15
Ka_0	63.15	142	8314	CS76521	AUT	47	14
Kar_1	50.30	33	763	CS76522	KGZ	42.3	74.3667
Kas_2	45.90	12	8424	CS76523	IND	35	77
Kb_0	55.05	76	7202	CS76524	GER	50.1797	8.50861
Kelsterbach_4	62.31	132	8420	CS76525	GER	50.0667	8.5333
Kil_0	62.25	129	7192	CS76526	UK	55.6395	-5.66364
Kin_0	62.70	137	6926	CS76527	USA	44.46	-85.37
Kl_5	58.50	100	7199	CS76528	GER	50.95	6.9666
Knox_18	48.05	22	6928	CS76530	USA	41.2816	-86.621

Accession	Average ovule number per flower	Ovule number ranking	Ecotype. ID	CS. Number	Countries	Lat.	Long.
Ko_2	47.55	20	7427	CS76531	DEN	NA	NA
Kondara	53.15	59	6929	CS76532	TJK	38.48	68.49
Kro_0	59.25	109	7206	CS76533	GER	50.0742	8.96617
Krot_0	56.31	88	7203	CS76534	GER	49.631	11.5722
Kyoto	60.55	120	7207	CS76535	JPN	35.0085	135.752
Kyr_1	54.25	68	770	CS76536	KGZ	40.04653	72.68361
Kz_9	61.95	127	6931	CS76537	KAZ	49.5	73.1
La_0	74.65	184	7209	CS76538	POL	52.7333	15.2333
Lan_0	66.85	166	7208	CS76539	UK	55.6739	-3.78181
Le_0	59.20	107	7218	CS76540	NED	52.1611	4.49015
Li_2	62.63	135	7223	CS76541	GER	50.3833	8.0666
Lip_0	66.70	164	8325	CS76542	POL	50	19.3
Litva	73.38	180	7236	CS76543	LTU	NA	NA
Lm_2	55.55	81	7217	CS76545	FRA	48	0.5
Lp2_2	69.05	169	7520	CS76546	CZE	49.38	16.81
Lz_0	65.50	157	6936	CS76547	FRA	46	3.3
Mc_0	50.81	40	7252	CS76548	UK	54.6167	-2.3
Me_0	69.00	168	7250	CS76549	GER	51.9183	10.1138
Mh_0	74.10	182	7255	CS76550	POL	50.95	20.5
Mir_0	52.81	56	8337	CS76551	ITA	44	12.37
Mnz_0	62.65	136	7244	CS76552	GER	50.001	8.26664
Mrk_0	53.95	64	6937	CS76554	GER	49	9.3
Ms_0	51.70	48	6938	CS76555	RUS	55.7522	37.6322
Mt_0	72.68	178	NA	NA	NA	NA	NA
Mv_0	46.13	13	7248	CS76556	USA	41.3923	-70.6652

Accession	Average ovule number per flower	Ovule number ranking	Ecotype. ID	CS. Number	Countries	Lat.	Long.
Mz_0	54.94	74	6940	CS76557	GER	50.3	8.3
Na_1	59.31	110	8343	CS76558	FRA	47.5	1.5
Nc_1	62.25	130	7430	CS76559	FRA	48.6167	6.25
Neo_6	59.60	112	772	CS76560	TJK	37.35	72.4667
Nok_0	51.69	46	NA	NA	NA	NA	NA
Nok_3	47.19	18	6945	CS76562	NED	52.24	4.45
Np_0	62.90	139	7268	CS76563	GER	52.6969	10.981
Nw_0	57.94	95	7258	CS76564	GER	50.5	8.5
Ob_0	54.25	69	7276	CS76566	GER	50.2	8.5833
Old_1	63.50	146	7280	CS76567	GER	53.1667	8.2
Or_0	55.10	77	7282	CS76568	GER	50.3827	8.01161
Ove_0	61.00	123	7287	CS76569	GER	53.3422	8.42255
Per_1	82.31	189	8354	CS76571	RUS	58	56.3167
Pi_0	59.45	111	7298	CS76572	AUT	47.04	10.51
Pla_0	53.10	58	8357	CS76573	ESP	41.5	2.25
Pla_1	46.17	14	NA	NA	NA	NA	NA
Pna_0	66.95	167	NA	NA	NA	NA	NA
Pna_10	46.90	16	7526	CS76574	USA	42.0945	-86.3253
Pna_17	48.35	23	7523	CS76575	USA	42.0945	-86.3253
Pog_0	74.50	183	7306	CS76576	CAN	49.2655	-123.206
Pu2_23	52.85	57	6951	CS76579	CZE	49.42	16.36
Pu2_7	55.88	84	6956	CS76580	CZE	49.42	16.36
Ra_0	66.69	163	6958	CS76582	FRA	46	3.3
Ragl_1	64.55	151	7314	CS76583	UK	54.3512	-3.41697

Accession	Average ovule number per flower	Ovule number ranking	Ecotype. ID	CS. Number	Countries	Lat.	Long.
Rd_0	64.80	153	8366	CS76584	GER	50.5	8.5
Rld_1	54.80	71	7471	CS76588	UNK		NaN
Rmx_A02	65.15	155	7524	CS76589	USA	42.036	-86.511
Rome_1	64.88	154	7319	CS76590	ITA	42	12.1
Rou_0	64.10	148	7320	CS76591	FRA	49.4424	1.09849
RRS_10	47.40	19	7515	CS76592	USA	41.5609	-86.4251
RRS_7	61.60	125	7514	CS76593	USA	41.5609	-86.4251
Rubezhnoe_1	64.70	152	7323	CS76594	UKR	49	38.28
Sap_0	56.20	87	8378	CS76595	CZE	49.49	14.24
Sapporo_0	66.05	159	7330	CS76596	JPN	43.0553	141.346
Se_0	62.25	131	6961	CS76597	ESP	38.3333	-3.53333
Seattle_0	71.45	174	7332	CS76598	USA	47	-122.2
Sei_0	71.60	175	7333	CS76599	ITA	46.5438	11.5614
Sg_1	60.10	118	7344	CS76600	GER	47.6667	9.5
Sha	69.28	172	NA	NA	NA	NA	NA
Si_0	60.00	116	7337	CS76601	GER	50.8738	8.02341
Sorbo	56.00	86	6963	CS76602	TJK	38.35	68.48
Sp_0	53.80	63	7343	CS76603	GER	52.5339	13.181
Sq_8	66.75	165	6967	CS76604	UK	51.4083	-0.6383
Stw_0	65.45	156	7347	CS76605	RUS	52	36
Su_0	52.50	51	7342	CS76606	UK	53.6473	-3.00733

Accession	Average ovule number per flower	Ovule number ranking	Ecotype. ID	CS. Number	Countries	Lat.	Long.
Sus_1	62.95	140	765	CS76607	KGZ	42.18 33	73.4
Ta_0	58.05	97	7349	CS76608	CZE	49.5	14.5
Tac_0	55.65	82	7350	CS76609	USA	47.24 13	-122.4 59
Tamm_2	49.60	25	6968	CS76610	FIN	60	23.5
Tiv_1	59.75	114	7355	CS76613	ITA	41.96	12.8
Tol_0	55.45	80	7356	CS76614	USA	41.66 39	-83.55 53
Ts_1	60.55	121	6970	CS76615	ESP	41.71 94	2.930 56
Tscha_1	59.70	113	7372	CS76616	AUT	47.07 48	9.904 2
Tu_0	58.25	98	8395	CS76617	ITA	45	7.5
Tul_0	46.95	17	7377	CS76618	USA	43.27 08	-85.25 63
Ty_0	46.65	15	7351	CS76619	UK	56.42 78	-5.234 39
Uk_1	72.95	179	7378	CS76620	GER	48.03 33	7.766 7
Uod_1	65.55	158	6975	CS76621	AUT	48.3	14.45
Utrecht	55.15	78	7382	CS76622	NED	52.09 18	5.114 5
Van_0	61.70	126	7383	CS76623	CAN	49.26 55	-123.2 06
Ven_1	48.40	24	7384	CS76624	NED	52.03 33	5.55
Vind_1	62.75	138	7387	CS76625	UK	54.99 02	-2.367 1
Wa_1	59.13	106	7394	CS76626	POL	52.3	21
Wc_1	59.20	108	7404	CS76627	GER	52.6	10.06 67
Wei_0	59.85	115	6979	CS76628	SUI	47.25	8.26
Westkar	58.70	102	9766	CS76629	KGZ	42.26	74.16

Accession	Average ovule number per flower	Ovule number ranking	Ecotype. ID	CS. Number	Countries	Lat.	Long.
Wl_0	57.65	94	7411	CS76630	GER	47.92 99	10.81 34
Ws_2	50.80	39	6981	CS76631	RUS	52.3	30
Wt_5	57.96	96	6982	CS76632	GER	52.3	9.3
Yo_0	45.10	10	7416	CS76633	USA	37.45	- 119.3 5
Zal_1	52.25	50	768	CS76634	KGZ	42.8	76.35
Zdr_1	71.70	176	6984	CS76635	CZE	49.38 53	16.25 44

Table 3.4 Chromosome 3 candidate genes and insertion mutants

SNP Position	GWAS P-value	Target AGI	Description	ABRC stock#
18881073	3.47E-07	AT3G50790	Esterase	SALK_202612C
18916764	9.55E-07	AT3G50890	homeobox protein 28 (HB28)	SALK_037180
18930470	9.55E-07	AT3G50930	cytochrome BC1 synthesis (BCS1)	SAIL_1266_A05
18941053	9.55E-07	AT3G50970	LOW TEMPERATURE-INDUCED 30 (LTI30)	SALK_114915.55.75.x
18942604	9.55E-07	AT3G50980	dehydrin xero 1 (XERO1)	SALK_003375.51.60.x
18947845	9.55E-07	AT3G51010	protein translocase subunit	SALK_066359.38.15.x
18947884	9.55E-07			
18948019	9.55E-07			
18949653	9.55E-07	AT3G51020	Unknown	SALK_032007
18949661	9.55E-07			
18949972	9.55E-07			
18954034	9.55E-07	AT3G51050	NERD1, NEW ENHANCER OF ROOT DWARFISM1	SALK_018060C
18955603	2.45E-08			WiscDsLoxHs056_01C /CS905283
18955604	2.45E-08			
19764124	5.25E-07	AT3G53305	cytochrome P450	SALK_075211C
19764897	6.46E-07			
19960188	5.75E-08	AT3G53910	malate dehydrogenase-like protein	NA
21460719	1.70E-08	AT3G57950	cotton fiber protein	NA
22398234	1.38E-11	AT3G60590	Unknown	SALK_006242C
22398245	1.38E-11			
22398301	1.38E-11			
22398311	1.38E-11			
22398313	1.38E-11			
22398340	1.38E-11			
22398357	1.38E-11			
22398913	1.38E-11			
22398955	1.38E-11			
22398971	1.38E-11			

SNP Position	GWAS P-value	Target AGI	Description	ABRC stock#
22398988	1.38E-11			
22399010	1.38E-11			
22399012	1.38E-11			
22399081	1.38E-11			

Table 3.5 List of primers used for genotyping and cloning.

Description	Direction	Primer sequence
For genotyping SALK 006242C	Forward	CAAAGTCTCCTTTCCCAAACC
	Reverse	AGACGATACATGGACACAGGG
For genotyping SALK 041743C	Forward	GCAAATTTGCAATATTTTCATCC
	Reverse	CTTCTGCAACTTCCCTTGTTG
For genotyping SALK 010684C	Forward	TTCCACAATTGATCACACACG
	Reverse	ATCAGGCTTGGTTGATGTGTG
For genotyping SALK 075211C	Forward	GACAACAACAGTGCACGACAC
	Reverse	AGTTATCGCATCCGTGAACAG
For genotyping SALK 018060C	Forward	TTCCTTTTGATGAGCCACAAC
	Reverse	CCTTGGACTGTTTCGTAGCTG
For genotyping SALK 202612C	Forward	ATAAGACGGATGTGGACAACG
	Reverse	GCCGTTAATCTCATCAGTTCG
For genotyping SALK 150134C	Forward	CGACCTTCCAAGAGAAAAATG
	Reverse	CGATTCTCGAGTCATTCGAAG
For genotyping SALK 082847	Forward	GAGGATTTGGTGCACAAAAG
	Reverse	AGCCTCTCGATCTTCAATTCC
For genotyping SALK 032007	Forward	GAGAAATCCCTCCACGAAATC
	Reverse	AGTGTACCGCGGGTTAAATTC
For genotyping WiscDsLoxHs056_01C/ CS905283	Forward	GGCGAAGTGTCGTGAGTAATC
	Reverse	TTACAAGCTTGATGTGCATGC
For genotyping SALK_079938	Forward	TTCTCATCCCCAGAGATGATG
	Reverse	AACTTTTAACCACATCGCTGC
For genotyping SALK_037180	Forward	ACACAGCTGTGGGAAACAAAG
	Reverse	GGGGAGGAGTAGTGGAAGATG
For genotyping SAIL_1266_A05	Forward	CTGTTTAGGCCACTTGACTCAG
	Reverse	GTTGTGGAAGTGCTTGGACTC
For genotyping SALK_114915.55.75.x	Forward	TAACAGGATTTGATCCTTGCG
	Reverse	ACCATAAGCCGTGTTAGTCCC
For genotyping SALK_003375.51.60.x	Forward	CCACAAAACCAACGTCTTACG
	Reverse	TTTGTCTTCCTTTGTGTTGGG
For genotyping SALK_066359.38.15.x	Forward	TCTCTTCTTCCTCTTCGCCTC
	Reverse	GGTAAATCCAGGAGCTTTTGG

Description	Direction	Primer sequence
For genotyping SALK_003757.29.99	Forward	GTAATGTTAGCACACGGGTGG
	Reverse	ATCGGTGAGATCAAGTCCTTG
For genotyping SAIL_736_B11	Forward	TGTGTTTGGCATGTTCTCTTG
	Reverse	TTATCCAATCTGGAATCGTCG
For genotyping GABI_700G12	Forward	CCCAAAACAAACCAAATCAAG
	Reverse	ATGGTAACGTTTGCAAGATGC
For genotyping GABI_881A04	Forward	TGAAAATTAATGCGAAACAAAAC
	Reverse	TCAAAATGGCGATGATTTCTC
SALK_003044.55.35.x	Forward	CTCCTGCGACATCATTGAAAC
	Reverse	TCCACGCCAGATTCATATCTC
For genotyping GABI_832H12	Forward	CAGTATCGTTTCTCCTCAGCG
	Reverse	GGTTAAGAACAAAACCCCTGC
For genotyping SAIL_701_A08/CS830886	Forward	TCAGGACGAGAATATTGCGAC
	Reverse	TTCTCATGTCTTTGGGCAAAG
For genotyping SALK_002829	Forward	TCCAAGGTTGCGTAGTTGATC
	Reverse	TTTTGCATAGTCGGAGGATTG
For genotyping SALK_069209C	Forward	TGGTGTTGCCATAATTATGGC
	Reverse	AGCTCTTAAAGCAAACCCTGC
For genotyping SAIL_201_F06C1	Forward	TTGTGAAGACCTTGAGGAACG
	Reverse	TGTCATTCCTTGAGCAATTCC
For genotyping SALK_205553C	Forward	CCGATTTGATTTCGTTTATGC
	Reverse	TTGGTTGTGCCTACATAAGCC
For genotyping SALK_128605C	Forward	TCAAGAAACCCAACGGAGTAG
	Reverse	TCTCTTTTATGCGATTCTCGC
35S::NERD1-GFP Construct	Forward	GGGGACAAGTTTGTACAAAAAAGCAGGCTTCAC CATG AGG AAA CGC GAT TTG
	Reverse	GGGGACCACTTTGTACAAGAAAGCTGGGTGAAA GCTAGATGATGGTCGAGGC
pNERD1::NERD1-tdTomato Construct	Forward	GGGGACAAGTTTGTACAAAAAAGCAGGCTTCAC CGGATTCATTAGCCTTCTGAAGCTG
	Reverse	GGGGACCACTTTGTACAAGAAAGCTGGGTGAAA GCTAGATGATGGTCGAGGC
For NERD1 qpcr	Forward	ACTAATGATGCCAAAATTCAG
	Reverse	CAACACGGATCTTGTCAG

CHAPTER 4.   THE CORRELATIONS BETWEEN OVULE NUMBER AND FLOWERING TIME IN NATURAL ACCESSIONS

4.1   Introduction

In flowering plants, proper timing of the transition from vegetative phase to reproductive phase is critical for ensuring that offspring are produced. The time period from plants starting their vegetative growth till the flowering initiation is usually measured by the number of days to flower (flowering time, FT), which is often estimated by the total number of rosette leaves that the plants produce in the vegetative phase (Koornneef et al., 1991). Flowering time is controlled by many internal and external factors including both genetic variation and environmental conditions (Simpson and Dean, 2002; Andres and Coupland, 2012). Importantly, flowering time affects plant fitness in natural ecosystems and agricultural productivity. Thus, it is necessary to have a clearer understanding of how flowering time affects other aspects of plant reproduction.

During the last several years, a complex network that contains different regulatory pathways of floral transition have been identified (Koornneef et al., 1998; Levy and Dean, 1998; Putterill et al., 2004). The major genetic pathways controlling flowering time in the model plant *Arabidopsis thaliana* are photoperiod, gibberellin, autonomous pathways, and vernalization pathways. The two major floral integrator genes *FLOWERING LOCUS T (FT)* and *SUPPRESSOR OF OVEREXPRESSION OF CONSTANS 1(SOC1)* participate in multiple pathways (Ratcliffe and Riechmann, 2002). As for those signaling pathways, one of the most important genetic pathways is the photoperiod pathway, which is mainly affected by daylength (Ratcliffe et al., 1998; Hayama and Coupland, 2004). The photoreceptors known as phytochromes (PHYA, PHYB, PHYC, PHYD, PHYE) and cryptochromes (CRY1, CRY2) perceive the red and blue light signals, respectively,

leading to the circadian regulation of *CONSTANS (CO)* expression. When CO expression passes a critical threshold, FT and SOC1 are upregulated to promote the floral transition (Onouchi et al., 2000; Suarez-Lopez et al., 2001). Another upstream regulator of *FT* and *SOC1* is *FLOWERING LOCUS C (FLC)*, which is involved in both the vernalization and autonomous pathways (Ratcliffe and Riechmann, 2002). In the vegetative stage of plant development, high levels of *FLC* represses *FT* and *SOC1*. Vernalization decreases the *FLC* expression level and after vernalization *FLC* expression is maintained at low levels to allow *FT* and *SOC1* to be expressed (Burn et al., 1993; Lee et al., 1993; Samach et al., 2000; Moon et al., 2003; Lee and Lee, 2010; Wellmer and Riechmann, 2010). Similarly, autonomous pathway also represses the *FLC* expression under the regulation of a group of genes. For instance, *FLOWERING CONTROL LOCUS A (FCA),* an RNA binding protein, negatively regulates *FLC* expression (Simpson et al., 2003). *FLOWERING LOCUS D (FLD)* and *FVE* were reported to modulate the chromatin status of *FLC* leading to decreased *FLC* expression (Koornneef et al., 1991; Lee et al., 1994; Chou and Yang, 1998; Lim et al., 2004). Additionally, the phytohormone gibberellic acid (GA) was reported to play a role in promoting the floral transition by upregulating *LEAFY (LFY)* expression (Blazquez et al., 1998). Taken together, a complex networks of multiple pathways work together to control the plant transition from vegetative growth to reproductive growth (Ratcliffe and Riechmann, 2002).

A better understanding of flowering time pathways is helpful to manipulate plants to flower at an appropriate time and increase their survivability under unpredictable environmental changes. A system of controlling this complexity network for floral transition is gradually building up in recent years. The light signals and the day-length have been adjusted for controlling the flowering time underlying the photoperiodic pathway (Song et al., 2015). Since the RNA processing has been

widely characterized in the autonomous and vernalization pathways, chromatin modification and epigenetic regulation were also used for exploring and further controlling the flowering time (Berry and Dean, 2015). In addition, application of the phytohormone such as gibberellins also benefit to regulate flowering time. All the genetic and epigenetic regulations, as well as multiple well-developed database help all the researchers to take advantage of this complex network manipulating flowering time.

Over the last 20 years, the mechanisms controlling the floral transition have been characterized in great detail. In contrast, relatively little is known about how flowering time relates to floral traits such as plant fertility, fruits number, and ovule number. Natural accessions in Arabidopsis have been widely reported that display phenotypic variation. After the transition to flowering, changes in gene expression lead to the production of inflorescence and floral meristems. Arabidopsis accessions also display variation in floral traits such as the fresh flower mass, pistil length and the number of ovules (Juenger et al., 2000; Yuan and Kessler, 2019). Among this variation, the number of ovules per flower is an important trait since it limits the future seed number within the flower. In Arabidopsis, ovules develop from the carpel margin meristem (CMM), and several genes have been identified that affect ovule development as well as the number of ovules. These include *AINTEGUMENTA* (*ANT*), *SEEDSTICK*, *ARABIDOPSIS HISTIDINE KINASE* (*AHK*), *GA-INSENSITVE (GAI)*, and *NEW ENHANCER of ROOT DWARFISM* (*NERD1*) (Galbiati et al., 2013; Cucinotta et al., 2014; Gomez et al., 2018; Yuan and Kessler, 2019).

In our previous study on natural variation in ovule number per flower, we noticed that very late flowering accessions tended to produce fewer ovules per flower than earlier flowering accessions.

So, we hypothesize that their variable flowering time may be associated with the number of ovules that they can produce. Our goals in this study were to investigate the correlation between flowering time and the number of ovules per flower, and to explore correlations between flowering time and other reproductive traits. Having a better understanding of the links between flowering time and reproductive traits will help us further improve the adaptability of plants and could potentially help to increase crop yield.

4.2   Materials and Methods

4.2.1   Plant Materials and Growth Conditions

Arabidopsis thaliana accessions and flowering time related mutants (in table 4.3) were ordered from the Arabidopsis Biological Resource Center at Ohio State University (ABRC). Seeds were sterilized and plated on ½ Murashige and Skoog (MS) plates and stratified at 4 ˚C for two days. The seedlings will germinate around 5-7 days and then they were transplanted to soil and moved to the growth chamber (long day conditions, 16h of light and 8 h of dark at 22˚C). The natural accession seedlings undergo 4 weeks vernalization, then they were returned to the growth chamber and grown under the long day conditions described above. The flowering time mutants seedlings were grown in long day growth chamber conditions without vernalization.

4.2.2   Genome-Wide Association Study

A GWAS web application for Genome-Wide Association Mapping in *Arabidopsis* was performed for our analysis (http://gwas.gmi.oeaw.ac.at). The ovule number GWAS was referred to previous publication (Yuan and Kessler, 2019). In the flowering time study, the detailed days to flower information were acquired from previous publication (Atwell et al., 2010). There are 176 accessions that were available for both ovule number and flowering time phenotype, which also

had single nucleotide polymorphisms (SNPs) data available on the 1001 Full-sequence dataset; TAIR 9. BOXCOX transformation was applied to make the results more reliable for parametric tests. The Manhattan plot was generated by a simple linear regression model (LM). SNPs with P values $\leq 1 \times 10^{-6}$ (determined by the Benjamini-Hochberg-Yekutieli method) were further considered as candidate loci linked to alleles that regulate flowering time. SNPs with < 15 minor allele count (MAC) were not considered to help control false positive rates.

4.2.3 Statistical analysis

In order to investigate the relationship between Ovule number trait/flowering time trait and other published traits, there are the phenotype data of 12 traits were download from 1001 genome public database. The correlation analysis were performed by 'cor.test()' function in R (R version 3.5.1), which used Pearson's product moment correlation coefficient to test for association between paired sample. Then, the r and p-value as two parameters were calculated by this function.

All the box plots and scatter plots were generated by Prism software (www.graphpad.com) with significance determined using a Student's *t*-test.

4.2.4 Microscopy

For all the embryo sac defect observation in the natural accessions, ovules were dissected out from emasculated flowers and put in a drop of water on a microscope slide. The Differential interference contrast (DIC) images were acquired by using a 40× dry objective (NA = 0.75) on a Nikon Eclipse Ni-U compound microscope. The brightness and contrast of the images were adjusted by the Fiji image software (Version 2.0.0-rc-68/1.52e).

4.3   Results

4.3.1   Natural accessions with low ovule number tend to be late-flowering

Based on our previous GWAS on ovule number in *Arabidopsis thaliana*, we noticed that earlier flowering accessions tended to have higher ovule number per flower, whereas the later flowering accessions produced fewer ovules per flower. During our investigation on ovule number, we grew 189 accessions in long-day growth chamber conditions after 4 weeks of vernalization as previously reported (Amasino, 2005) (Table 4.3). Every ten days, the population was assessed and accessions that had flowered were recorded. The reference genotype Col-0 flowered in around 30 days under our conditions. The FT1 group contained those accessions that flowered within 25-35 days, the FT2 group contained the accessions that flowered moderately later (36- 45 days). The FT3 group contained the rest of the accessions which flowered in 46 days or more (Figure 4.1A and Table 4.3). The box plot in Figure 4.1B shows that there were both high ovule number accessions and medium ovule number accessions in the FT1 group, however, there were only low ovule number accessions in FT3. This result indicates there is a potential negative correlation between ovule number and their flowering time in Arabidopsis natural accessions. In order to verify that the flowering time records observed under our growth conditions matched previous studies on the genetic variation in flowering time, we took advantage of published data for flowering time phenotype which recorded the exact days to flower among different natural accessions (Atwell et al., 2010). We tested the 176 accessions from our ovule number data set that overlapped with the publicly available flowering time data sets from (Atwell et al., 2010) with a the Pearson correlation test (Table 4.3). A correlation test revealed a significant negative correlation between ovule number and flowering time (Figure 4.1C).

Flowering time has been extensively studied by Genome wide association and has been shown to be affected by geographical distribution (Stinchcombe et al., 2004; Aranzana et al., 2005; Atwell et al., 2010; Brachi et al., 2013). Since our correlation analysis was done with only a relatively small subset of the accessions that have been used to study flowering time, we assessed the geographical distribution of our accessions and confirmed that they were distributed throughout of the world with most of them originating in Europe (Figure 4.2A). There is no correlation between flowering time and longitude. In contrast to previous studies that detected the positive correlation between flowering time and latitude (Stinchcombe et al., 2004; Debieu et al., 2013), we did not detect a correlation between flowering time and latitude (Figure 4.2B and 4.2C). This discrepancy could be due to the limited number of accessions in our study.

4.3.2   Some specific SNPs highly associated with both ovule number and flowering time

Since we identified a negative correlation between flowering time and ovule number, we wondered if there are also correlations at the genetic level. We hypothesized that specific SNPs may be associated with both traits. In order to explore the relationship between the SNPs associated with the number of ovules and flowering time, we performed a genome-wide association analysis (GWAS) in each trait by using the genotypes of the 176 overlapping accessions described above. We found that there are eight SNPs in chromosome 3 that are significantly associated with both ovule number and flowering time (-$\log_{10}$ p-value >6, cut-off value 6 were defined by the 5% FDR threshold -$\log_{10}$p-value = 6.2 in both ovule number and flowering time GWAS, which was computed by the Benjamini-Hochberg-Yekutieli method) (Figure 4.3 and Table 4.1). This result suggests that the same gene(s) might control ovule number and flowering time. There are seven genes containing these associated SNPs. Interestingly, although none of them was described as a known flowing time related gene, *NERD1,* a gene controls the number of ovules per flower (Yuan

and Kessler, 2019), had SNPs that are significantly associated with flowering time (Table 4.1). We further analyzed the flowering time in the *nerd1-2* mutant. *nerd1-2* flowering was delayed by around fifteen days compared to the reference wild-type, Col-0 (Figure 4.4). This data suggests that *NERD1* could be involved in the regulation of both ovule number and flowering time.

Although we did not detect any flowering time related genes directly located at the significant loci in both ovule number and flowering time GWA study (Figure 4.3), we wondered whether the flowering time-related genes were near any of the significant loci detected in our ovule number GWA study. We mapped 12 well-known flowering time genes (Figure 4.5), as well as their flanking ~200kb genomic region (Figure 4.6) on the ovule number Manhattan plot. The result revealed that CO was the only flowering time that was near an ovule number-associated peak, with CO's flanking ~200kb region containing significant SNPs associated with ovule number (-$\log_{10}$ (p - value) >6, Figure 4.5). This result suggests CO could be a potential candidate for further analysis of the correlation between flowering time and ovule number.

4.3.3   Mutants affecting flowering time also have variation in ovule number

Furthermore, it will be interesting to test if the reduced number of ovules from those late flowering accessions is under the gene regulation from one or more of the flowering time pathways, or due to the overall extended vegetative growth period. For instance, from our observations during the experiments, the extremely late flowering accessions always produce much more leaves and they also tended to produce less branches from the main stem. This suggests a different mode of meristem regulation that includes both the vegetative to inflorescence meristem conversion and the activation of lateral meristems. Likewise, it is possible that in late flowering accessions, other floral meristems are also affected, such as the carpel margin meristem that regulates the number

of ovules per flower. If this is true, then we would expect that the ovule number phenotype of lower ovule numbers per flower in late flowering mutants and higher in early flowering mutants, with no dependence on the flowering time pathway that is mutated. In order to test this hypothesis, we selected the late flowering mutants *constans (co), flowering time (ft), leafy (lfy)* and the early flowering mutant *flowering locus c (flc)* for our study and grew them under the same growth chamber conditions without vernalization. There are multiple reasons for selecting these mutants for our test. One reason is *CO* was identified previously located near the significant loci that highly associated with ovule number (Figure 4.6). Another reason is that these genes are involved in different flowering regulation pathways: *CO* and *FT* are involved in photoperiod pathway, *LFY* participates the GA pathway, *FLC* is involved in vernalization and the autonomous pathways (Koornneef et al., 1991; Suarez-Lopez et al., 2001; Putterill et al., 2004). Flowering times were determined by counting the leaf number when the first bud was visible (Table 4.2). *co, ft* and *lfy* have longer flowering time with more leaves and *flc* had earlier flowering time compared to their background ecotype Col-0 (Figure 4.7A and table 4.2). We found that all three late flowering mutants had significantly lower ovule numbers per flower than wild-type Col-0. Conversely, the earlier flowering mutant *flc* had more ovules per flower (Figure 4.7B). This result confirms our hypothesis for the negative correlation between ovule number and flowering time. Moreover, it also indicates that the effect of flowering time on ovule number is not correlated with only one flowering time pathway.

4.3.4   Flowering time, Ovule number and ovule quality

Since we revealed that an extended vegetative phase/ longer flowering time might affect specific meristem activity in developing flowers leading to reduced ovule number, we also wondered if other reproductive traits are affected by the variation of flowering time and/or ovule number.

During our experiments, we noticed the natural accessions also have variation in fertility as previously reported (Zinn et al., 2010; Bac-Molenaar et al., 2015; Muller et al., 2016) (Figure 4.8A). In the accessions we examined, reduced fertility was associated with female gametophytic development defects leading to abnormal embryo sacs. In Arabidopsis, a normal mature embryo sac contains a large central cell, an egg cell, two synergid cells, and three antipodal cells (Figure 4.8B). However, low fertility accessions such as Kb-0 have aborted or undeveloped embryo sacs in many ovules (Figure 4.8C). We quantified embryo sac development in several low fertility accessions and confirmed that the low the fertility accessions often had abnormal embryo sacs percentages that were almost the same as the unfertilized ovule percentage (Figure 4.8D). Then we hypothesized that the abnormal embryo sacs made by those infertile accessions may be linked to the number of ovules, or they could be affected by the variation of flowering time. Perhaps accessions that have low fertility due to abnormal embryo sac development also tend to produce more ovules per flower. In order to test this hypothesis, we utilized our fertility data for natural accessions that were recorded at the same time in our ovule number experiments. The correlation test showed that there is almost no correlation between ovule number and fertility in Arabidopsis accessions, suggesting that the number of ovules that a flower produced will not be affected by its growth quality and they may use separate regulatory pathways (Figure 4.8E). Furthermore, since the fertility of plants is very sensitive to the environment, we wondered whether the different timing of floral transition might also affect fertility as well as the abnormal embryo sacs. But the correlation test indicates there is no correlation between fertility and flowering time as well (Figure 4.8F). These results suggest that flowering time affects some aspects of plant reproductive development due to the effect in overall plant physiology.

4.4   Discussion

The days to flower and the number of ovules produced per flower are both important factors affecting plant productivity. In this study, we found that these two traits have a significant negative correlation. Moreover, *NERD1*, a gene that was reported to function in regulating ovule number and fertility, was identified that containing some SNPs highly associated with both ovule number and flowering time, suggesting the *NERD1* could be a common regulator for both floral transition and the ovule number. In addition, we found that delayed floral transition will affect floral development, leading to reduced ovule number per flower. We also identified that there are some gametophytic defects leading to reduced fertility during plant development in natural accessions, but those defects are not correlated with the number of ovules that a flower produced, nor influenced by flowering time. Having a better understanding of the links between flowering time and ovule number benefits us to manipulate the agricultural traits in response to climate change.

Plant growth and development are sensitive to the environment (Zinn et al., 2010; Muller and Rieu, 2016). For instance, extreme hot or cold temperature will disrupt the normal developmental process, even sometimes will cause senescence or death of the plants (Zinn et al., 2010; Hatfield and Prueger, 2015). Through natural selection, Arabidopsis accessions have adapted to the challenges of their local environments. Flowering time is one of the key adaptive strategies during the plant life cycle, and is regulated by a complex signaling network (Putterill et al., 2004; Cho et al., 2017; Sasaki et al., 2017). Some of the plants have adapted to be earlier flowering with a shorter vegetative growth period being more efficient and can save a lot of resource for floral growth, whereas others prefer flowering late in case unpredictable weather such as late snowfall or freezing happens.

Since natural Arabidopsis accessions grow in diverse conditions throughout the world, it is not surprising that they displayed a variation in different traits such as flowering time and ovule numbers (Weigel, 2012; Blackman, 2017; Yuan and Kessler, 2019). However, it is interesting that we found a significant negative correlation between these two traits, with the later flowering accessions tending to produce fewer ovules per flower, and vice versa. This correlation indicates there might be some common pathways or similar regulators that were shared or utilized by both flowering time and ovule number. The floral transition is under the regulation of a complex network and initiates from floral meristem (Mouradov et al., 2002; Simpson and Dean, 2002). Similarly, ovules initiated from the carpel margin meristem (CMM) (Smyth et al., 1990). So the meristem regions play an important role in these two processes, which could be the key point that linked flowering time and ovule number.

In our study, we explored the correlation between the flowering time and ovule number at a genetic level by using GWAS and determined the specific SNPs that are highly associated with both flowering time and ovule number. Interestingly, we found eight SNPs in a distinct in region chromosome 3 that had previously been found to associate with ovule number variation. Mutation of one of the genes in this region, *NERD1*, caused both reduced ovule number and delayed flowering time, revealing that flowering time and ovule number may be under similar regulation in a NERD1-dependent pathway. For instance, *NERD1* could be the common regulator in both floral meristem and carpel margin meristem to initiating the floral transition and ovule initiation. Furthermore, *nerd1-2* has been reported to have a root growth defect in which the root meristem was shortened (Cole et al., 2018). This also provides us a hint for *NERD1*, which could play an important role in regulating general meristem regions. For future experiments, it would be

interesting to examine NERD1 expression levels in of early and late flowering accessions before and after floral transition, which could provide evidence that the *NERD1* have function in regulating these two traits. The result may also explain whether *NERD1* is the common regulator for floral transition and the further ovule initiation and development. It is also important to explore in which flowering pathways *NERD1* participates (i.e. why do nerd1 mutants flower late?) There are other genes in the NERD1 chromosomal region that is associated with both ovule number and flowering time. Mutants in the rest of genes that lie in the unique chromosome 3 region should be examined in future experiments. If some of them have either delayed or earlier flowering time, then further work should be done to determine their functions in different flowering pathways.

On the other hand, when we tested the flowering time related mutants, we noticed the earlier flowering mutant produced more ovules and the later flowering mutants produced fewer ovules as well as fewer branches. This indicates that the flowering time genes may also have an important role in meristem activation throughout plant development. For future experiments, more traits can be examined among the natural accessions such as the total flower number, branch number, and plant height. It is also important to explore the genetic basis of how these traits are affected by flowering time. Understanding the mechanisms of this regulation may be helpful for manipulating the plants to be better able to respond to the environmental extremes and seasonal signals.

The number of ovules produced per flower directly links to the seed number and potential crop yield in later stage of plant development. The potential yield is determined by the number of seeds per flower, the total flower number and the seed weight (Fischer, 2015). Previous studies showed that flowering gene *SINGLE FLOWER TRUSS (SFT)*, a tomato ortholog of *FLOWERING LOCUS*

T , plays a role in growth termination. Mutation of the *SPT* gene increased total flowers per plant and the fruits weight that leading to increased total yield in tomato (Krieger et al., 2010). In rice, there is also a correlation between the heading date and potential yield, both traits are regulated by the quantitative traits locus Ghd7, which isolated from elite rice hybird (Xue et al., 2008). In our study, we did not count the total seed number for each accession, but in future study, it would be interesting to count the Arabidopsis seed number, seed weight as well as the total flower number and to determine if any of these traits are correlated with flowering time. Based on our ovule number results, we predict that the total seed number may also have a negative correlation with flowering time in Arabidopsis.

Global climate change is expected to change many of the environmental cues that regulate flowering time. Since flowering time may affect not only ovule number, but also overall seed yield, future work should focus on understanding the links between these processes so that plants can be manipulated to have optimal productivity in suboptimal environments.

4.5   Figures and Tables
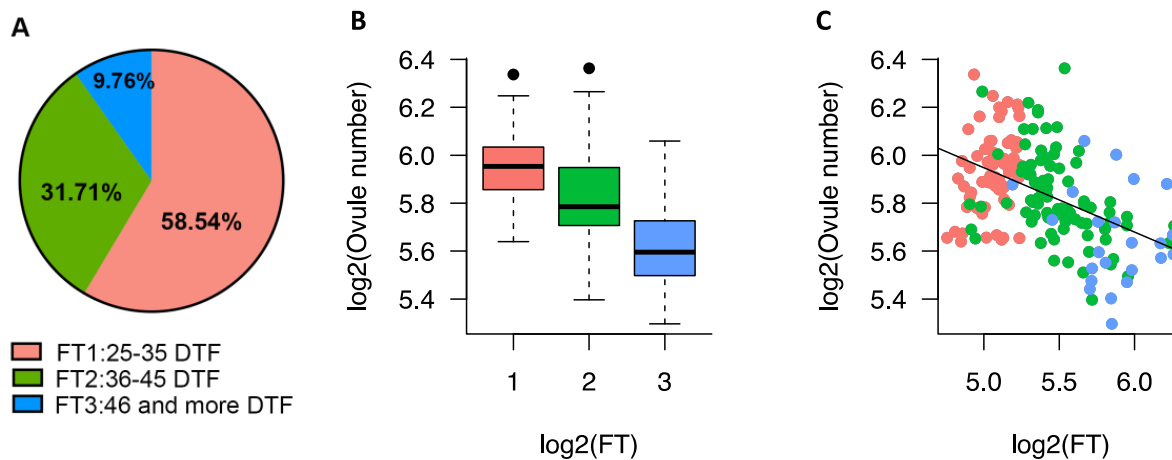
Figure 4.1 The ovule number per flower has negative correlation with their flowering time in natural accessions.

(A) Based on the days to flower, 189 accessions were divided into three groups. (B) Those accessions which were late flowering tend to have less ovule per flower. DTF: Days to flowering. FT1: 25-35 DTF (pink), FT2: 36-45 DTF (green), FT3: 46 and more DTF (blue). (C) The flowering time have negative correlation with their ovule number per flower. 176 overlapped accessions were used for Pearson's product-moment correlation test, r=-0.5***, p value=1.154e^{-10} ***.
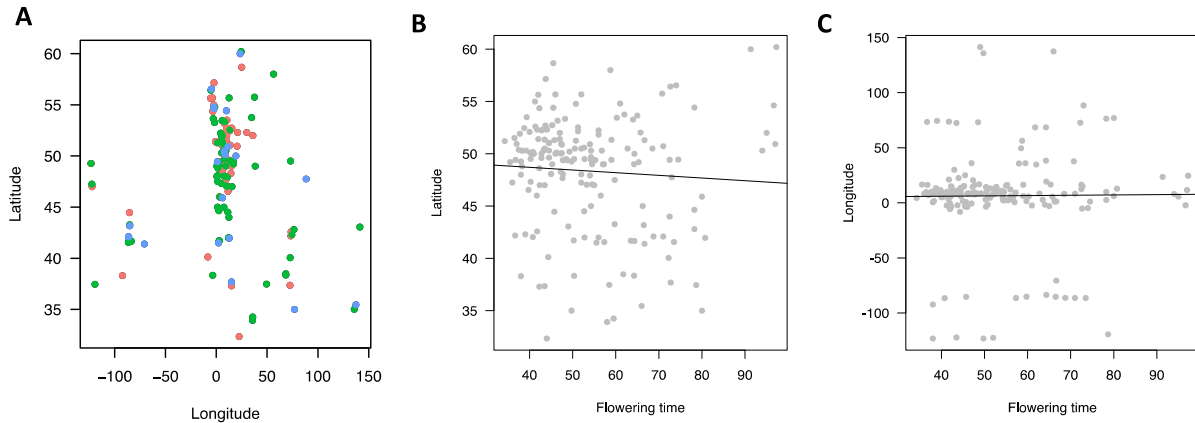
Figure 4.2 Natural accessions and their distribution.

(A) Arabidopsis accessions spread all over the world in our study. FT1: 25-35 DTF (pink), FT2: 36-45 DTF (green), FT3: 46 and more DTF (blue). (B) The flowering time of the accessions in this study have no correlation with their latitude. Pearson's product-moment correlation test with r=-0.06, *p* value=0.39. (C) The flowering time of the accessions in our study have no correlation with their longitude. Pearson's product-moment correlation test with r=0.01, *p* value=0.90.
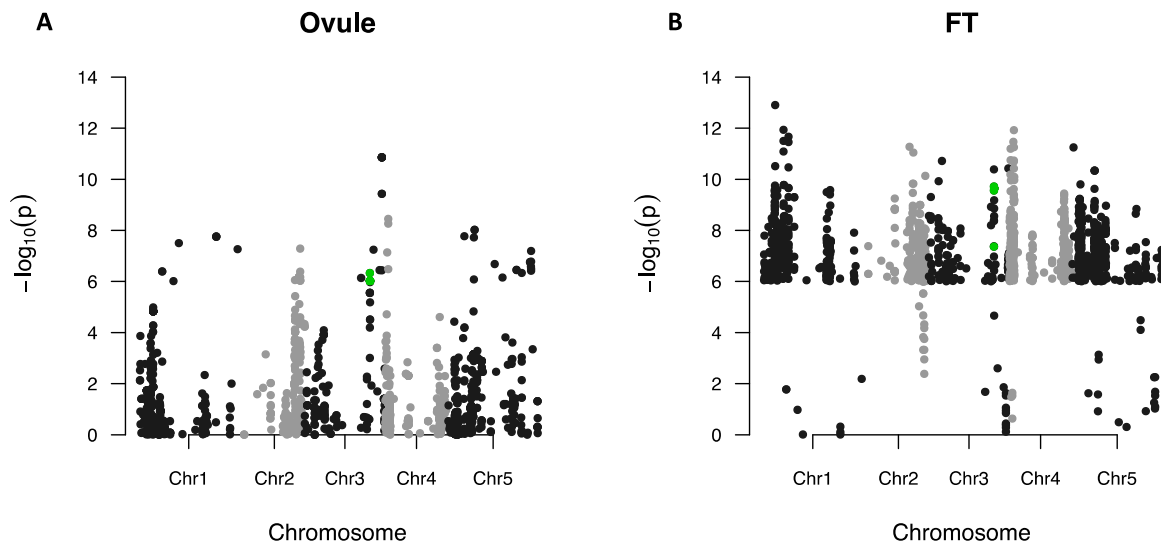
Figure 4.3 GWAS identifies candidate loci associated with both ovule number per flower and the flowering time.

(A) Manhattan plot for the selected SNPs associated with ovule number per flower. (B) Manhattan plot for the selected SNPs associated with flowering time. The loci were selected if $-\log_{10}$ transformed p value lager than 6 either in the result of ovule number per flower or the flowering time (grey and black dots). The light green dots represent the loci if $-\log_{10}$ transformed p value larger than 6 in both ovule number per flower and the flowering time.
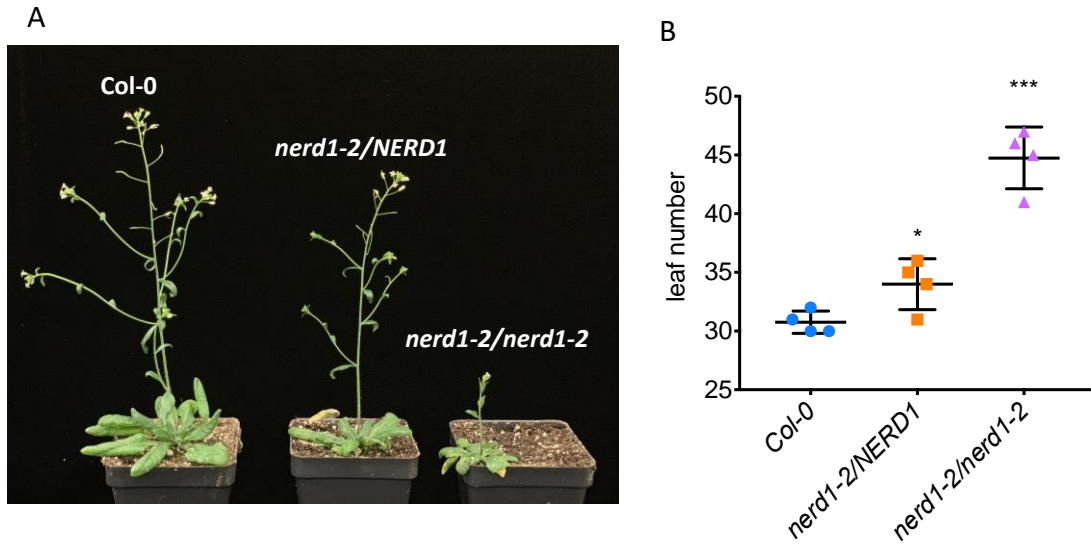
Figure 4.4 *nerd1-2* displays delayed flowering time.

(A) Compared to Col-0, the homozygous *nerd1-2* mutant produced more leaves and flowered later. (B) Leaf number counts for Col-0, *nerd1-2/NERD1,* and *nerd1-2/nerd1-2.* "***" indicates statistical significance (*p* value<0.001 determined by Student's t-test). "*" indicates statistical significance (*p* value<0.01 determined by Student's t-test).
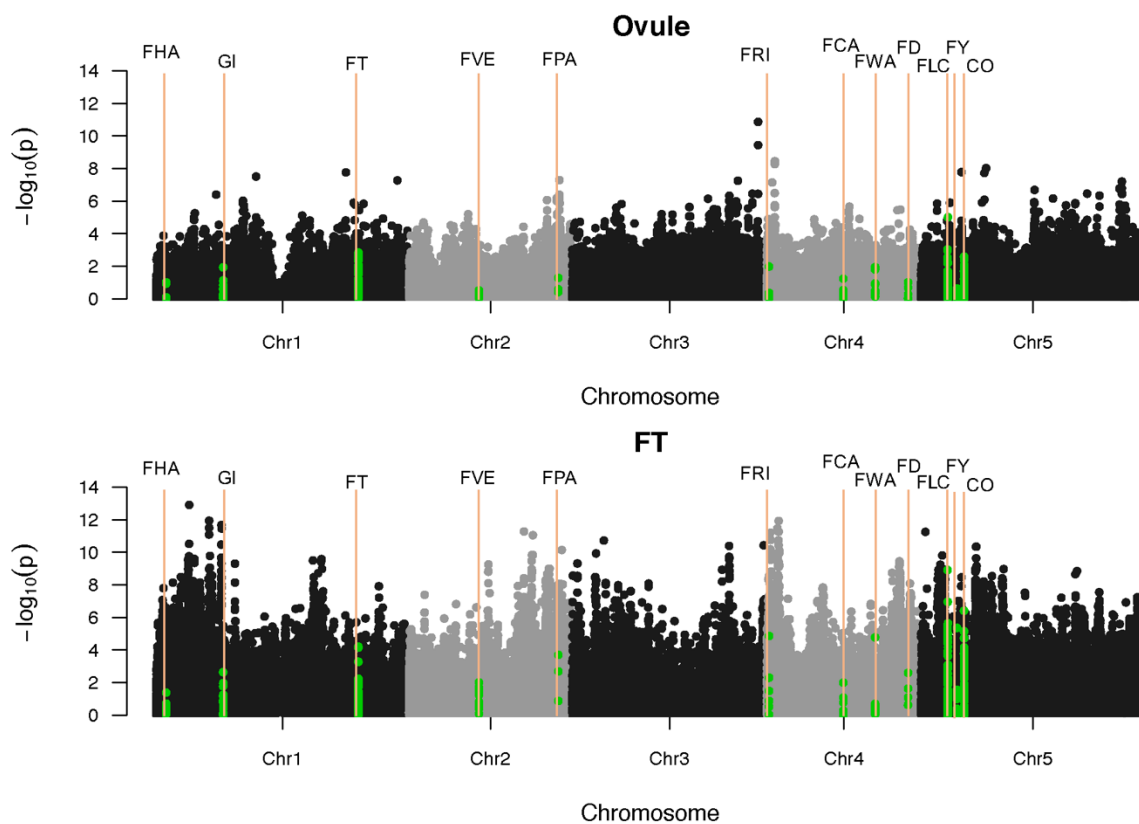
Figure 4.512 flowering time related genes were mapped on Manhattan plots of the ovule number and flowering time GWAS.

Orange lines indicate the position of flowering time related genes. Green dots are the SNPs in the flowering time related genes.
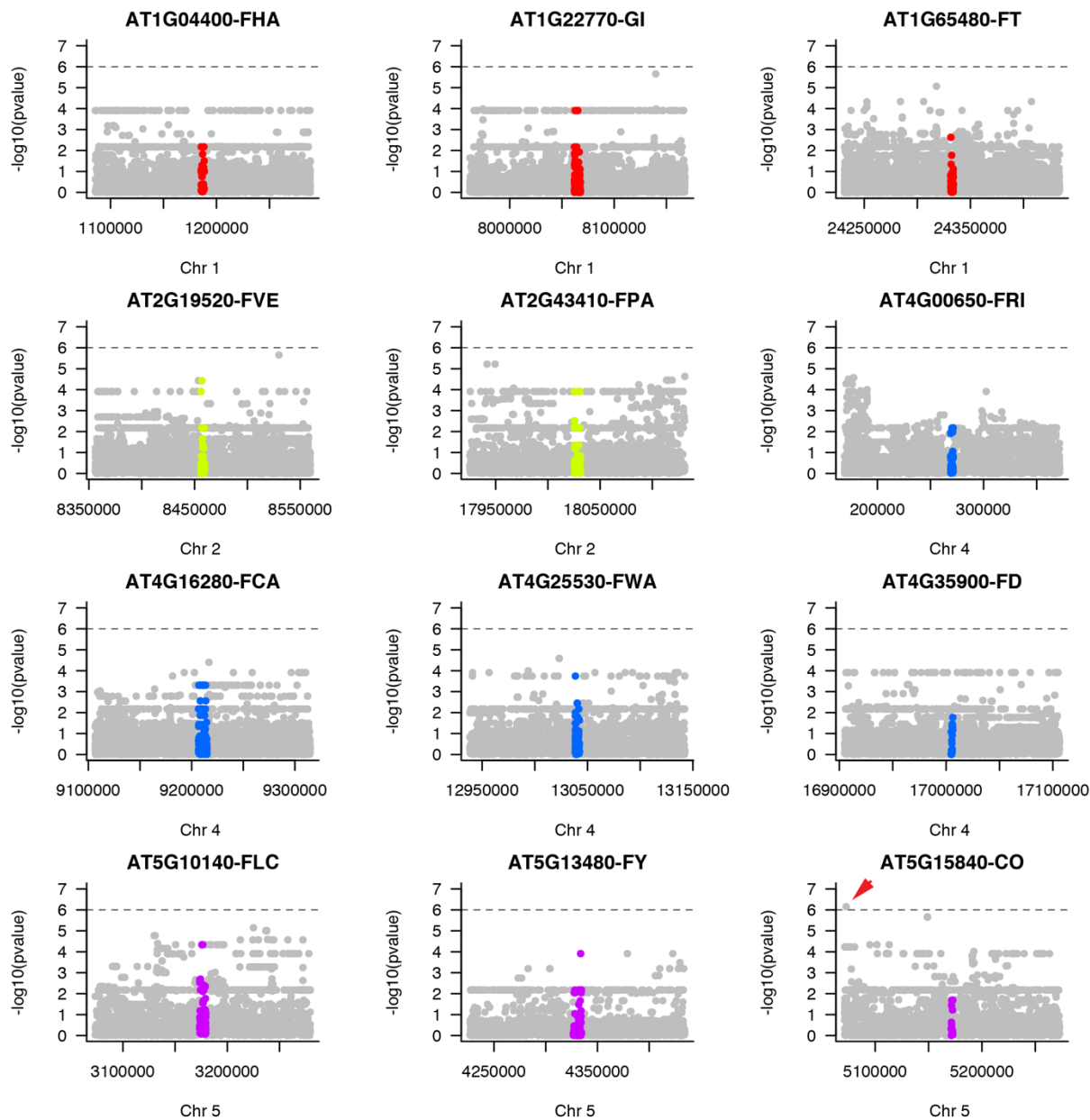
Figure 4.6 The flanking 200kb regions of 12 well-known flowering time related genes mapped on the ovule number Manhattan plot.

In each panel, the grey dots represent the SNPs' *p* value, the x-axis represents the position on the chromosome that the given gene located, the colored dots are the SNPs in the gene. In the *CO* flanking region panel, there is a SNP that -$\log_{10} p$ value >6.2 (arrow). The 5% FDR thresholds (-$\log_{10} p$ value =6.2) are represented as the dashed line on each plot.
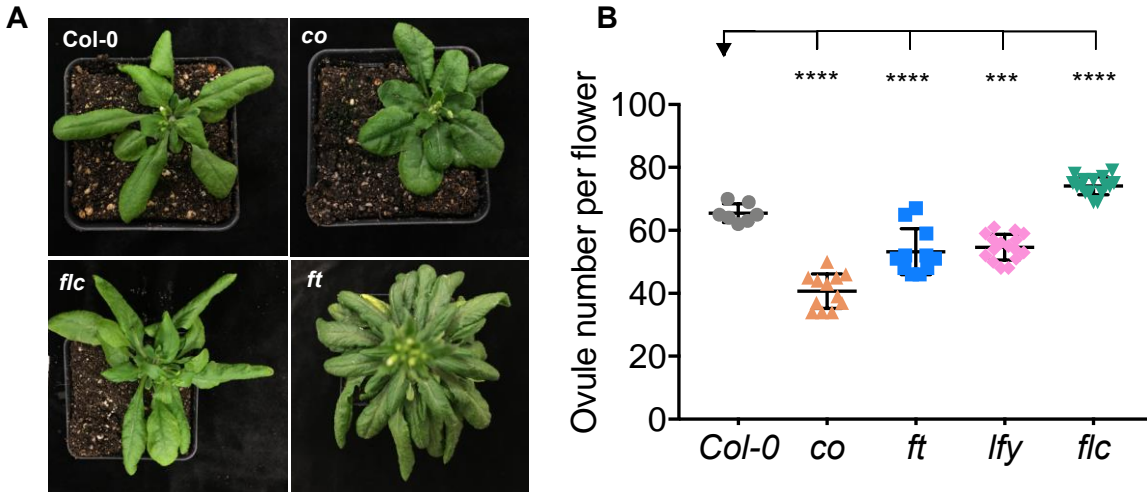
Figure 4.7 The flowering time mutants have a variation in ovule number.

(A) The flowring time mutants produced different leaf number when the first bud was visible. (B) Scatter plot of ovule number per flower in flowering time mutants. "***" indicates statistical significance (p value<0.05 determined by Student's t-test). "****" indicates statistical significance (p value<0.001 determined by Student's t-test).
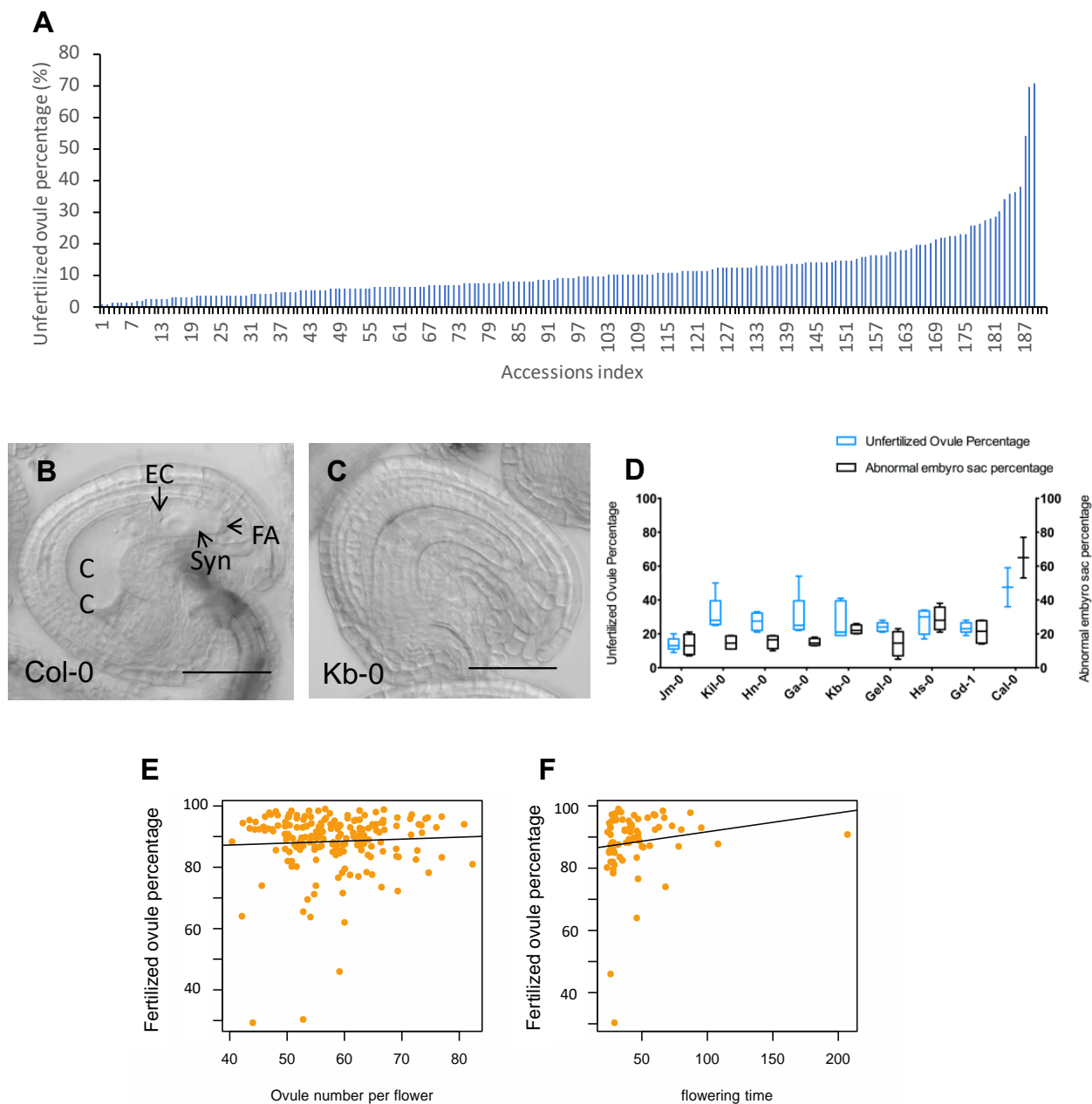
Figure 4.8 The diversity links among flowering time, ovule number and other reproductive traits.

(A) Natural accessions displayed a significant variation in plant fertility. (B)Differential interference contrast (DIC) image of a mature wild type (Col-0) embryo sac. Bar=40μm. CC, Central cell; EC, egg cell; Syn, Synergid cells; FA, filiform apparatus. (C) DIC image of an abnormal embryo sac in natural accession Kb-0. The Kb-0 displayed aborted embryo sac that no egg cell, central cell, synergid cells and antipodal cells developed. Bar=40μm. (D) Boxplot of unfertilized ovule percentage and abnormal embryo sac percentage in some natural accessions. (E) There is no correlation between the fertility and flowering time. Pearson's product-moment correlation test with r= 0.15, p value= 0.198. (F) There is no correlation between the fertility and ovule number. Pearson's product-moment correlation test with r= 0.05, p value= 0.465.

Table 4.1 The candidate genes associated with both ovule number per flower (ON) and flowering time (FT)

Chr.	Position	Gene ID	Description	P_{ON}	P_{FT}
3	18917649	AT3G50890	homeobox protein 28	9.51E-07	1.92E-10
3	18918049	AT3G50900	unknown protein	9.51E-07	2.76E-10
3	18934040	AT3G50940	P-loop containing nucleoside triphosphate hydrolases superfamily protein	4.69E-07	4.34E-08
3	18942604	AT3G50980	dehydrin xero 1 (XERO1)	9.51E-07	2.27E-10
3	18948019	AT3G51010	unknown protein	9.51E-07	2.27E-10
3	18949972	AT3G51020	unknown protein	9.51E-07	2.27E-10
3	18953930	AT3G51050	NERD1	9.51E-07	2.27E-10
3	18954034	AT3G51050	NERD1	9.51E-07	2.27E-10

Table 4.2 Leaf number counts for different flowering time mutants

Gene ID	Description	Leaf number	Gene ID	Description	Leaf number
	Col-0	31	AT5G15840	*co*	36
AT1G65480	*ft*	164	AT5G10140	*flc*	23
AT5G61850	*lfy*	52			

Table 4.3 List of Arabidopsis accessions used in the study and their ovule number data

Accession	FT Group	Days to flower (Atwell *et al*. 2010)	Ovule number	Longitude	Latitude	Country
Aa_0	2	54.00	69.20	9.57	50.92	GER
Abd_0	1	43.75	58.94	-2.22	57.15	UK
Ag_0	2	66.25	55.00	1.30	45.00	France
Ak_1	1	47.75	50.35	7.63	48.07	GER
Alst_1	3	61.00	57.56	-2.43	54.80	UK
Altai_5	3	73.00	39.30	88.40	47.75	China
Amel_1	2	60.25	54.15	5.73	53.45	NED
An_1	1	34.25	50.40	4.40	51.22	Belgium
Ang_0	2	54.25	63.45	5.30	50.30	Belgium
Anholt_1	3	NA	43.50	NA	NA	NA
Ann_1	3	80.00	49.69	6.13	45.90	France
Anz_0	2	58.50	51.70	49.47	37.47	Iran
Appt_1	2	56.00	64.20	5.58	51.83	NED
Ba_1	3	74.00	52.70	-4.80	56.55	UK
Baa_1	2	59.00	53.30	6.10	51.33	NED
Baz_0	2	38.25	51.63	1.66	48.81	France
Bch_1	1	40.25	54.07	9.32	49.52	GER
Bd_0	1	38.75	80.85	13.29	52.46	GER
Be_0	2	54.25	56.75	8.62	49.68	GER
Benk_1	2	95.00	49.65	5.68	52.00	NED
Ber	2	52.00	56.53	12.57	55.68	DEN
Bik_1	2	58.00	54.88	35.70	33.92	Lebanon
Bl_1	2	52.67	49.65	11.34	44.50	Italy
Bla_1	2	63.50	52.63	2.80	41.68	Spain
Bla_5	2	NA	44.00	NA	NA	NA
Boot_1	1	45.50	60.95	-3.27	54.40	UK
Bor_1	2	55.25	51.00	16.23	49.40	Czech Republic
Br_0	2	65.33	50.75	16.62	49.20	Czech Republic
Bsch_0	1	47.25	66.45	8.67	50.02	GER
Bu_0	2	50.50	52.80	9.50	50.50	GER
Ca_0	1	38.25	57.45	8.27	50.30	GER
Cal_0	2	64.00	45.58	-1.64	53.27	UK

Accession	FT Group	Days to flower (Atwell *et al*. 2010)	Ovule number	Longitude	Latitude	Country
Cen_0	2	57.00	54.81	0.50	49.00	France
Cerv_1	2	56.00	50.15	12.10	42.00	Italy
Chat_1	2	45.00	55.75	1.34	48.07	France
Chi_0	2	62.00	62.63	34.74	53.75	Russia
Cit_0	3	NA	40.42	NA	NA	NA
Cnt_1	2	66.67	42.13	1.10	51.30	UK
Co_1	1	44.33	50.40	-8.25	40.12	POR
Col_0	1	38.00	56.65	-92.30	38.30	US
Com_1	2	54.25	54.20	2.82	49.42	France
Ct_1	1	42.25	76.00	15.00	37.30	Italy
Da1-12	3	NA	51.65	NA	NA	NA
Db_1	2	43.25	64.20	8.32	50.31	GER
Di_G	2	40.25	76.94	5.04	47.32	France
Dja_1	1	41.75	60.30	73.63	42.58	Kyrgyzstan
Do_0	2	71.00	50.15	8.24	50.72	GER
Dr_0	1	44.50	58.40	13.73	51.05	GER
Dra_0	1	36.75	51.05	16.27	49.42	Czech Republic
Dra_1	1	NA	76.95	NA	NA	NA
Durh_1	2	50.75	55.90	-1.57	54.78	UK
Ei_2	2	56.75	69.42	6.30	50.30	GER
El_0	1	36.50	49.85	9.68	51.51	GER
Ema_1	1	45.75	66.44	0.50	51.30	UK
En_2	1	41.00	50.44	8.50	50.00	GER
En_D	1	42.75	63.40	8.50	50.00	GER
Er_0	1	42.75	58.56	11.01	49.60	GER
Es_0	2	97.25	52.19	24.57	60.20	Finland
Est	1	45.50	55.45	24.99	58.67	Estonia
Et_0	2	78.25	53.56	2.56	44.64	France
Etna_2	3	72.75	42.30	14.98	37.69	Italy
Fi_0	3	68.50	52.81	8.02	50.50	GER
Fr_2	3	46.25	58.81	8.68	50.11	GER
Ga_0	3	94.00	58.90	8.00	50.30	GER
Gd_1	1	39.33	63.85	10.50	53.50	GER
Gel_1	1	44.50	62.44	5.87	51.02	NED
Gie_0	2	52.67	63.06	8.68	50.58	GER

Accession	FT Group	Days to flower (Atwell *et al*. 2010)	Ovule number	Longitude	Latitude	Country
Gifu_2	3	66.00	43.45	137.42	35.45	Japan
Gr_1	2	55.00	62.06	15.50	47.00	Austria
Gre_0	3	66.50	44.50	-85.25	43.18	US
Gu_0	1	44.50	63.35	8.00	50.30	GER
Gy_0	2	54.50	53.45	2.00	49.00	France
Ha_0	1	44.00	50.13	9.74	52.37	GER
Had_1b	2	59.50	54.70	35.92	34.25	Lebanon
Hey_1	2	50.75	69.06	5.90	51.25	NED
Hh_0	3	78.25	44.33	9.89	54.42	GER
Hn_0	1	43.50	73.50	8.29	51.35	GER
HR_5	1	47.00	61.50	-0.64	51.41	UK
Hs_0	1	42.75	60.06	9.44	52.24	GER
Is_0	2	52.00	72.44	7.50	50.50	GER
Je_0	3	97.00	48.05	11.59	50.93	GER
Jl_3	1	35.50	51.30	16.62	49.20	Czech Republic
Jm_0	1	45.25	66.30	15.00	49.00	Czech Republic
Ka_0	1	42.33	63.15	14.00	47.00	Austria
Kar_1	2	39.00	50.30	74.37	42.30	Kyrgyzstan
Kas_2	3	80.00	45.90	77.00	35.00	India
Kb_0	1	40.75	55.05	8.51	50.18	GER
Kelsterbach_4	1	47.50	62.31	8.53	50.07	GER
Kil_0	1	42.00	62.25	-5.66	55.64	UK
Kin_0	1	45.75	62.70	-85.37	44.46	US
Kl_5	1	37.00	58.50	6.97	50.95	GER
Knox_18	3	NA	48.05	NA	NA	NA
Ko_2	3	91.50	47.55	NA	NA	DEN
Kondara	2	61.75	53.15	68.49	38.48	Tajikistan
Kro_0	1	40.25	59.25	8.97	50.07	GER
Krot_0	1	44.50	56.31	11.57	49.63	GER
Kyoto	2	49.75	60.55	135.75	35.01	Japan
Kyr_1	2	72.25	54.25	72.68	40.05	Kyrgyzstan
Kz_9	2	48.50	61.95	73.10	49.50	Kazakhstan
La_0	1	45.25	74.65	15.23	52.73	Poland
Lan_0	1	46.00	66.85	-3.78	55.67	UK

Accession	FT Group	Days to flower (Atwell *et al*. 2010)	Ovule number	Longitude	Latitude	Country
Le_0	2	51.25	59.20	4.49	52.16	NED
Li_2	2	NA	62.63	NA	NA	NA
Lip_0	3	64.33	66.70	19.30	50.00	Poland
Litva	1	47.50	73.38	NA	NA	Lithuania
Lm_2	2	38.00	55.55	0.50	48.00	France
Lp2_2	2	48.75	69.05	16.81	49.38	Czech Republic
Lz_0	2	56.50	65.50	3.30	46.00	France
Mc_0	3	96.67	50.81	-2.30	54.62	UK
Me_0	1	37.75	69.00	10.11	51.92	GER
Mh_0	1	47.33	74.10	20.50	50.95	Poland
Mir_0	2	72.50	52.81	12.37	44.00	Italy
Mnz_0	1	46.00	62.65	8.27	50.00	GER
Mrk_0	2	57.25	53.95	9.30	49.00	GER
Ms_0	2	70.75	51.70	37.63	55.75	Russia
Mt_0	1	44.00	72.68	22.46	32.34	LIB
Mv_0	3	66.67	46.13	-70.67	41.39	US
Mz_0	1	39.25	54.94	8.30	50.30	GER
Na_1	2	59.75	59.31	1.50	47.50	France
Nc_1	1	42.25	62.25	6.25	48.62	France
Neo_6	1	43.50	59.60	72.47	37.35	Tajikistan
Nok_0	2	NA	51.69	NA	NA	NA
Nok_3	2	56.00	47.19	4.45	52.24	NED
Np_0	1	43.67	62.90	10.98	52.70	GER
Nw_0	1	43.50	57.94	8.50	50.50	GER
Ob_0	2	49.25	54.25	8.58	50.20	GER
Old_1	1	46.50	63.50	8.20	53.17	GER
Or_0	1	37.50	55.10	8.01	50.38	GER
Ove_0	2	48.25	61.00	8.42	53.34	GER
Per_1	2	58.75	82.31	56.32	58.00	Russia
Pi_0	2	53.25	59.45	10.51	47.04	Austria
Pla_0	3	55.50	53.10	2.25	41.50	Spain
Pla_1	2	NA	46.17	NA	NA	NA
Pna_0	2	NA	66.95	NA	NA	NA
Pna_10	3	71.00	46.90	-86.33	42.09	US
Pna_17	3	68.75	48.35	-86.33	42.09	US

Accession	FT Group	Days to flower (Atwell *et al*. 2010)	Ovule number	Longitude	Latitude	Country
Pog_0	2	49.75	74.50	-123.21	49.27	Canada
Pu2_23	2	59.00	52.85	16.36	49.42	Czech Republic
Pu2_7	2	72.50	55.88	16.36	49.42	Czech Republic
Ra_0	1	41.67	66.69	3.30	46.00	France
Ragl_1	1	42.25	64.55	-3.42	54.35	UK
Rd_0	2	62.75	64.80	8.50	50.50	GER
Rld_1	2	NA	54.80	NA	NA	NA
Rmx_A02	1	40.75	65.15	-86.51	42.04	US
Rome_1	2	52.75	64.88	12.10	42.00	Italy
Rou_0	3	74.50	64.10	1.10	49.44	France
RRs_10	2	73.50	47.40	-86.43	41.56	US
RRS_7	2	57.33	61.60	-86.43	41.56	US
Rubezhnoe_1	2	64.25		38.28	49.00	Ukraine
Sap_0	2	50.33	56.20	14.24	49.49	Czech Republic
Sapporo_0	2	49.00	66.05	141.35	43.06	Japan
Se_0	2	50.33	62.25	-3.53	38.33	Spain
Seattle_0	1	43.50	71.45	-122.20	47.00	US
Sei_0	1	39.75	71.60	11.56	46.54	Italy
Sg_1	1	47.67	60.10	9.50	47.67	GER
Sha_1	2	NA	69.28	NA	NA	NA
Si_0	1	47.50	60.00	8.02	50.87	GER
Sorbo	2	64.25	56.00	68.48	38.35	Tajikistan
Sp_0	2	51.25	53.80	13.18	52.53	GER
Sq_8	1	42.00	66.75	-0.64	51.41	UK
Stw_0	1	47.00	65.45	36.00	52.00	Russia
Su_0	2	65.00	52.50	-3.01	53.65	UK
Sus_1	1	36.67	62.95	73.40	42.18	Kyrgyzstan
Ta_0	2	52.75	58.05	14.50	49.50	Czech Republic
Tac_0	2	52.00	55.65	-122.46	47.24	US
Tamm_2	3	91.33	49.60	23.50	60.00	Finland
Tiv_1	3	80.75	59.75	12.80	41.96	Italy
Tol_0	2	64.33	55.45	-83.56	41.66	US
Ts_1	2	50.25	60.55	2.93	41.72	Spain

Accession	FT Group	Days to flower (Atwell *et al*. 2010)	Ovule number	Longitude	Latitude	Country
Tscha_1	2	54.50	59.70	9.90	47.07	Austria
Tu_0	2	54.25	58.25	7.50	45.00	Italy
Tul_0	2	59.75	46.95	-85.26	43.27	US
Ty_0	2	72.67	46.65	-5.23	56.43	UK
Uk_1	2	52.00	72.95	7.77	48.03	GER
Uod_1	1	47.25	65.55	14.45	48.30	Austria
Utrecht	2	40.00	55.15	5.11	52.09	NED
Van_0	1	38.00	61.70	-123.21	49.27	Canada
Ven_1	2	65.75	48.40	5.55	52.03	NED
Vind_1	1	41.25	62.75	-2.37	54.99	UK
Wa_1	1	41.75	59.13	21.00	52.30	Poland
Wc_1	1	41.33	59.20	10.07	52.60	GER
Wei_0	1	36.00	59.85	8.26	47.25	SUI
Westkar	2	NA	58.70	NA	NA	NA
Wl_0	2	54.00	57.65	10.81	47.93	GER
Ws_2	1	43.00	50.80	30.00	52.30	Russia
Wt_5	1	44.00	57.96	9.30	52.30	GER
Yo_0	2	78.67	45.10	-119.35	37.45	US
Zal_1	2	78.25	52.25	76.35	42.80	Kyrgyzstan
Zdr_1	1	47.75	71.70	16.25	49.39	Czech Republic

CHAPTER 5.   CONCLUSIONS AND FUTURE DIRECTIONS

How plants achieve reproductive success is an important topic for plant biology researchers, since it directly links to agricultural productivity. Pollination is an interesting field to explore and it is also a fundamental process that occurs in flowering plants. In this dissertation, I summarized my PhD research for the sexual reproduction in flowering plants from multiple directions. By exploring those unknown questions, I was able to have a better understanding of the detailed mechanisms of plants, which also helps me to generate some new ideas for future research.

5.1   Manipulating the Cell-cell communication improves the quality of reproductive success

Successful pollen tube reception and double fertilization is important and critical to plant fertility. In chapter 2, I introduced some genes' function during pollen tube reception, which is the behavior of NTA and its related networks. Now we know that during PT arrival, NTA redistribution to the filiform apparatus takes about one and half hours, and this redistribution starts from when the PT is just arriving at the micropyle of the ovule. However, in *lre* and *fer* mutants, NTA redistribution did not happen, indicating that the NTA function in pollen tube reception is regulated by FRE/LRE pathway. I also found that RabA1g labeled endosomes accumulated at the filiform apparatus during PT arrival. My hypothesis for the NTA redistribution is that after perceiving the signal from PT, *FER/LRE* will act as coreceptors and initiate a signal transduction cascade that leads to selective trafficking of NTA protein from the Golgi to the filiform apparatus. However, more detailed information of this collaboration still needs to be explored. As for the future directions, the actual interaction among FER/LRE/NTA pathways should be determined during PT reception. It is possible that there are some signals released from the pollen tube to facilitate the NTA movement. Another future direction is to test the behavior of other type of endosome makers

during pollen tube reception. Then NTA and endosomes can be tracked at the same time during PT approaching at a higher resolution. Moreover, it is interesting to explore if the endosome will still have the polar accumulation at the filiform apparatus in *nta-1* mutants and if the NTA-GFP will redistribute to filiform apparatus in endosome mutants such as Rab4 negative mutant (Rab4AS22N), Rab5 negative mutant (Rab5S34N) (McCaffrey et al., 2001). If the endosome does not redistribute to filiform apparatus in *nta-1* mutants, and the NTA-GFP still redistribute to filiform apparatus in endosome mutants, which suggests that the endosome re-accumulation depends on NTA signaling pathway, vice versa.

As for the whole pollination event, it will be interesting to explore the diversity of intercellular communication between the male gametophyte (pollen tube) and all of the female tissues along the reproductive tract. For instance, it is still unclear how do PTs exit from the transmitting tract. There may be a region that acts as a "door" for PTs. It is also possible that PTs just randomly penetrate into any part of the pistil via tip grow. Since there are 15 proteins in MLO family, it is also interesting to explore whether other MLOs are involved in different processes during pollen tube reception such as the dynamic changes of Calcium and ROS in multiple male-female interaction stage. Moreover, during PTs attraction, it is not clear how multiple LUREs interact with the different receptor like kinases. Whether the LUREs need to always bind to them, or they just deliver some small molecules and active the process still needs to be explored. Furthermore, the more diverse function of filiform apparatus in synergid is worth to be characterized, why dose the pollen tube pause a while before entering to synergid still not clear, whether the filiform apparatus needs to secrets some contents, or the pollen tube needs to perceive enough signals to be able to enter the synergids are the opening questions.

5.2   Controlling the number of ovules improves the quantity of reproductive success

In chapter 3, I used the GWA study to identify a novel gene in regulating fertility and ovule number, which is the *NERD1*. The *nerd1* mutant is male sterile and has reduced ovule number as well as short roots (Cole et al., 2018; Yuan and Kessler, 2019). However, the mechanisms of how *NERD1* affect the number of ovules is still unclear. It would be interesting to test if *NERD1* has some functional redundancy or correlations with other well-known ovule number genes such as *ANT* and *SEU* (Klucher et al., 1996; Azhakanandam et al., 2008). It will be important to characterize the actual mechanism of *NERD1* and explore which pathway *NERD1* participates in. Moreover, some hormones expression may also vary among the *nerd1* mutant and overexpression plants. Since we observed that the branch number increases in NERD1 overexpression plants, it will be interesting to test if the NERD1 is also involved in branch initiation. If *NERD1* has some links or involves in some novel pathways for controlling the number of ovules, it will useful for generating a more efficient way to increase the number of ovules, as well as improving the potential yield in future. Furthermore, we found the negative correlation between the ovule and flowering time, and some of the highly associated SNPs are in *NERD1*. It will be interesting to test whether *NERD1* participates in the different flowering pathways. It also possible that *NERD1* highly expressed in meristem, or interact with some meristem genes such as WUSCHEL (WUS), CLAVATA (CLV), HAIRY MERISTEM (HAM), etc. to regulate the floral transition (Leibfried et al., 2005; Somssich et al., 2016; Zhou et al., 2018).

5.3   Plant reproduction and application

Pollination is very sensitive and can be easily affected by lots of random and unpredictable factors in environment. In the last part of my dissertation, I discussed the negative correlation between ovule number and flowering time. Improving the plant fertilization and maximining the quantity

of the fruits, as well as the future seeds, not only benefit their related plant family in closely environment, but also help other species like animals and humans. For instance, optimizing the fertility within plants and increasing the seed number can help in maintaining the diversity of plant species in response to climate change. As for human beings, many activities will also depend on the reproductive success of plants, such as clothes and foods. Specially, food resource is an important topic in agronomy and our daily life. With the increasing number of the populations, more and more food will be required. During my PhD study, I used the model plant *Arabidopsis thaliana.* After having a better understanding of their mechanisms, it will be useful to apply them for different crop plants. For instance, for those genes that involved in regulating the ovule number can be applied to crop plant to increase the yield in agronomy. So taking advantage of environment conditions is another way to achieve reproductive success.

5.4　To the end

During my PhD, I took advantage of genetic, molecular biology and microscopy to learn more about the female control of reproductive success in the model plant *Arabidopsis thaliana*. My research forms the framework for future studies of plant development and reproduction such as female gametophyte development, cell to cell communication during pollen tube reception, as well as the whole plant development. Based on those explorations during my PhD study, I was able to get a better scientific ability for future research.

REFERENCES

Acevedo-Garcia J, Kusch S, Panstruga R (2014) Magical mystery tour: MLO proteins in plant immunity and beyond. New Phytol **204:** 273-281

Alexander MP (1969) Differential staining of aborted and nonaborted pollen. Stain Technol **44:** 117-122

Alonso-Blanco C, Blankestijn-de Vries H, Hanhart CJ, Koornneef M (1999) Natural allelic variation at seed size loci in relation to other life history traits of Arabidopsis thaliana. Proc Natl Acad Sci U S A **96:** 4710-4717

Amasino RM (2005) Vernalization and flowering time. Current Opinion in Biotechnology **16:** 154-158

Andres F, Coupland G (2012) The genetic basis of flowering responses to seasonal cues. Nat Rev Genet **13:** 627-639

Aranzana MJ, Kim S, Zhao K, Bakker E, Horton M, Jakob K, Lister C, Molitor J, Shindo C, Tang C, Toomajian C, Traw B, Zheng H, Bergelson J, Dean C, Marjoram P, Nordborg M (2005) Genome-wide association mapping in Arabidopsis identifies previously known flowering time and pathogen resistance genes. PLoS Genet **1:** e60

Arazi T, Baum G, Snedden WA, Shelp BJ, Fromm H (1995) Molecular and Biochemical-Analysis of Calmodulin Interactions with the Calmodulin-Binding Domain of Plant Glutamate-Decarboxylase. Plant Physiology **108:** 551-561

Atwell S, Huang YS, Vilhjalmsson BJ, Willems G, Horton M, Li Y, Meng DZ, Platt A, Tarone AM, Hu TT, Jiang R, Muliyati NW, Zhang X, Amer MA, Baxter I, Brachi B, Chory J, Dean C, Debieu M, de Meaux J, Ecker JR, Faure N, Kniskern JM, Jones JDG, Michael T, Nemri A, Roux F, Salt DE, Tang CL, Todesco M, Traw MB, Weigel D, Marjoram P, Borevitz JO, Bergelson J, Nordborg M (2010) Genome-wide association study of 107 phenotypes in Arabidopsis thaliana inbred lines. Nature **465:** 627-631

Azhakanandam S, Nole-Wilson S, Bao F, Franks RG (2008) SEUSS and AINTEGUMENTA mediate patterning and ovule initiation during gynoecium medial domain development. Plant Physiology **146:** 1165-1181

Bac-Molenaar JA, Fradin EF, Becker FFM, Rienstra JA, van der Schoot J, Vreugdenhil D, Keurentjes JJB (2015) Genome-Wide Association Mapping of Fertility Reduction upon Heat Stress Reveals Developmental Stage-Specific QTLs in Arabidopsis thaliana. Plant Cell **27:** 1857-1874

Bartrina I, Otto E, Strnad M, Werner T, Schmulling T (2011) Cytokinin regulates the activity of reproductive meristems, flower organ size, ovule formation, and thus seed yield in Arabidopsis thaliana. Plant Cell **23:** 69-80

Beale KM, Johnson MA (2013) Speed dating, rejection, and finding the perfect mate: advice from flowering plants. Curr Opin Plant Biol **16:** 590-597

Beale KM, Leydon AR, Johnson MA (2012) Gamete Fusion Is Required to Block Multiple Pollen Tubes from Entering an Arabidopsis Ovule. Current Biology **22:** 1090-1094

Bencivenga S, Simonini S, Benkova E, Colombo L (2012) The transcription factors BEL1 and SPL are required for cytokinin and auxin signaling during ovule development in Arabidopsis. Plant Cell **24:** 2886-2897

Bent A (2006) Arabidopsis thaliana Floral Dip Transformation Method. *In* K Wang, ed, Methods in Molecular Biology, Vol 343. Humana Press Inc., Totowa, NJ

Berry S, Dean C (2015) Environmental perception and epigenetic memory: mechanistic insight through FLC. Plant Journal **83:** 133-148

Best NB, Hartwig T, Budka J, Fujioka S, Johal G, Schulz B, Dilkes BP (2016) nana plant2 Encodes a Maize Ortholog of the Arabidopsis Brassinosteroid Biosynthesis Gene DWARF1, Identifying Developmental Interactions between Brassinosteroids and Gibberellins. Plant Physiol **171:** 2633-2647

Best NB, Johal G, Dilkes BP (2017) Phytohormone inhibitor treatments phenocopy brassinosteroid–gibberellin dwarf mutant interactions in maize. Plant Direct **1**

Blackman BK (2017) Changing Responses to Changing Seasons: Natural Variation in the Plasticity of Flowering Time. Plant Physiology **173:** 16-26

Blazquez MA, Green R, Nilsson O, Sussman MR, Weigel D (1998) Gibberellins promote flowering of Arabidopsis by activating the LEAFY promoter. Plant Cell **10:** 791-800

Boisson-Dernier A, Frietsch S, Kim TH, Dizon MB, Schroeder JI (2008) The peroxin loss-of-function mutation abstinence by mutual consent disrupts male-female gametophyte recognition. Curr Biol **18:** 63-68

Brachi B, Faure N, Bergelson J, Cuguen J, Roux F (2013) Genome-wide association mapping of flowering time in Arabidopsis thaliana in nature: genetics for underlying components and reaction norms across two successive years. Acta Bot Gallica **160:** 205-219

Burgoyne RD, Clague MJ (2003) Calcium and calmodulin in membrane fusion. Biochim Biophys Acta **1641:** 137-143

Burn JE, Smyth DR, Peacock WJ, Dennis ES (1993) Genes Conferring Late Flowering in Arabidopsis-Thaliana. Genetica **90:** 147-155

Buschges R, Hollricher K, Panstruga R, Simons G, Wolter M, Frijters A, van Daelen R, van der Lee T, Diergaarde P, Groenendijk J, Topsch S, Vos P, Salamini F, Schulze-Lefert P (1997) The barley Mlo gene: a novel control element of plant pathogen resistance. Cell **88:** 695-705

Capron A, Gourgues M, Neiva LS, Faure JE, Berger F, Pagnussat G, Krishnan A, Alvarez-Mejia C, Vielle-Calzada JP, Lee YR, Liu B, Sundaresan V (2008) Maternal control of male-gamete delivery in Arabidopsis involves a putative GPI-anchored protein encoded by the LORELEI gene. Plant Cell **20:** 3038-3049

Chen J, Gutjahr C, Bleckmann A, Dresselhaus T (2015) Calcium signaling during reproduction and biotrophic fungal interactions in plants. Mol Plant **8:** 595-611

Chen Z, Noir S, Kwaaitaal M, Hartmann HA, Wu MJ, Mudgil Y, Sukumar P, Muday G, Panstruga R, Jones AM (2009) Two seven-transmembrane domain MILDEW RESISTANCE LOCUS O proteins cofunction in Arabidopsis root thigmomorphogenesis. Plant Cell **21:** 1972-1991

Chin D, Means AR (2000) Calmodulin: a prototypical calcium sensor. Trends Cell Biol **10:** 322-328

Cho LH, Yoon J, An G (2017) The control of flowering time by environmental factors. Plant J **90:** 708-719

Chou ML, Yang CH (1998) FLD interacts with genes that affect different developmental phase transitions to regulate Arabidopsis shoot development. Plant Journal **15:** 231-242

Christensen CA, King EJ, Jordan JR, Drews GN (1997) Megagametogenesis in Arabidopsis wild type and the Gf mutant. Sexual Plant Reproduction **10:** 49-64

Clough SJ, Bent AF (1998) Floral dip: a simplified method for Agrobacterium-mediated transformation of Arabidopsis thaliana. Plant J **16:** 735-743

Coen ES, Meyerowitz EM (1991) The war of the whorls: genetic interactions controlling flower development. Nature **353:** 31-37

Cole RA, Peremyslov VV, Van Why S, Moussaoui I, Ketter A, Cool R, Moreno MA, Vejlupkova Z, Dolja VV, Fowler JE (2018) A broadly conserved NERD genetically interacts with the exocyst to affect root growth and cell expansion. Journal of Experimental Botany **69:** 3625-3637

Consonni C, Humphry ME, Hartmann HA, Livaja M, Durner J, Westphal L, Vogel J, Lipka V, Kemmerling B, Schulze-Lefert P, Somerville SC, Panstruga R (2006) Conserved requirement for a plant host cell protein in powdery mildew pathogenesis. Nature Genetics **38:** 716-720

Cucinotta M, Colombo L, Roig-Villanova I (2014) Ovule development, a new model for lateral organ formation. Frontiers in Plant Science **5**

Curtis MD, Grossniklaus U (2003) A gateway cloning vector set for high-throughput functional analysis of genes in planta. Plant Physiol **133:** 462-469

Davis TC, Jones DS, Dino AJ, Cejda NI, Yuan J, Willoughby AC, Kessler SA (2017) Arabidopsis thaliana MLO genes are expressed in discrete domains during reproductive development. Plant Reprod **30:** 185-195

Debieu M, Tang C, Stich B, Sikosek T, Effgen S, Josephs E, Schmitt J, Nordborg M, Koornneef M, de Meaux J (2013) Co-variation between seed dormancy, growth rate and flowering time changes with latitude in Arabidopsis thaliana. PloS one **8:** e61075

Denninger P, Bleckmann A, Lausser A, Vogler F, Ott T, Ehrhardt DW, Frommer WB, Sprunck S, Dresselhaus T, Grossmann G (2014) Male-female communication triggers calcium signatures during fertilization in Arabidopsis. Nat Commun **5:** 4645

Devoto A, Piffanelli P, Nilsson I, Wallin E, Panstruga R, von Heijne G, Schulze-Lefert P (1999) Topology, subcellular localization, and sequence diversity of the Mlo family in plants. J Biol Chem **274:** 34993-35004

Domagalska MA, Leyser O (2011) Signal integration in the control of shoot branching. Nature Reviews Molecular Cell Biology **12:** 211

Dresselhaus T, Franklin-Tong N (2013) Male-female crosstalk during pollen germination, tube growth and guidance, and double fertilization. Mol Plant **6:** 1018-1036

Drews GN, Koltunow AM (2011) The female gametophyte. Arabidopsis Book **9:** e0155

Duan Q, Kita D, Johnson EA, Aggarwal M, Gates L, Wu HM, Cheung AY (2014) Reactive oxygen species mediate pollen tube rupture to release sperm for fertilization in Arabidopsis. Nat Commun **5:** 3129

Eames AJ (1961) Morphology of the angiosperms. McGraw-Hill, New York,

Elliott RC, Betzner AS, Huttner E, Oakes MP, Tucker WQ, Gerentes D, Perez P, Smyth DR (1996) AINTEGUMENTA, an APETALA2-like gene of Arabidopsis with pleiotropic roles in ovule development and floral organ growth. The Plant Cell **8:** 155-168

Escobar-Restrepo JM, Huck N, Kessler S, Gagliardini V, Gheyselinck J, Yang WC, Grossniklaus U (2007) The FERONIA receptor-like kinase mediates male-female interactions during pollen tube reception. Science **317:** 656-660

Faure JE, Rotman N, Fortune P, Dumas C (2002) Fertilization in Arabidopsis thaliana wild type: Developmental stages and time course. Plant Journal **30:** 481-488

Felsenstein J (1985) Confidence-Limits on Phylogenies - an Approach Using the Bootstrap. Evolution **39:** 783-791

Fernandez-Mazuecos M, Glover BJ (2017) The evo-devo of plant speciation. Nat Ecol Evol **1:** 110

Fischer R (2015) Definitions and determination of crop yield, yield gaps, and of rates of change. Field Crops Research **182:** 9-18

Foo E, Bullier E, Goussot M, Foucher F, Rameau C, Beveridge CA (2005) The branching gene RAMOSUS1 mediates interactions among two novel signals and auxin in pea. Plant Cell **17:** 464-474

Galbiati F, Sinha Roy D, Simonini S, Cucinotta M, Ceccato L, Cuesta C, Simaskova M, Benkova E, Kamiuchi Y, Aida M, Weijers D, Simon R, Masiero S, Colombo L (2013) An integrative model of the control of ovule primordia formation. Plant Journal **76:** 446-455

Ge Z, Bergonci T, Zhao Y, Zou Y, Du S, Liu MC, Luo X, Ruan H, Garcia-Valencia LE, Zhong S, Hou S, Huang Q, Lai L, Moura DS, Gu H, Dong J, Wu HM, Dresselhaus T, Xiao J, Cheung AY, Qu LJ (2017) Arabidopsis pollen tube integrity and sperm release are regulated by RALF-mediated signaling. Science **358:** 1596-1600

Geldner N, Denervaud-Tendon V, Hyman DL, Mayer U, Stierhof YD, Chory J (2009) Rapid, combinatorial analysis of membrane compartments in intact plants with a multicolor marker set. Plant J **59:** 169-178

Gifford EM, Foster AS, Foster AS (1989) Morphology and evolution of vascular plants, Ed 3rd. W.H. Freeman and Co., New York

Gomez MD, Barro-Trastoy D, Escoms E, Saura-Sanchez M, Sanchez I, Briones-Moreno A, Vera-Sirera F, Carrera E, Ripoll JJ, Yanofsky MF, Lopez-Diaz I, Alonso JM, Perez-Amador MA (2018) Gibberellins negatively modulate ovule number in plants. Development **145**

Gunning BES, Pate JS (1969) Transfer Cells Plant Cells with Wall Ingrowths, Specialized in Relation to Short Distance Transport of Solutes - Their Occurrence, Structure, and Development. Protoplasma **68:** 107-&

Hamamura Y, Nagahara S, Higashiyama T (2012) Double fertilization on the move. Curr Opin Plant Biol **15:** 70-77

Hamamura Y, Nishimaki M, Takeuchi H, Geitmann A, Kurihara D, Higashiyama T (2014) Live imaging of calcium spikes during double fertilization in Arabidopsis. Nat Commun **5:** 4722

Hamamura Y, Saito C, Awai C, Kurihara D, Miyawaki A, Nakagawa T, Kanaoka MM, Sasaki N, Nakano A, Berger F, Higashiyama T (2011) Live-cell imaging reveals the dynamics of two sperm cells during double fertilization in Arabidopsis thaliana. Curr Biol **21:** 497-502

Hatfield JL, Prueger JH (2015) Temperature extremes: Effect on plant growth and development. Weather and climate extremes **10:** 4-10

Hayama R, Coupland G (2004) The molecular basis of diversity in the photoperiodic flowering responses of Arabidopsis and rice. Plant Physiol **135:** 677-684

Higashiyama T (2002) The synergid cell: attractor and acceptor of the pollen tube for double fertilization. J Plant Res **115:** 149-160

Higashiyama T, Kuroiwa H, Kawano S, Kuroiwa T (1998) Guidance in vitro of the pollen tube to the naked embryo sac of torenia fournieri. Plant Cell **10:** 2019-2032

Higashiyama T, Yabe S, Sasaki N, Nishimura Y, Miyagishima S, Kuroiwa H, Kuroiwa T (2001) Pollen tube attraction by the synergid cell. Science **293:** 1480-1483

Himschoot E, Pleskot R, Van Damme D, Vanneste S (2017) The ins and outs of Ca(2+) in plant endomembrane trafficking. Curr Opin Plant Biol **40:** 131-137

Hofmeister WFB, Currey F (1862) On the germination, development, and fructification of the higher Cryptogamia, and on the fructification of the Coniferæ. Pub. for the Ray society by R. Hardwicke, London,

Hou Y, Guo X, Cyprys P, Zhang Y, Bleckmann A, Cai L, Huang Q, Luo Y, Gu H, Dresselhaus T, Dong J, Qu LJ (2016) Maternal ENODLs Are Required for Pollen Tube Reception in Arabidopsis. Curr Biol **26:** 2343-2350

Huang B-Q, Russell SD (1992) Female germ unit: organization, isolation, and function. *In* International Review of Cytology, Vol 140. Elsevier, pp 233-293

Huang HY, Jiang WB, Hu YW, Wu P, Zhu JY, Liang WQ, Wang ZY, Lin WH (2013) BR Signal Influences Arabidopsis Ovule and Seed Number through Regulating Related Genes Expression by BZR1. Molecular Plant **6:** 456-469

Huck N, Moore JM, Federer M, Grossniklaus U (2003) The Arabidopsis mutant feronia disrupts the female gametophytic control of pollen tube reception. Development **130:** 2149-2159

Huckelhoven R, Panstruga R (2011) Cell biology of the plant-powdery mildew interaction. Curr Opin Plant Biol **14:** 738-746

Iwanami Y (1984) The Viability of Pollen Grains of a Lily (Lilium-Auratum) and the Eggs of the Brine-Shrimp (Artemia-Salina) Soaked in Organic-Solvents for 10 Years. Experientia **40:** 568-569

Iwano M, Ngo QA, Entani T, Shiba H, Nagai T, Miyawaki A, Isogai A, Grossniklaus U, Takayama S (2012) Cytoplasmic Ca2+ changes dynamically during the interaction of the pollen tube with synergid cells. Development **139:** 4202-4209

Jensen WA (1965) The Ultrastructure and Histochemistry of the Synergids of Cotton. Am J Bot **52:** 238-256

Johnson MA, Harper JF, Palanivelu R (2019) A Fruitful Journey: Pollen Tube Navigation from Germination to Fertilization. Annu Rev Plant Biol **70:** 809-837

Jones DS, Kessler SA (2017) Cell type-dependent localization of MLO proteins. Plant Signaling & Behavior **12**

Jones DS, Liu X, Willoughby AC, Smith BE, Palanivelu R, Kessler SA (2018) Cellular distribution of secretory pathway markers in the haploid synergid cells of Arabidopsis thaliana. Plant J **94:** 192-202

Jones DS, Yuan J, Smith BE, Willoughby AC, Kumimoto EL, Kessler SA (2017) MILDEW RESISTANCE LOCUS O Function in Pollen Tube Reception Is Linked to Its Oligomerization and Subcellular Distribution. Plant Physiol **175:** 172-185

Juenger T, Purugganan M, Mackay TFC (2000) Quantitative trait loci for floral morphology in Arabidopsis thaliana. Genetics **156:** 1379-1392

Kasahara RD, Maruyama D, Hamamura Y, Sakakibara T, Twell D, Higashiyama T (2012) Fertilization Recovery after Defective Sperm Cell Release in Arabidopsis. Current Biology **22:** 1084-1089

Kessler SA, Grossniklaus U (2011) She's the boss: signaling in pollen tube reception. Curr Opin Plant Biol **14:** 622-627

Kessler SA, Shimosato-Asano H, Keinath NF, Wuest SE, Ingram G, Panstruga R, Grossniklaus U (2010) Conserved molecular components for pollen tube reception and fungal invasion. Science **330:** 968-971

Kim MC, Lee SH, Kim JK, Chun HJ, Choi MS, Chung WS, Moon BC, Kang CH, Park CY, Yoo JH, Kang YH, Koo SC, Koo YD, Jung JC, Kim ST, Schulze-Lefert P, Lee SY, Cho MJ (2002) Mlo, a modulator of plant defense and cell death, is a novel calmodulin-binding protein. Isolation and characterization of a rice Mlo homologue. J Biol Chem **277:** 19304-19314

Kim MC, Panstruga R, Elliott C, Muller J, Devoto A, Yoon HW, Park HC, Cho MJ, Schulze-Lefert P (2002) Calmodulin interacts with MLO protein to regulate defence against mildew in barley. Nature **416:** 447-451

Klucher KM, Chow H, Reiser L, Fischer RL (1996) The AINTEGUMENTA gene of Arabidopsis required for ovule and female gametophyte development is related to the floral homeotic gene APETALA2. Plant Cell **8:** 137-153

Koornneef M, Alonso-Blanco C, Peeters AJ, Soppe W (1998) Genetic Control of Flowering Time in Arabidopsis. Annu Rev Plant Physiol Plant Mol Biol **49:** 345-370

Koornneef M, Hanhart CJ, van der Veen JH (1991) A genetic and physiological analysis of late flowering mutants in Arabidopsis thaliana. Mol Gen Genet **229:** 57-66

Krieger U, Lippman ZB, Zamir D (2010) The flowering gene SINGLE FLOWER TRUSS drives heterosis for yield in tomato. Nature Genetics **42:** 459-U138

Kumar S, Stecher G, Tamura K (2016) MEGA7: Molecular Evolutionary Genetics Analysis Version 7.0 for Bigger Datasets. Mol Biol Evol **33:** 1870-1874

Lee I, Aukerman MJ, Gore SL, Lohman KN, Michaels SD, Weaver LM, John MC, Feldmann KA, Amasino RM (1994) Isolation of Luminidependens - a Gene Involved in the Control of Flowering Time in Arabidopsis. Plant Cell **6:** 75-83

Lee I, Bleecker A, Amasino R (1993) Analysis of Naturally-Occurring Late Flowering in Arabidopsis-Thaliana. Molecular & General Genetics **237:** 171-176

Lee J, Lee I (2010) Regulation and function of SOC1, a flowering pathway integrator. J Exp Bot **61:** 2247-2254

Leibfried A, To JP, Busch W, Stehling S, Kehle A, Demar M, Kieber JJ, Lohmann JU (2005) WUSCHEL controls meristem function by direct regulation of cytokinin-inducible response regulators. Nature **438:** 1172-1175

Lempe J, Balasubramanian S, Sureshkumar S, Singh A, Schmid M, Weigel D (2005) Diversity of flowering responses in wild Arabidopsis thaliana strains. PLoS Genet **1:** 109-118

Levy YY, Dean C (1998) The transition to flowering. Plant Cell **10:** 1973-1990

Leydon AR, Beale KM, Woroniecka K, Castner E, Chen J, Horgan C, Palanivelu R, Johnson MA (2013) Three MYB transcription factors control pollen tube differentiation required for sperm release. Curr Biol **23:** 1209-1214

Leydon AR, Tsukamoto T, Dunatunga D, Qin Y, Johnson MA, Palanivelu R (2015) Pollen Tube Discharge Completes the Process of Synergid Degeneration That Is Initiated by Pollen Tube-Synergid Interaction in Arabidopsis. Plant Physiology **169:** 485-+

Leydon AR, Weinreb C, Venable E, Reinders A, Ward JM, Johnson MA (2017) The Molecular Dialog between Flowering Plant Reproductive Partners Defined by SNP-Informed RNA-Sequencing. Plant Cell **29:** 984-1006

Li C, Yeh FL, Cheung AY, Duan Q, Kita D, Liu MC, Maman J, Luu EJ, Wu BW, Gates L, Jalal M, Kwong A, Carpenter H, Wu HM (2015) Glycosylphosphatidylinositol-anchored proteins as chaperones and co-receptors for FERONIA receptor kinase signaling in Arabidopsis. Elife **4**

Li SP, Chen L, Zhang LW, Li X, Liu Y, Wu ZK, Dong FM, Wan LL, Liu KD, Hong DF, Yang GS (2015) BnaC9.SMG7b Functions as a Positive Regulator of the Number of Seeds per Silique in Brassica napus by Regulating the Formation of Functional Female Gametophytes. Plant Physiology **169:** 2744-2760

Liang Y, Tan ZM, Zhu L, Niu QK, Zhou JJ, Li M, Chen LQ, Zhang XQ, Ye D (2013) MYB97, MYB101 and MYB120 Function as Male Factors That Control Pollen Tube-Synergid Interaction in Arabidopsis thaliana Fertilization. Plos Genetics **9**

Lim MH, Kim J, Kim YS, Chung KS, Seo YH, Lee I, Kim J, Hong CB, Kim HJ, Park CM (2004) A new Arabidopsis gene, FLK, encodes an RNA binding protein with K homology motifs and regulates flowering time via FLOWERING LOCUS C. Plant Cell **16:** 731-740

Lindner H, Kessler SA, Muller LM, Shimosato-Asano H, Boisson-Dernier A, Grossniklaus U (2015) TURAN and EVAN mediate pollen tube reception in Arabidopsis Synergids through protein glycosylation. PLoS Biol **13:** e1002139

Liu N, Tu L, Wang L, Hu H, Xu J, Zhang X (2017) MicroRNA 157-targeted SPL genes regulate floral organ size and ovule production in cotton. BMC Plant Biol **17:** 7

Liu X, Castro C, Wang Y, Noble J, Ponvert N, Bundy M, Hoel C, Shpak E, Palanivelu R (2016) The Role of LORELEI in Pollen Tube Reception at the Interface of the Synergid Cell and Pollen Tube Requires the Modified Eight-Cysteine Motif and the Receptor-Like Kinase FERONIA. Plant Cell **28:** 1035-1052

Liu ZC, Franks RG, Klink VP (2000) Regulation of gynoecium marginal tissue formation by LEUNIG and AINTEGUMENTA. Plant Cell **12:** 1879-1891

Lo SF, Yang SY, Chen KT, Hsing YI, Zeevaart JA, Chen LJ, Yu SM (2008) A novel class of gibberellin 2-oxidases control semidwarfism, tillering, and root development in rice. Plant Cell **20:** 2603-2618

Mackiewicz T (1970) Pollen Grain Morphology, Viability, and Pollen Tube Development in-Vitro and in-Situ in Octoploid White Clover (Trifolium-Repens L). Genetica Polonica **11:** 249-+

Maheshwari P (1950) An introduction to the embryology of angiosperms, Ed 1st. McGraw-Hill, New York,

McCaffrey MW, Bielli A, Cantalupo G, Mora S, Roberti V, Santillo M, Drummond F, Bucci C (2001) Rab4 affects both recycling and degradative endosomal trafficking. FEBS letters **495:** 21-30

Modrusan Z, Reiser L, Feldmann KA, Fischer RL, Haughn GW (1994) Homeotic Transformation of Ovules into Carpel-like Structures in Arabidopsis. The Plant Cell **6:** 333-349

Moon J, Suh SS, Lee H, Choi KR, Hong CB, Paek NC, Kim SG, Lee I (2003) The SOC1 MADS-box gene integrates vernalization and gibberellin signals for flowering in Arabidopsis. Plant J **35:** 613-623

Moriyama EN, Strope PK, Opiyo SO, Chen Z, Jones AM (2006) Mining the Arabidopsis thaliana genome for highly-divergent seven transmembrane receptors. Genome Biol **7:** R96

Mouradov A, Cremer F, Coupland G (2002) Control of flowering time: Interacting pathways as a basis for diversity. Plant Cell **14:** S111-S130

Mulcahy DL (1979) The rise of the angiosperms: a genecological factor. Science **206:** 20-23

Muller F, Rieu I (2016) Acclimation to high temperature during pollen development. Plant Reprod **29:** 107-118

Muller LM, Lindner H, Pires ND, Gagliardini V, Grossniklaus U (2016) A subunit of the oligosaccharyltransferase complex is required for interspecific gametophyte recognition in Arabidopsis. Nature Communications **7**

Nahar MA, Ishida T, Smyth DR, Tasaka M, Aida M (2012) Interactions of CUP-SHAPED COTYLEDON and SPATULA genes control carpel margin development in Arabidopsis thaliana. Plant Cell Physiol **53:** 1134-1143

Nam YJ, Herman D, Blomme J, Chae E, Kojima M, Coppens F, Storme V, Van Daele T, Dhondt S, Sakakibara H, Weigel D, Inze D, Gonzalez N (2017) Natural Variation of Molecular and Morphological Gibberellin Responses. Plant Physiol **173:** 703-714

Nelson BK, Cai X, Nebenfuhr A (2007) A multicolored set of in vivo organelle markers for co-localization studies in Arabidopsis and other plants. Plant J **51:** 1126-1136

Nemhauser JL, Feldman LJ, Zambryski PC (2000) Auxin and ETTIN in Arabidopsis gynoecium morphogenesis. Development **127:** 3877-3888

Ngo QA, Vogler H, Lituiev DS, Nestorova A, Grossniklaus U (2014) A Calcium Dialog Mediated by the FERONIA Signal Transduction Pathway Controls Plant Sperm Delivery. Dev Cell **29:** 491-500

Okuda S, Tsutsui H, Shiina K, Sprunck S, Takeuchi H, Yui R, Kasahara RD, Hamamura Y, Mizukami A, Susaki D, Kawano N, Sakakibara T, Namiki S, Itoh K, Otsuka K, Matsuzaki M, Nozaki H, Kuroiwa T, Nakano A, Kanaoka MM, Dresselhaus T, Sasaki N, Higashiyama T (2009) Defensin-like polypeptide LUREs are pollen tube attractants secreted from synergid cells. Nature **458:** 357-361

Onouchi H, Igeno MI, Perilleux C, Graves K, Coupland G (2000) Mutagenesis of plants overexpressing CONSTANS demonstrates novel interactions among Arabidopsis flowering-time genes. Plant Cell **12:** 885-900

Palanivelu R, Preuss D (2006) Distinct short-range ovule signals attract or repel Arabidopsis thaliana pollen tubes in vitro. BMC Plant Biol **6:** 7

Palanivelu R, Tsukamoto T (2012) Pathfinding in angiosperm reproduction: pollen tube guidance by pistils ensures successful double fertilization. Wiley Interdiscip Rev Dev Biol **1:** 96-113

Palmer RG, Albertsen MC, Heer H (1978) Pollen production in soybeans with respect to genotype, environment, and stamen position. Euphytica **27:** 427-433

Panstruga R (2005) Serpentine plant MLO proteins as entry portals for powdery mildew fungi. Biochem Soc Trans **33:** 389-392

Peaucelle A, Braybrook SA, Le Guillou L, Bron E, Kuhlemeier C, Hofte H (2011) Pectin-induced changes in cell wall mechanics underlie organ initiation in Arabidopsis. Curr Biol **21:** 1720-1726

Peaucelle A, Louvet R, Johansen JN, Hofte H, Laufs P, Pelloux J, Mouille G (2008) Arabidopsis phyllotaxis is controlled by the methyl-esterification status of cell-wall pectins. Curr Biol **18:** 1943-1948

Platre MP, Noack LC, Doumane M, Bayle V, Simon MLA, Maneta-Peyret L, Fouillen L, Stanislas T, Armengot L, Pejchar P, Caillaud MC, Potocky M, Copic A, Moreau P, Jaillais Y (2018) A Combinatorial Lipid Code Shapes the Electrostatic Landscape of Plant Endomembranes. Dev Cell **45:** 465-480 e411

Punwani JA, Drews GN (2008) Development and function of the synergid cell. Sexual Plant Reproduction **21:** 7-15

Putterill J, Laurie R, Macknight R (2004) It's time to flower: the genetic control of flowering time. Bioessays **26:** 363-373

Qin Y, Leydon AR, Manziello A, Pandey R, Mount D, Denic S, Vasic B, Johnson MA, Palanivelu R (2009) Penetration of the stigma and style elicits a novel transcriptome in pollen tubes, pointing to genes critical for growth in a pistil. PLoS Genet **5:** e1000621

Rameau C, Bertheloot J, Leduc N, Andrieu B, Foucher F, Sakr S (2014) Multiple pathways regulate shoot branching. Front Plant Sci **5:** 741

Ratcliffe OJ, Amaya I, Vincent CA, Rothstein S, Carpenter R, Coen ES, Bradley DJ (1998) A common mechanism controls the life cycle and architecture of plants. Development **125:** 1609-1615

Ratcliffe OJ, Riechmann JL (2002) Arabidopsis transcription factors and the regulation of flowering time: a genomic perspective. Curr Issues Mol Biol **4:** 77-91

Reyes-Olalde JI, Zuniga-Mayo VM, Chavez Montes RA, Marsch-Martinez N, de Folter S (2013) Inside the gynoecium: at the carpel margin. Trends Plant Sci **18:** 644-655

Robinson-Beers K, Pruitt RE, Gasser CS (1992) Ovule Development in Wild-Type Arabidopsis and Two Female-Sterile Mutants. Plant Cell **4:** 1237-1249

Ross JD (1985) The Physiology of Flowering Plants - Their Growth and Development, 3rd Edition - Street,He, Opik,H. Nature **314:** 42-43

Rotman N, Rozier F, Boavida L, Dumas C, Berger F, Faure JE (2003) Female control of male gamete delivery during fertilization in Arabidopsis thaliana. Curr Biol **13:** 432-436

Ruge H, Flosdorff S, Ebersberger I, Chigri F, Vothknecht UC (2016) The calmodulin-like proteins AtCML4 and AtCML5 are single-pass membrane proteins targeted to the endomembrane system by an N-terminal signal anchor sequence. J Exp Bot **67:** 3985-3996

Russell SD (1992) Double Fertilization. International Review of Cytology-a Survey of Cell Biology **140:** 357-387

Sachs T, Thimann KV (1967) THE ROLE OF AUXINS AND CYTOKININS IN THE RELEASE OF BUDS FROM DOMINANCE. American Journal of Botany **54:** 136-144

Samach A, Onouchi H, Gold SE, Ditta GS, Schwarz-Sommer Z, Yanofsky MF, Coupland G (2000) Distinct roles of CONSTANS target genes in reproductive development of Arabidopsis. Science **288:** 1613-1616

Sandaklie-Nikolova L, Palanivelu R, King EJ, Copenhaver GP, Drews GN (2007) Synergid cell death in Arabidopsis is triggered following direct interaction with the pollen tube. Plant Physiol **144:** 1753-1762

Sasaki E, Frommlet F, Nordborg M (2017) The genetic architecture of the network underlying flowering time variation in Arabidopsis thaliana. BioRxiv**:** 175430

Schaller GE, Bishopp A, Kieber JJ (2015) The Yin-Yang of Hormones: Cytokinin and Auxin Interactions in Plant Development. The Plant Cell **27:** 44-63

Schindelin J, Arganda-Carreras I, Frise E, Kaynig V, Longair M, Pietzsch T, Preibisch S, Rueden C, Saalfeld S, Schmid B, Tinevez JY, White DJ, Hartenstein V, Eliceiri K, Tomancak P, Cardona A (2012) Fiji: an open-source platform for biological-image analysis. Nat Methods **9:** 676-682

Schiott M, Romanowsky SM, Baekgaard L, Jakobsen MK, Palmgren MG, Harper JF (2004) A plant plasma membrane Ca2+ pump is required for normal pollen tube growth and fertilization. Proceedings of the National Academy of Sciences of the United States of America **101:** 9502-9507

Schneitz K, Hulskamp M, Kopczak SD, Pruitt RE (1997) Dissection of sexual organ ontogenesis: a genetic analysis of ovule development in Arabidopsis thaliana. Development **124:** 1367-1376

Seren U, Vilhjalmsson BJ, Horton MW, Meng D, Forai P, Huang YS, Long Q, Segura V, Nordborg M (2012) GWAPP: a web application for genome-wide association mapping in Arabidopsis. Plant Cell **24:** 4793-4805

Shimizu-Sato S, Tanaka M, Mori H (2009) Auxin-cytokinin interactions in the control of shoot branching. Plant Mol Biol **69:** 429-435

Silverstone AL, Mak PY, Martinez EC, Sun TP (1997) The new RGA locus encodes a negative regulator of gibberellin response in Arabidopsis thaliana. Genetics **146:** 1087-1099

Simon ML, Platre MP, Marques-Bueno MM, Armengot L, Stanislas T, Bayle V, Caillaud MC, Jaillais Y (2016) A PtdIns(4)P-driven electrostatic field controls cell membrane identity and signalling in plants. Nat Plants **2:** 16089

Simpson GG, Dean C (2002) Flowering - Arabidopsis, the rosetta stone of flowering time? Science **296:** 285-289

Simpson GG, Dijkwel PP, Quesada V, Henderson I, Dean C (2003) FY is an RNA 3 ' end-processing factor that interacts with FCA to control the Arabidopsis floral transition. Cell **113:** 777-787

Smyth DR, Bowman JL, Meyerowitz EM (1990) Early Flower Development in Arabidopsis. Plant Cell **2:** 755-767

Somssich M, Je BI, Simon R, Jackson D (2016) CLAVATA-WUSCHEL signaling in the shoot meristem. Development **143:** 3238-3248

Song YH, Shim JS, Kinmonth-Schultz HA, Imaizumi T (2015) Photoperiodic Flowering: Time Measurement Mechanisms in Leaves. Annual Review of Plant Biology, Vol 66 **66:** 441-464

Sprunck S, Rademacher S, Vogler F, Gheyselinck J, Grossniklaus U, Dresselhaus T (2012) Egg cell-secreted EC1 triggers sperm cell activation during double fertilization. Science **338:** 1093-1097

Stinchcombe JR, Weinig C, Ungerer M, Olsen KM, Mays C, Halldorsdottir SS, Purugganan MD, Schmitt J (2004) A latitudinal cline in flowering time in Arabidopsis thaliana modulated by the flowering time gene FRIGIDA. Proc Natl Acad Sci U S A **101:** 4712-4717

Stoorvogel W, Strous GJ, Geuze HJ, Oorschot V, Schwartz AL (1991) Late endosomes derive from early endosomes by maturation. Cell **65:** 417-427

Suarez-Lopez P, Wheatley K, Robson F, Onouchi H, Valverde F, Coupland G (2001) CONSTANS mediates between the circadian clock and the control of flowering in Arabidopsis. Nature **410:** 1116-1120

Takeuchi H, Higashiyama T (2012) A species-specific cluster of defensin-like genes encodes diffusible pollen tube attractants in Arabidopsis. PLoS Biol **10:** e1001449

Thimann KV, Skoog F (1933) Studies on the Growth Hormone of Plants: III. The Inhibiting Action of the Growth Substance on Bud Development. Proc Natl Acad Sci U S A **19:** 714-716

Tsukamoto T, Qin Y, Huang Y, Dunatunga D, Palanivelu R (2010) A role for LORELEI, a putative glycosylphosphatidylinositol-anchored protein, in Arabidopsis thaliana double fertilization and early seed development. Plant J **62:** 571-588

Uribelarrea M, Cárcova J, Otegui ME, Westgate ME (2002) Pollen Production, Pollination Dynamics, and Kernel Set in Maize. Crop Science **42:** 1910-1918

Viotti C, Bubeck J, Stierhof YD, Krebs M, Langhans M, van den Berg W, van Dongen W, Richter S, Geldner N, Takano J, Jurgens G, de Vries SC, Robinson DG, Schumacher K (2010) Endocytic and secretory traffic in Arabidopsis merge in the trans-Golgi network/early endosome, an independent and highly dynamic organelle. Plant Cell **22:** 1344-1357

Volz R, Heydlauff J, Ripper D, von Lyncker L, Gross-Hardt R (2013) Ethylene Signaling Is Required for Synergid Degeneration and the Establishment of a Pollen Tube Block. Developmental Cell **25:** 310-316

Vu V, Verster AJ, Schertzberg M, Chuluunbaatar T, Spensley M, Pajkic D, Hart GT, Moffat J, Fraser AG (2015) Natural Variation in Gene Expression Modulates the Severity of Mutant Phenotypes. Cell **162:** 391-402

Waese J, Fan J, Pasha A, Yu H, Fucile G, Shi R, Cumming M, Kelley LA, Sternberg MJ, Krishnakumar V, Ferlanti E, Miller J, Town C, Stuerzlinger W, Provart NJ (2017) ePlant: Visualizing and Exploring Multiple Levels of Data for Hypothesis Generation in Plant Biology. Plant Cell **29:** 1806-1821

Wang Y, Sun S, Zhu W, Jia K, Yang H, Wang X (2013) Strigolactone/MAX2-induced degradation of brassinosteroid transcriptional effector BES1 regulates shoot branching. Dev Cell **27:** 681-688

Webb MC, Gunning BES (1990) Embryo Sac Development in Arabidopsis-Thaliana .1. Megasporogenesis, Including the Microtubular Cytoskeleton. Sexual Plant Reproduction **3:** 244-256

Weigel D (2012) Natural Variation in Arabidopsis: From Molecular Genetics to Ecological Genomics. Plant Physiology **158:** 2-22

Wellmer F, Riechmann JL (2010) Gene networks controlling the initiation of flower development. Trends Genet **26:** 519-527

Wetzsteini HY, Yi WG, Porter JA, Ravid N (2013) Flower Position and Size Impact Ovule Number per Flower, Fruitset, and Fruit Size in Pomegranate. Journal of the American Society for Horticultural Science **138:** 159-166

Wickson M, Thimann KV (1958) The Antagonism of Auxin and Kinetin in Apical Dominance. Physiologia Plantarum **11:** 62-74

Willemse M, Van Went J (1984) The female gametophyte. *In* Embryology of angiosperms. Springer, pp 159-196

Wilson ZA, Zhang DB (2009) From Arabidopsis to rice: pathways in pollen development. J Exp Bot **60:** 1479-1492

Xue WY, Xing YZ, Weng XY, Zhao Y, Tang WJ, Wang L, Zhou HJ, Yu SB, Xu CG, Li XH, Zhang QF (2008) Natural variation in Ghd7 is an important regulator of heading date and yield potential in rice. Nature Genetics **40:** 761-767

Yadegari R, Drews GN (2004) Female gametophyte development. Plant Cell **16 Suppl:** S133-141

Yamada M, Miyawaki A, Saito K, Nakajima T, Yamamoto-Hino M, Ryo Y, Furuichi T, Mikoshiba K (1995) The calmodulin-binding domain in the mouse type 1 inositol 1,4,5-trisphosphate receptor. Biochem J **308 (Pt 1):** 83-88

Yan J, Chia JC, Sheng H, Jung HI, Zavodna TO, Zhang L, Huang R, Jiao C, Craft EJ, Fei Z, Kochian LV, Vatamaniuk OK (2017) Arabidopsis Pollen Fertility Requires the Transcription Factors CITF1 and SPL7 That Regulate Copper Delivery to Anthers and Jasmonic Acid Synthesis. Plant Cell **29:** 3012-3029

Yin Y, Wang Z-Y, Mora-Garcia S, Li J, Yoshida S, Asami T, Chory J (2002) BES1 Accumulates in the Nucleus in Response to Brassinosteroids to Regulate Gene Expression and Promote Stem Elongation. Cell **109:** 181-191

Yuan J, Kessler SA (2019) A genome-wide association study reveals a novel regulator of ovule number and fertility in Arabidopsis thaliana. PLoS Genet **15:** e1007934

Zhong S, Liu M, Wang Z, Huang Q, Hou S, Xu YC, Ge Z, Song Z, Huang J, Qiu X, Shi Y, Xiao J, Liu P, Guo YL, Dong J, Dresselhaus T, Gu H, Qu LJ (2019) Cysteine-rich peptides promote interspecific genetic isolation in Arabidopsis. Science **364**

Zhou Y, Yan A, Han H, Li T, Geng Y, Liu X, Meyerowitz EM (2018) HAIRY MERISTEM
with WUSCHEL confines CLAVATA3 expression to the outer apical meristem layers.
Science **361:** 502-506

Zhu L, Chu LC, Liang Y, Zhang XQ, Chen LQ, Ye (2018) The Arabidopsis CrRLK1L
protein kinases BUPS1 and BUPS2 are required for normal growth of pollen tubes in the
pistil. Plant J **95:** 474-486

Zinn KE, Tunc-Ozdemir M, Harper JF (2010) Temperature stress and plant sexual
reproduction: uncovering the weakest links. J Exp Bot **61:** 1959-1968

PUBLICATIONS

1. **Yuan, J**., Ju, Y., Jones, D.S., Zhang, W., Lucca, N., Staiger, C.J. and Kessler, S.A., 2019. Redistribution of NORTIA in response to pollen tube arrival facilitates fertilization in *Arabidopsis thaliana*. *BioRxiv*, p.621599.

2. Boachon, B., Lynch, J.H., Ray, S., **Yuan, J**., Caldo, K.M.P., Junker, R.R., Kessler, S.A., Morgan, J.A. and Dudareva, N., 2019. Natural fumigation as a mechanism for volatile transport between flower organs. *Nature chemical biology*, 15(6), p.583.

3. **Yuan, J**, Kessler, S.A. A genome-wide association study reveals a novel regulator of ovule number and fertility in *Arabidopsis thaliana*. *PLoS Genetics*. 2019 ;15(2): e1007934.

4. Jones, D.S, **Yuan, J,** Smith, B.E, Willoughby, A.C, Kumimoto, E.L, and Kessler, S.A. Mildew Resistance Locus o function in pollen tube reception is linked to its oligomerization and subcellular distribution. *Plant Physiology*. 2017 ;175(1):172-185.

5. Davis, T.C, Jones, D.S, Dino, A.J, Cejda, N.I, **Yuan, J,** Willoughby, A.C, Kessler, S.A. Arabidopsis thaliana MLO genes are expressed in discrete domains during reproductive development. *Plant Reproduction.* 2017 ;30(4):185-195.